THE UNIVERSITY OF MANITOBA

Fundamental shear strength parameters

by

S.SEKLA

A THESIS

SUBMITED TO THE FACULTY OF GRADUATE STUDIES

IN PARTIAL FULFILMENT OF THE REQUIREMENTS FOR THE DEGREE

OF MASTER OF SCIENCE

DEPARTMENT OF CIVIL ENGINEERING

WINNIPEG,MANITOBA

October 1972

ABSTRACT

An experimental study on the fundamental shear strength parameters of a remoulded clay from Winnipeg, Manitoba was conducted.Three different experimental methods were used to determine the parameters by means of the triaxial apparatus. It was found that both Hvorslev's c_e and Schmertmann's (c_e) parameters are related to ;the water content at failure,the effective consolidation pressure, and the effective octahedral normal stress at failure. The parameter c_e was also found to be influenced by stress history.For the soil tested and for the range of pressures applied,it appears that Hvorslev's $\emptyset_e$ is not constant,but varies with the water content at failure and the stress history,and that Schmertmann's $(\emptyset_e)$ is virtually independent of water content at failure or effective consolidation pressure.

ACKNOWLEDGEMENT

I would like to acknowledge Dr.K.Y.Loh for his enthusiastic aid and guidance throughout my work and National Research Council who sponsored the project.

A special thanks is due to Dr.Domaschuk and Dr. Muir for reviewing the manuscript.

TABLE OF CONTENTS

Leaf blank to correct numbering.

Chapter | Page

LIST OF TABLES

LIST OF FIGURES

Page

LIST OF APPENDICES

Page

Chapter 1

INTRODUCTION

The shearing resistance of clays is not well understood. The lack of understanding arises from the complexity of the physical make-up of clays.

The conventional concept of expressing shearing resistance in terms of cohesion and friction is attributed to Coulomb. While this concept is relatively simple, it does not represent the fundamental properties of clays.

Hvorslev (1960) expressed the Coulomb criterion in terms of an effective cohesion (c_e),and an effective angle of friction (ϕ_e). Experimental studies have shown, however, that the fundamental parameters c_e and ϕ_e are not unique for a given soil.Conceivably,other factors may also influence c_e and ϕ_e.

The Coulomb-Hvorslev criterion is a failure theory and is not concerned with the mobilization of shearing resistance with deformation before failure. Schmertmann and Osterberg (1960) and Schmertmann (1963) extended the Coulomb-Hvorslev criterion to express shearing resistance as a function of a strain in terms of a component (I_ϵ) independent of effective stress,and a component (D_ϵ) dependent on effective stress. Schmertmann developed the

ID3* test and found that I_ϵ was fully mobilized at small strain, whereas much larger strain was required to fully develop D_ϵ . Similar finding were reported by Wu et al (1962).

For a fundamental understanding of shearing resistance, an examination of the structure of clays appears to be the logical starting point. A mechanistic picture of the development of shearing resistance of soils in terms of interaction between individual soil particles was presented by Lambe(1960). Factors influencing shear strength have been summarized by Whitman (1960).

There is no published data on Hvorslev strength parameters of Winnipeg clay. An experimental study has been carried out on a remoulded clay from Winnipeg, Manitoba. The objective were:

i) To obtain experimental strength data;

ii) To study the factors influencing the fundamental shear strength parameters of the clay.

* Details of the test are given in Appendix E.

Chapter 2

THEORETICAL CONSIDERATIONS

2.1 Conventional Shear Strength Parameters

The shear strength of a soil is commonly expressed by the Mohr-Coulomb failure criterion

$$s = c + \sigma_n \tan \phi \quad \ldots\ldots\ldots\ldots\ldots\ldots\ldots(1)$$

where :

s, is the shear strength which is equal to the shear stress on the failure plane,

c , is the unit cohesion,

σ_n,is the total normal stress on the plane of failure,

ϕ ,is the angle of friction.

As concluded by Terzaghi (1938), the stress conditions for failure in a soil depends on the intensity of effective stresses, and equation (1) should be written as

$$s = c' + \sigma'_n \tan \phi \quad \ldots\ldots\ldots\ldots\ldots\ldots\ldots(2)$$

where :

c' is the effective cohesion,

σ'_n is the effective normal stress on the failure plane,

ϕ is the angle of shearing resistance.

Equation (2) is illustrated in Figure (1)

where :

σ'_1 and σ'_3 are the effective major and minor principal stresses at failure respectively,

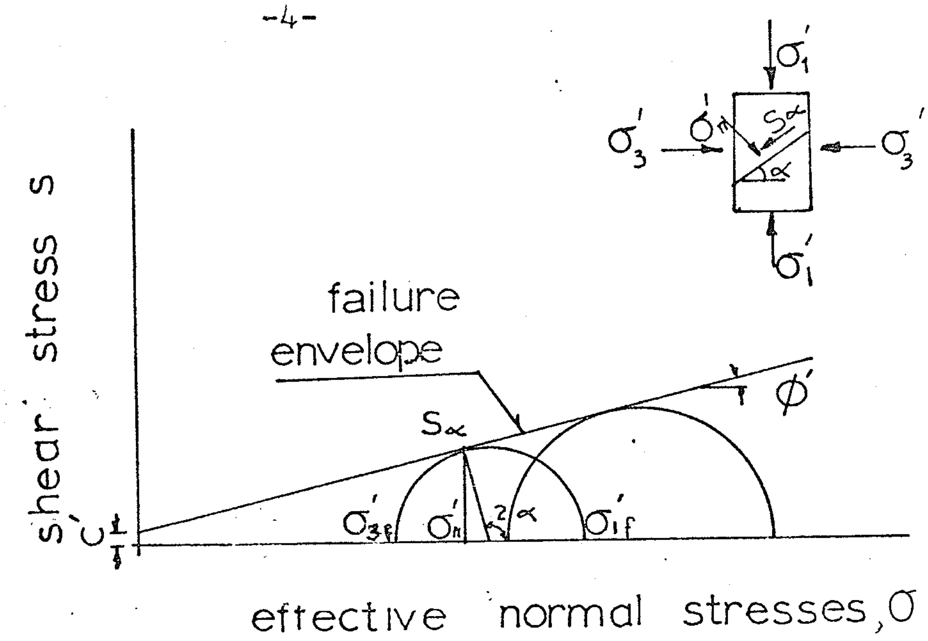

FIGURE 1 Mohr - Coulomb failure envelope in terms of s and σ

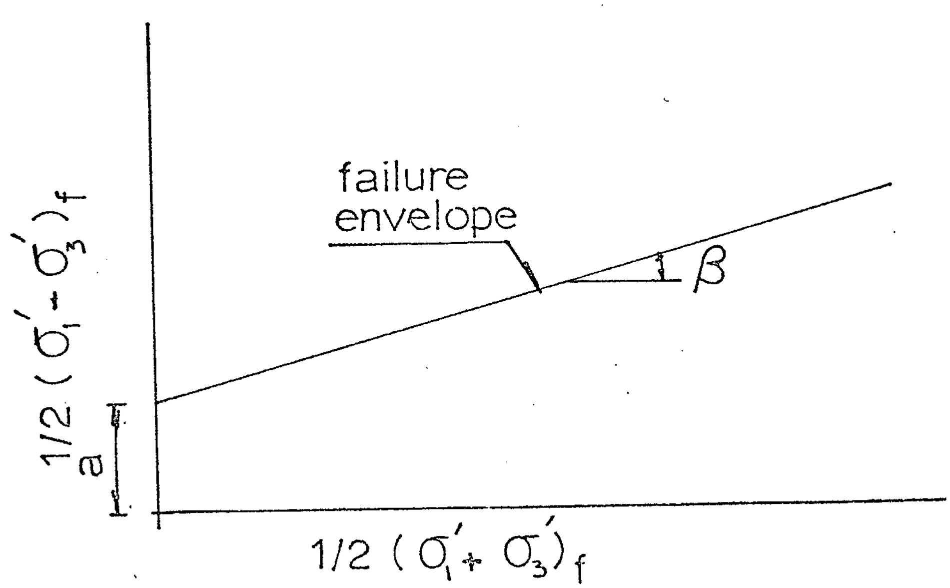

FIGURE 2 Mohr-Coulomb failure envelope in terms of $1/2\,(\sigma_1 + \sigma_3)_f$ and $1/2\,(\sigma_1 - \sigma_3)_f$

s_α is the shear stress at failure on the failure plane

$\alpha = 45 + \phi/2$ is the angle between the failure plane and the major principal plane.

In terms of the principal stresses, the Mohr-Coulomb equation can be written as :

$$1/2(\sigma_1' - \sigma_3')_f = a + 1/2\ (\sigma_1' + \sigma_3')_f \tan\beta \ldots\ldots(3)$$

where:

a is the intercept on the $1/2\ (\sigma_1' - \sigma_3')$ axis,

β is the angle of inclination of the straight line as illustrated in Figure 2 ,

$$\sin\phi = \tan\beta \ldots\ldots(4)$$

$$c' = a / \cos\phi' \ldots\ldots(5)$$

The Mohr-Coulomb equation can also be written as:

$$\sigma_1' = b + \sigma_3' \tan\gamma \ldots\ldots(6)$$

where:

b is the intercept on the σ_1' axis

γ is the angle of inclination of the straight line as illustrated in Figure 3 and

$$\sin\phi' = (\tan\gamma - 1)/(\tan\gamma + 1) \ldots\ldots(7)$$

$$c' = b/2 \sec\phi'\ (1 - \sin\phi') \ldots\ldots(8)$$

The shear strength of clay may therefore be considered to consist of two components that are physically different in nature as follows :

a) Cohesion

Cohesion contributes to shear strength of a soil as

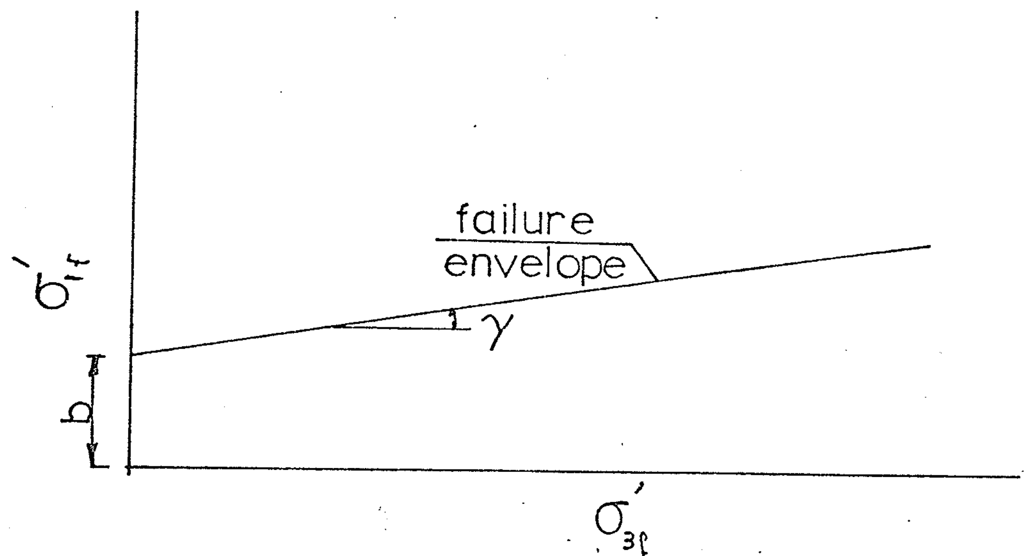

FIGURE 3 Mohr-Coulomb failure envelope in terms of σ_{1f} & σ_{3f}

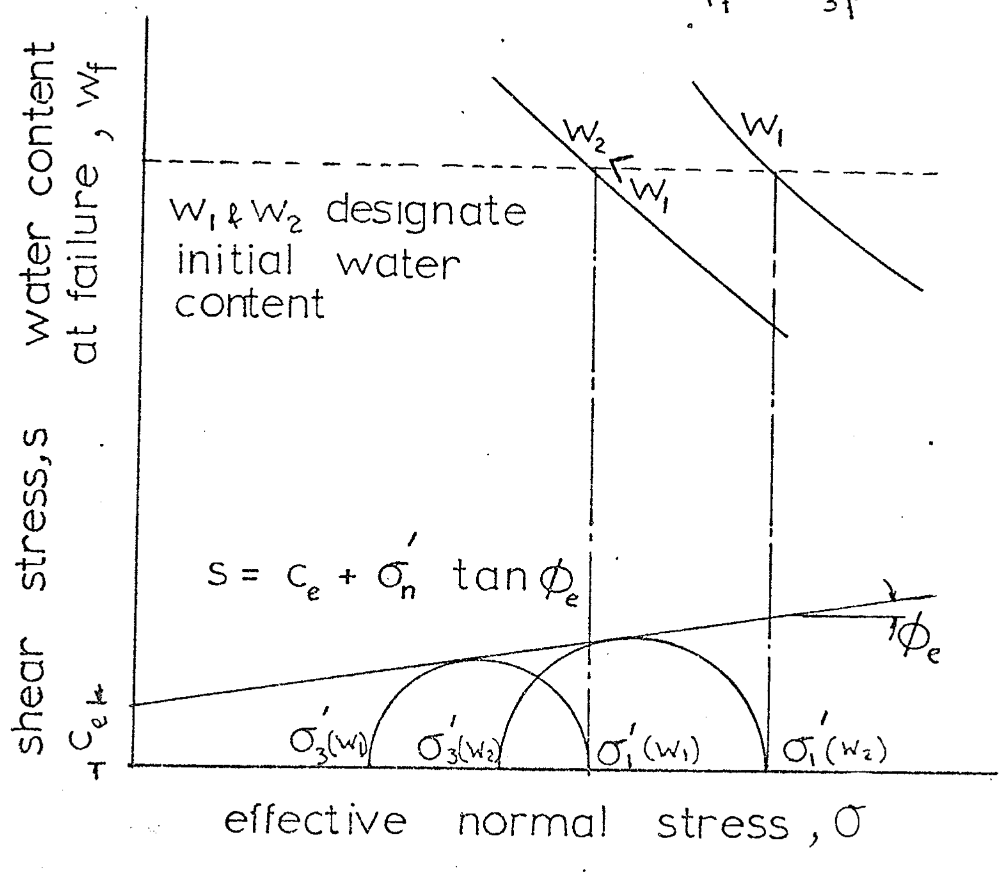

FIGURE 4 Determination of Hvorslev parameters (after Bjerrum, 1954)

a results of the physicochemical bond between the clay particles and is therefore governed by the physical nature of the particles as well as the void ratio,or the water content of the clay.Hence for a saturated clay,if the effective stress acting on the soil is changed, the water content will also change,and the cohesion will adopt another value corresponding to the new water content.

b) Friction

Friction contributes to shear strength as a result of frictional resistance to shear upon movements of the particles of the clay.Frictional resistance,therefore, is dependent on the effective normal stress σ'

2.2 Hvorslev's Shear Strength Parameters

Hvorslev (1960) expressed the Mohr-Coulomb equation as

$$s = c_e + \sigma'_n \tan \phi_e \quad \ldots\ldots\ldots\ldots\ldots (9)$$

where :

c_e is the effective cohesion which is a function of the void ratio at failure only,

ϕ_e is the effective angle of friction.

Equation (9) is seen to be based on the premise that shear strength of cohesive soils may be expressed in terms of two parameters c_e and ϕ_e with c_e reflecting the structural state of the particle system in terms of the void ratio at failure;and ϕ_e reflecting the frictional characteristics of the clay. A change in void ratio, or water content in case of saturated soil, causes a change in shear strength through a change in c_e only.

Working exclusively with remoulded clays,Hvorslev (1960) found that ϕ_e was virtually a constant and that the cohesion was directly proportional to the equivalent consolidation pressure.

$$c = K\sigma'_e \quad \ldots\ldots\ldots\ldots\ldots\ldots\ldots\ldots\ldots\ldots\ldots (10)$$

where

K is a coefficient of cohesion,

σ'_e is the equivalent consolidation pressure. For remoulded clays subjected to axial compression following isotropic consolidation, σ'_e may be taken as equal to σ'_c ,the effective consolidation pressure.

Equation (10) is based on the premise that a clay slurry has no cohesive strength,and subsequent cohesion exists as a result of consolidation only.The equation is applicable,therefore,only if the soil is initially consolidated from a water content equal to or higher than the liquid limit of the soil.

Bjerrum (1954) has verified the validity of equation (10) for cohesive soil remoulded at high water contents, but found that for clays remoulded at low water contents equation (10) should be replaced by :

$$c = c_o + K'\sigma'_c \quad \ldots\ldots\ldots\ldots\ldots\ldots\ldots\ldots\ldots\ldots\ldots\ldots\ldots(11)$$

where:

c_o is the initial cohesion,

K' is the coefficient of cohesion for clays remoulded at low water contents.

Equation (9) can therefore be written as :

$$s/\sigma'_e = K + \sigma'_n/\sigma'_e \tan \phi_e \quad \ldots\ldots\ldots\ldots\ldots\ldots\ldots(12)$$

or

$$s/\sigma'_e = c/\sigma'_e + K' + \sigma'_n/\sigma'_e \tan \phi_e \quad \ldots\ldots\ldots(13)$$

If values of s/σ'_e are plotted against values of σ'_n/σ'_e, the intercept on the s/σ'_e axis determines K in equation (12) or $c/\sigma'_e + K'$ in equation (13), and ϕ_e is obtained from the angle of inclination of the straight line through the points.

A method for the determination of c_e and ϕ_e suggested by Bjerrum (1954) is as follows. A series of consolidated undrained triaxial compression tests with pore pressure measurements are carried out on a clay remoulded at a given water content. Another series of the same type of tests are also carried out on the same clay remoulded at a different initial water content. Two different consolidation as well as strength curves therefore result . As equal water content at failure implies equal c_e, the difference in shear strength between any two samples having the same water content at failure is due entirely to a difference in frictional resistance. Consequently c_e and $\emptyset_e$ can be determined as illustrated in Figure 4.

Noorany and Seed (1965) proposed a new experimental procedure for the determination of c_e and $\emptyset_e$ for sensitive clays as follows. A pair of identical samples is subjected to the same anisotropic consolidation pressure, and then, if the applied consolidation stresses on one sample are removed with no volume changes allowed, and the two samples axially compressed to failure, there will exist two samples at identical void ratio but under different effective stress system at failure. From a comparison between the effective stresses at failure for these two samples, the shear strength parameters c_e and $\emptyset_e$ can be determined. A disadvantage of this method is that the two Mohr's circles representing the effective stress conditions at failure for the pair of samples tested may be very close to each other for insensitive clays. However, for sensitive soils, they are sufficiently far apart to permit the desired interpretation of the test data. This method has the advantage that c_e and $\emptyset_e$ can be obtained with a limited number of samples.

2.3 Schmertmann's Shear Strength Parameters

A significant contribution to the understanding of shear strength was made by Schmertmann and Osterberg (1960),and Schmertmann (1962,1963), who expressed the shearing resistance mobilized at a given strain as

$$s_\epsilon = I_\epsilon + D_\epsilon \quad \ldots\ldots\ldots\ldots\ldots\ldots\ldots\ldots\ldots (14)$$

where:

s_ϵ is the total shearing resistance mobilized at a given strain on a given plane,

I_ϵ is the mobilized component of resistance independent of effective stress at the same strain and on the same plane,

D_ϵ is the mobilized component of shearing resistance dependent on effective stress at the same strain and on the same plane.

Equation (9) may be written as :

$$s = (c_e)_\epsilon + \sigma'_n \; (\tan \phi_e)_\epsilon \quad \ldots\ldots\ldots (15)$$

At failure one might expect

$$I_{\epsilon f} = c_e = (c_e)_{\epsilon f} \ldots\ldots\ldots\ldots\ldots\ldots\ldots\ldots (16)$$

$$D_{\epsilon f} = \sigma'_n \; \tan \phi_e \quad \ldots\ldots\ldots\ldots\ldots\ldots\ldots\ldots (17)$$

or

$$(\tan \phi_e)_f = \tan \phi_e \quad \ldots\ldots\ldots\ldots\ldots\ldots\ldots (18)$$

where the subscript f indicates failure.

The components I_ϵ and D_ϵ are determined by a testing technique developed by Schmertmann, referred to as the IDS test, in which soil specimens are subjected to axial compression under controlled pore pressures. Thus the IDS test is, in essence, a drained test under controlled effective stresses.

Schmertmann showed that, among other findings of his works, the maximum value of I_ϵ, ($I_{max.}$), was developed at a much lower strain than that of D_ϵ, and consequently at failure one or both of the strength components may not be at the maximum. He therefore concluded that Hvorslev's parameters c_e and ϕ_e may not be unique because they were determined from two specimens that may have failed at different strains, and consequently equal void ratio at failure may not reflect equal structure of the same clay. Schmertmann's finds were substantiated by Wu et al (1962) who found that the mobilized components of shearing resistance were influenced by the structure of the clay, depending on wether the same clay was in the "indisturbed" laboratory flocculated or remoulded state. A constant structure Mohr envelope, where fundamental parameters of shearing resistance may only be defined at the same strain, and hence at the same structure, has been proposed by Schmertmann (1972) for cohesive soils.

Kenney (1967) extended the Hvorslev-Schmertmann's criterion to include a " bond strength" component by expressing the shearing resistance of natural cemented clays as :

$$s = (b_n)_\epsilon + (c_e)_\epsilon + \sigma'_n (\tan \phi_e)_\epsilon \text{..........} (19)$$

where:

(b_n) is the bond strength at strain ϵ.

Chapter 3

EXPERIMENTAL PROGRAM

The experimental program consisted of performing consolidated-undrained triaxial compression tests with pore pressure measurments,and Schmertmann's IDS tests on remoulded clay.The clay in its "undisturbed" state was extracted from a depth of about 13 feet at the Imperial Oil storage tanks site in Winnipeg, Manitoba.Two remoulded batches of soil with different initial water contents were prepared.The details of the preparation are explained in a subsequent section. Samples from Batches 1 and 2 were tested in accordance with the method suggested by Bjerrum (1954),hereafter called Method (1);and the method proposed by Noorany and Seed (1965),hereafter called Method (2).Samples from Batch 2 only,were tested using Schmertmann's IDS technique,which hereafter will be called Method (3).

The purpose of the experimental program was to investigate the factors which influence the shear strength parameters of the clay.The conventional shear strength parameters c'and ϕ' were also obtained.

The average properties of the soil tested,the method of sample preparation,and the testing procedure employed, are described in the following sections.

3.1 Clay Tested

The remoulded clay in its original "undisturbed" condition is a lacustrine clay deposited during the times of glacial Lake Agassiz.The clay is highly plastic, dark greyish brown in colour,and is laminated with silt. The average index properties are shown in Table 1.

The consolidation characteristics of the remoulded clay are shown in Figure 5,where plots of void ratio, versus the logarithm of effective pressure;and the coefficient of consolidation,C_v,versus the logarithm of effective pressure,p,were presented in the same figure for a sample from Batch 1.Swelling was not allowed throughout the loading process.

3.2 Sample Preparation

Two batches of the same soil were prepared as follows: Small lumps of "unditurbed" soil were allowed to soak in distilled water for one week,and then thoroughly mixed and separated into two batches.They were then covered and stored in a moist room for three weeks in order to obtain a more uniform distribution of moisture

Table 1 Average properties of clays tested

Original average water content of undisturbed clay	54.0 %
Liquid Limit	120.0
Plastic Limit	46.7
Plasticity Index	73.3
Clay fraction	90.0 %
Activity ratio	9.815
Specific Gravity	2.75
Compression Index C_c	0.70

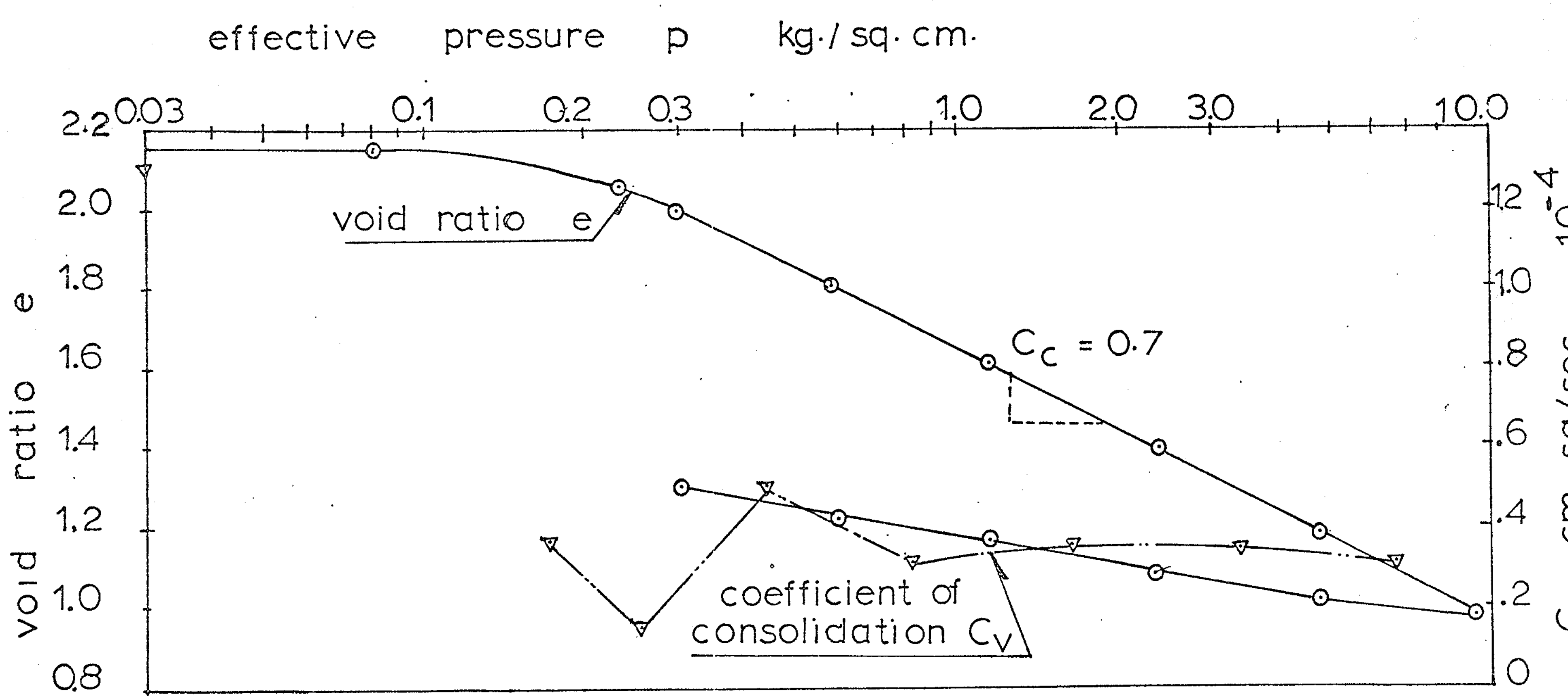

FIGURE 5 One dimensional consolidation characteristics; remoulded clay

content.The water content of the "batches" in this condition was approximately equal to the liquid limit of the soil.

One batch of the soil,hereafter called Batch 1, was allowed to dry to a water content of 75.0%,whereas the other batch hereafter called Batch 2,was dried to a water content of 91.0%.Both batches were continuously and thoroughly remoulded throughout the drying process.

All samples,were cut from the batches,and trimmed to 1.4 inches in diameter and 3.0 inches in height.

To accelerate consolidation and pore pressure response,all samples were provided with filter paper side drains and seven internal wool drains.

3.3 Testing Procedure

All samples were subjected to isotropic consolidation and were drained from the basal porous stone. To reduce the effect of end restraint,the top loading cap was lubricated with silicon grease.

To assure complete saturation,a back pressure was used.As described by Bishop and Henkel (1957),both cell pressure and back pressure were increased in increments in order to allow sufficient time for equalization of pore pressure at each stage.Pore pressures were measured at the sample base by means of a pressure gauge or mercury manometer.

The multiple-stage technique desribed by Bishop and Henkel (1957) and by Kenney and Watson (1961) was used for all tests. It was possible to perform two or three tests on each sample, resulting in a great saving of material.

All samples were axially loaded to failure under a constant rate of deformation, using a loading frame with a proving ring attachment. The average axial strain rates during tests were :

Method 1, 0.863 % strain /hour;

Method 2, 0.882 % strain /hour;

Method 3, 0.908 % strain/ hour.

The three different testing procedures, Methods (1), (2) and (3) are described below.

3.3.1 Method 1

Three samples from Batch 1 and two samples from Batch 2 were subjected to multiple-stage consolidated-undrained triaxial compression tests with pore pressure measurements, following the procedure described by Bishop and Henkel (1957). The effective isotropic consolidation pressure, σ_c', ranged from 10.0 psi. to 60.0 psi.. A back pressure of 20.0 psi. was used for all tests. In Stage 1 of the test,after failure was reached,the applied stress $(\sigma_1-\sigma_3)$ was removed and the sample was then allowed to come to equilibrium as indicated by the constant pore pressure.In Stage 2,the cell pressure on the same sample was increased to the desired value, the sample was allowed to consolidate,and the test was repeated as before.Stage 3 was merely a repetition of Stage 2 with a higher consolidation pressure.The heights and volume changes were carefully measured throughout the consolidation of the samples,and the height changes were measured throughout the testing. Where apparent,the mode of failure was also noted.

3.3.2 Method 2

In this Method,the samples were first consolidated to the same isotropic consolidation pressure used in section 3.3.1. The cell pressure was then reduced to a lower value under undrained conditions.Consequently a reduction in the pore pressure occured.The major drop in the pore pressure occured in a short time. The samples were then axially tested to failure before the samples had reached equilibrium under the reduced cell pressure.It was assumed in the analyses that the pore pressure at the time the axial load was applied, was constant throughout the sample and that subsequent pore pressure changes were due to the application of the axial load only.These assumptions are not necessary valid,which makes the method questionable.

Using the multiple-stage technique and in accordance with the procedure desribed above,one sample from Batch 1 and two samples from Batch 2 were tested. Eight test results in all were obtained,and they were used in conjunction with the other results obtained from the consolidated-undrained tests described in section 3.3.1 to determine Hvorslev parameters.

3.3.3 Method 3

Two-stage IDS tests were carried out on one sample from Batch 2.In the first stage,the sample was consolidated,then axially compressed to failure,with the major effective principal stress,σ_1' ,kept constant at two different stress levels by means of pore pressure control.The pore pressure was controlled by increasing or decreasing the pore pressure at the base of the sample.After failure was reached,the applied deviator stress ($\sigma_1'-\sigma_3'$) was removed,and the sample was allowed to come to equilibrium.In the second stage,the cell pressure was increased to the desired value, consolidation was allowed to take place, and the test was repeated as before. Volume changes of the sample were recorded when drainage was used to control pore pressure.

Chapter 4

TEST DATA AND ANALYSES OF RESULTS

The water content, w, the effective consolidation pressure, σ'_c, the void ratio, e, and the degree of saturation s, at various stage of the multiple-stage tests are summarized in Table 2. In the table the subscript "i" designates the initial condition prior to consolidation, whereas the subscript "f" indicates the final or failure condition. The test numbers are designated as 101.1 for Stage 1, 101.2 for Stage 2, and 101.3 for Stage 3, for the same sample. This system of designation is used for all samples.

The stress-strain curves for all tests are included in Figures A-1 through A-31 of Appendix A.

Failure was taken as the peak point of the plot of the effective principal stress ratio (σ'_1/σ'_3) versus the axial strain, ϵ, of a sample. The failure conditions for tests carried on by Methods (1) and (2) are presented in Tables 3 and 4,

where :

ϵ is the axial strain at failure,

Δu_f is the pore pressure change at failure,

$\bar{A}_f = \Delta u_f / (\Delta\sigma'_1 - \Delta\sigma'_3)$ is Skempton's pore pressure parameter A at failure.

Table 2 Summary of test conditions of multiple-stage tests

Test Number		Batch 1				Batch 2				
		101	102	103	104	201	202	203	204	301
σ'_c psi.	Stage (1)	12.20	21.40	14.80	17.60	12.20	17.60	12.20	17.60	12.20
w_i %	Stage (1)	74.30	74.00	76.00	80.00	92.00	91.50	91.00	90.90	64.88*
e_i	Stage (1)	2.07	2.06	2.09	2.25	2.56	2.55	2.56	2.67	1.84*
w_f %	Stage (1)	61.10	57.20	61.70	60.00	64.70	61.80	66.10	63.10	68.50**
e_f	Stage (1)	1.71	1.57	1.71	1.69	1.79	1.72	1.87	1.85	1.94**
σ'_c psi.	Stage (2)	21.50	31.00	24.70	31.00	21.50	31.50	21.30	31.20	31.80
w_i %	Stage (2)	61.10	57.20	61.70	60.00	64.70	61.80	66.10	63.10	55.40*
e_i	Stage (2)	1.71	1.57	1.71	1.69	1.79	1.72	1.87	1.85	1.58*
w_f %	Stage (2)	57.20	53.50	57.00	53.50	59.40	56.20	59.50	57.30	59.50**
e_f	Stage (2)	1.60	1.47	1.58	1.51	1.65	1.56	1.69	1.68	1.69**
σ'_c psi.	Stage (3)	41.10		41.60	62.30	41.20	61.50	40.50		
w_i %	Stage (3)	57.20		57.00	53.50	59.40	56.20	59.50		
e_i	Stage (3)	1.60		1.58	1.51	1.65	1.56	1.69		
w_f %	Stage (3)	51.20		50.00	47.41	53.50	49.30	53.60		
e_f	Stage (3)	1.44		1.42	1.33	1.49	1.37	1.49		

* At start of test

** At end of test

Table 3 Failure conditions for samples from Batch 1, by Method (1) and (2);

Test number	σ'_c psi.	w_f %	e_f	ϵ_f %	σ'_1 psi.	σ'_3 psi.	Δu_f psi.	$\bar{A}_f$	$1/2(\sigma'_1-\sigma'_3)_f$ psi.	$1/2(\sigma'_1+\sigma'_3)_f$ psi.
101.1	12.2	61.1	1.71	3.995	16.268	7.2	4.1	0.452	4.5340	11.7340
101.2	21.5	57.2	1.60	4.142	26.269	13.1	7.5	0.570	6.5845	19.6850
101.3	41.1	51.2	1.44	4.805	45.895	26.8	13.3	0.362	9.5475	36.3450
102.1	21.4	57.2	1.57	5.224	24.797	13.0	8.4	0.713	5.8985	18.8990
102.2	31.0	53.5	1.47	4.753	38.008	20.6	10.0	0.574	8.7040	29.3040
*103.1	14.8	61.7	1.71	4.540	16.989	8.8	4.2	0.513	4.0945	12.8950
*103.2	24.7	57.0	1.58	4.427	26.423	14.2	6.5	0.531	6.1115	20.3120
*103.3	41.6	50.0	1.42	4.619	46.229	26.4	11.4	0.576	9.9145	36.3140
104.1	17.6	60.0	1.69	4.770	19.519	9.6	5.5	0.555	4.9595	14.5600
104.2	31.0	53.5	1.51	4.332	39.685	20.8	9.5	0.504	9.4425	30.2430
104.3	62.3	47.4	1.34	4.851	74.959	41.6	20.2	0.606	16.6795	58.2800

* Results obtained by Method (2)

Table 4 Failure conditions for samples from Batch 2, by Methods (1) and (2);

Test number	σ'_c psi.	w_f %	e_f	ϵ_f %	σ'_1 psi.	σ'_3 psi.	Δu_f psi.	$\bar{A}_f$	$1/2(\sigma'_1-\sigma'_3)_f$ psi.	$1/2(\sigma'_1+\sigma'_3)_f$ psi.
201.1	12.2	64.7	1.79	4.041	15.297	7.3	4.9	0.615	3.9985	11.298
201.2	21.5	59.4	1.65	4.900	26.797	13.2	8.1	0.596	6.7985	19.998
201.3	41.2	53.5	1.49	4.802	49.438	27.8	12.9	0.596	10.8190	36.619
202.1	17.6	61.8	1.72	4.268	20.829	10.0	6.0	0.554	5.4145	15.414
202.2	31.5	56.2	1.56	4.210	38.202	19.9	9.8	0.536	9.1510	29.051
202.3	61.5	49.3	1.37	4.301	71.365	42.0	19.3	0.657	14.6825	56.682
* 203.1	12.2	66.1	1.87	4.054	13.931	6.7	2.4	0.337	3.6155	10.316
* 203.2	21.3	59.5	1.69	4.343	22.833	13.2	4.4	0.457	4.8165	18.016
* 203.3	40.2	53.6	1.49	3.147	47.553	26.2	9.9	0.464	10.6765	36.108
* 204.1	17.6	63.1	1.85	4.820	17.556	8.6	3.8	0.424	4.4780	13.078
* 204.2	31.2	57.3	1.68	4.643	37.232	18.8	9.2	0.500	9.2160	28.016

* Results obtained by Method (2)

It may be observed from the tables that the values of $\overline{A}_f$ varried between 0.337 to 0.713 ,and averaged about 0.582 ,and the ratio $\Delta u/\ \sigma'_c$ ranged from 0.30 to 0.39 and average 0.35.

4.1 Effective Shear Strength Parameters

Figure 6 shows the stress paths and the failure envelopes in effective principal stress space for the consolidated undrained tests performed on samples from Batch 1 and Batch 2. By applying equations (6),(7) and (8),the average shear strength parameters were : $c' = 0$ and $\phi' = 15$ degree.

4.2 Hvorslev Parameters c_e and ϕ_e

4.2.1 Determination of c_e & ϕ_e by Method (1)

To determine the parameters c_e & ϕ_e according to Method (1),it was essential that the pair of samples considered had an identical water content at failure. The water content at failure,w_f,was plotted against the logarithm of the corresponding effective consolidation pressure, σ'_c ,for samples from Batches 1 and 2 in Figure 7 .It can be seen from the figure that two different consolidation curves,which were approximated

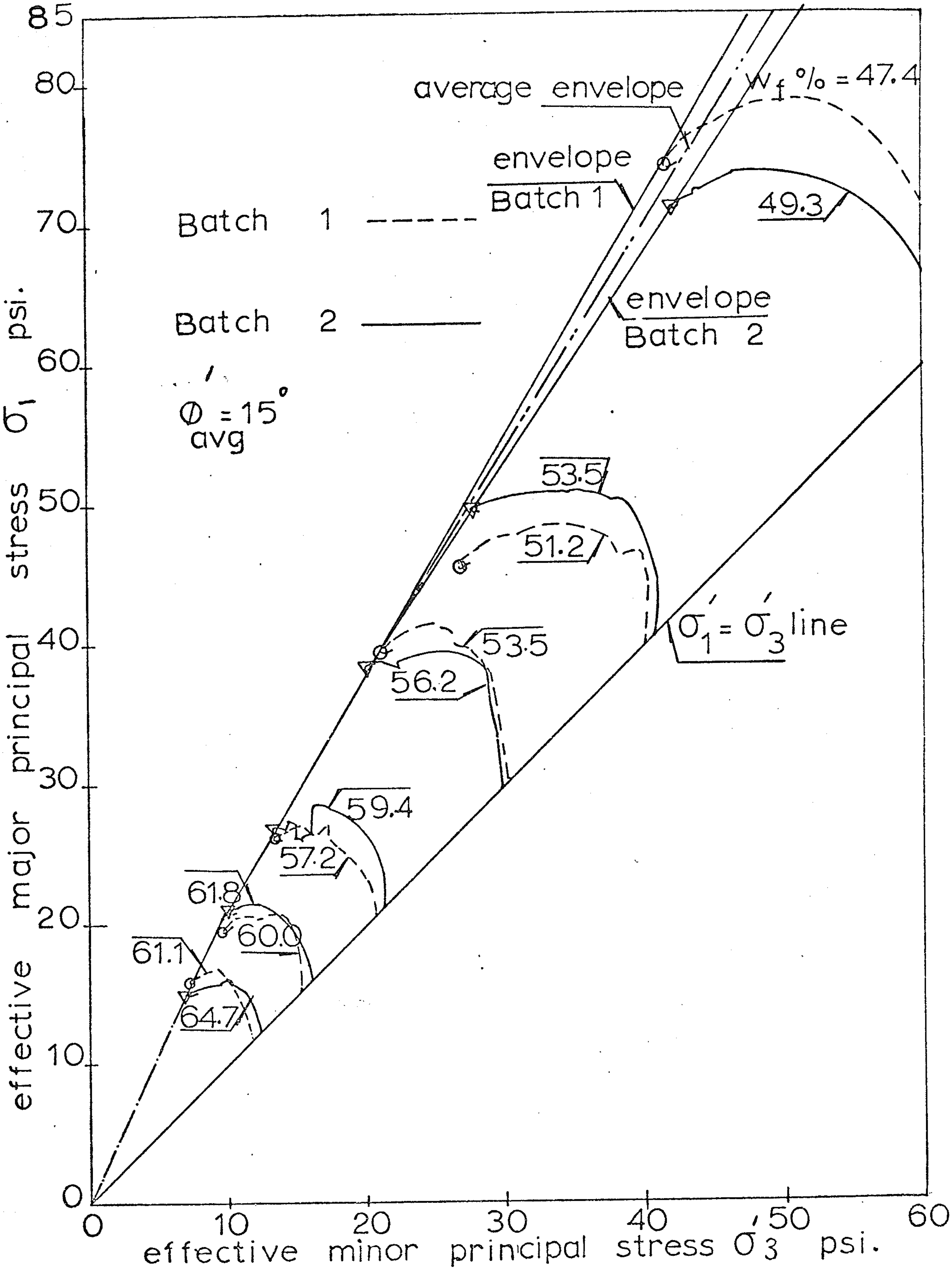

FIGURE 6 Stress path & failure envelope

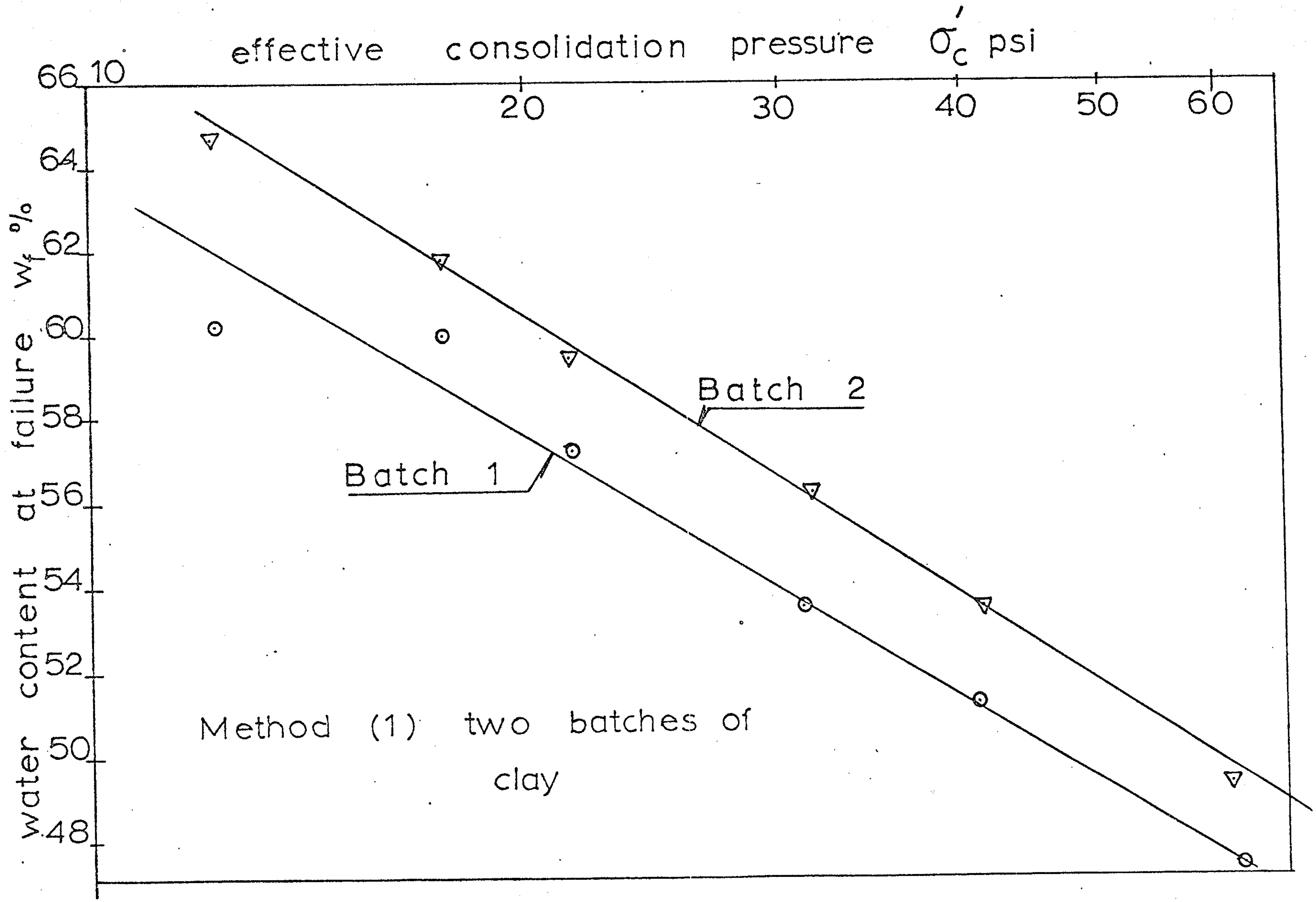

FIGURE 7 water content at failure vs effective consolidation pressure by straight lines, were obtained for Batches 1 and 2. This indicated that the structure of the soil in the two batches probably differed due to different stress histories. Similar graphs would be obtained if the void ratio was plotted against the logarithms of the effective consolidation pressure σ'_c .

In Figure 8 , the water content at failure , w_f, was plotted against the logarithm of $1/2\ (\sigma'_1 - \sigma'_3)_f$ and $1/2(\sigma'_1 + \sigma'_3)_f$ for samples from Batches 1 and 2, and a straight line relationship was obtained. At a given water content at failure, w_f, two values of $1/2(\sigma'_1 - \sigma'_3)_f$ and two values of $1/2(\sigma'_1 + \sigma'_3)_f$ are obtained for soils from Batches 1 and 2, yielding two points in a $1/2(\sigma'_1 - \sigma'_3)_f$ versus $1/2(\sigma'_1 + \sigma'_3)_f$ plot, representing the Mohr circles of stresses at failure. By drawing a straight line through these two points, c_e was obtained from the intercept on the $1/2(\sigma'_1 - \sigma'_3)_f$ axis and ϕ_e from the angle of inclination of the line by applying equations (3), (4) and (5). Figures 9, 10, and 11 shows the plots of $1/2(\sigma'_1 - \sigma'_3)_f$ against $1/2(\sigma'_1 + \sigma'_3)_f$ for different water content at failure, w_f, values. The parameters thus obtained are tabulated in Table 5.

In Figure 12, c_e and ϕ_e were plotted versus the water content at failure, w_f. It can be seen from the figure that values of c_e increased with decreasing

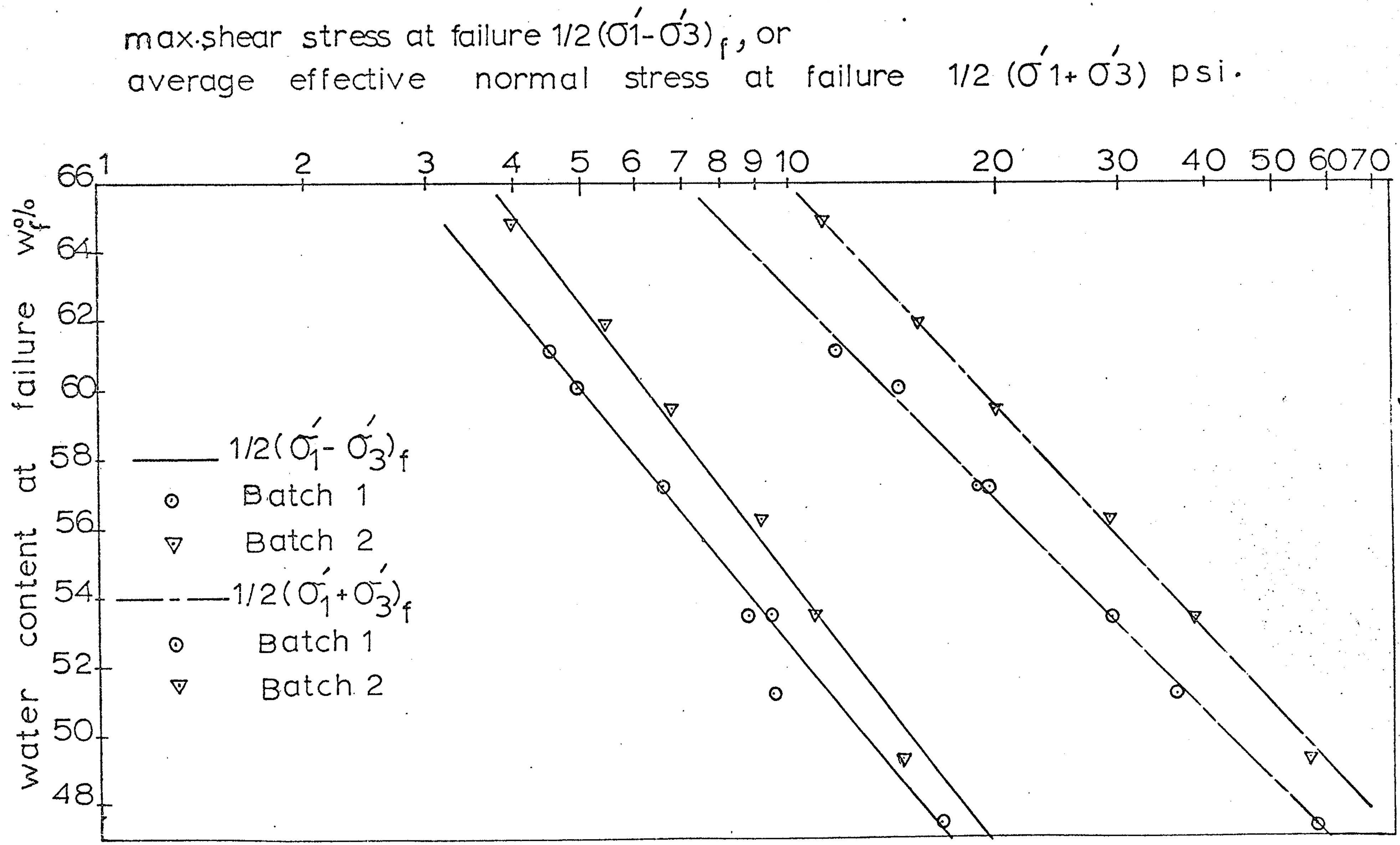

FIGURE 8 Water content at failure vs $1/2(\sigma_1' + \sigma_3')$ & $1/2(\sigma_1' - \sigma_3')_f$; Method (1)

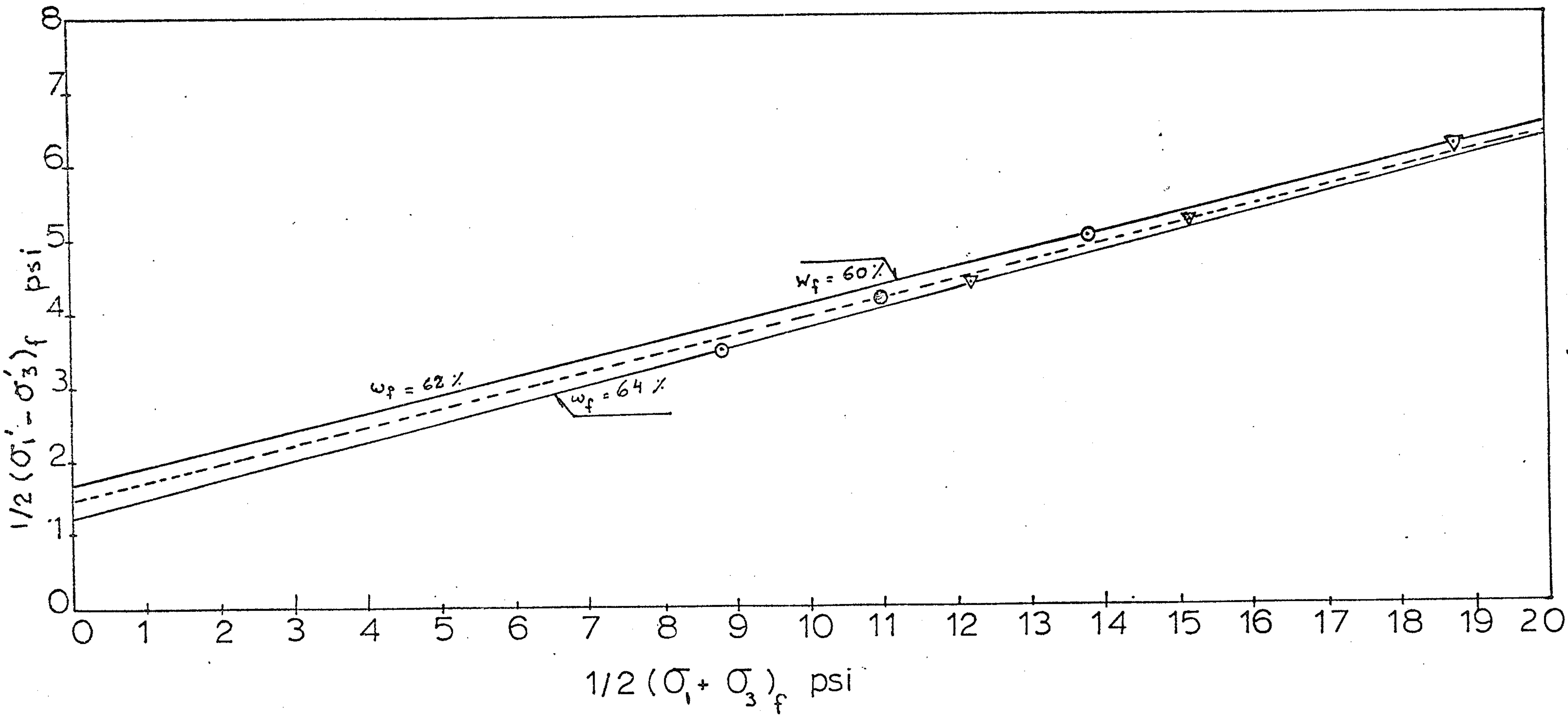

FIGURE 9 $1/2(\sigma_1' + \sigma_3')_f$ vs $1/2(\sigma_1' - \sigma_3')_f$; Method (1); $w_f = 60\%, 62\%, 64\%$

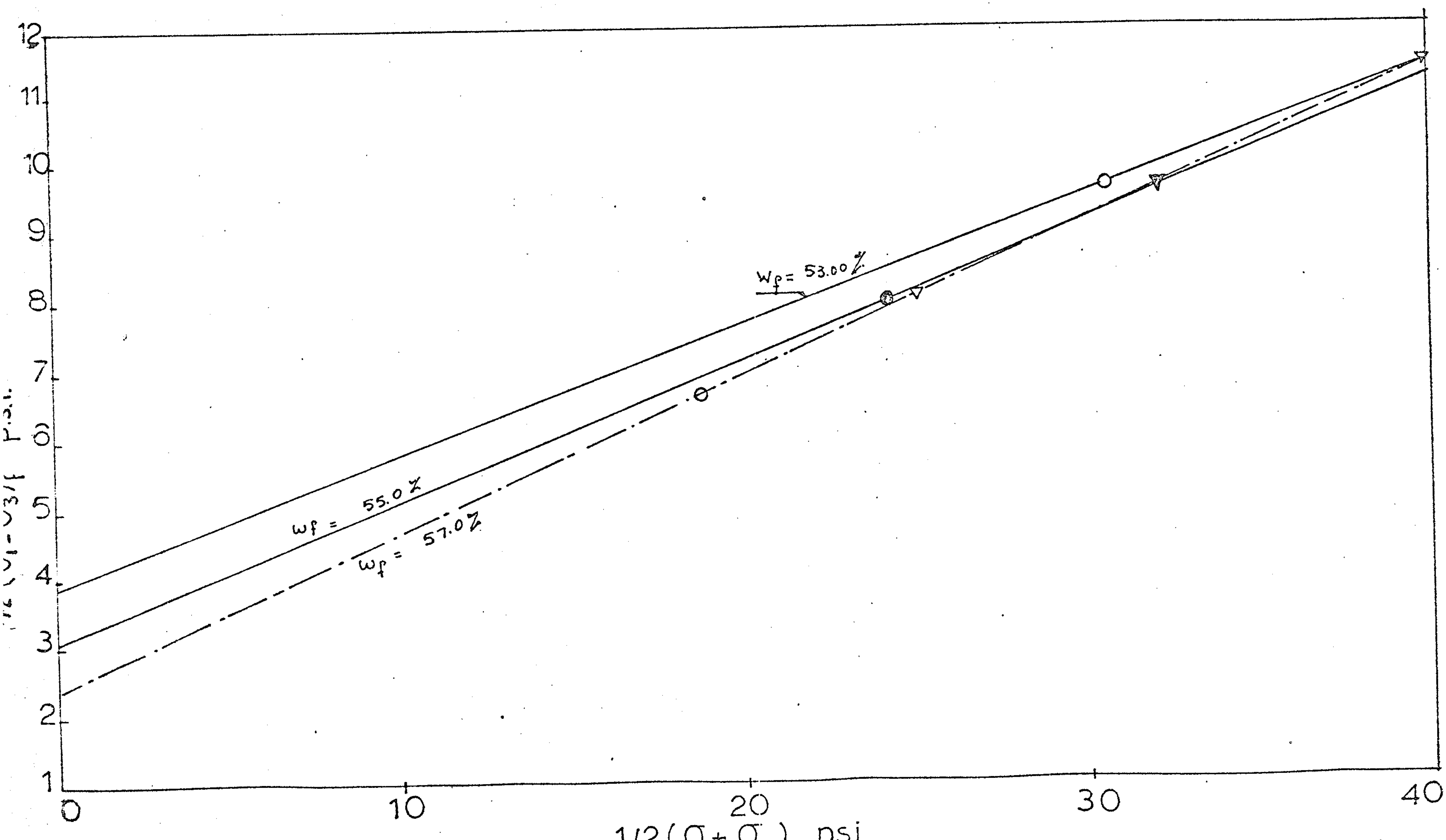

FIGURE 10. $1/2(\sigma_1' + \sigma_3')$ vs. $1/2(\sigma_1' - \sigma_3')$; Method (1) ; W_f = 53%, 55%, 57%

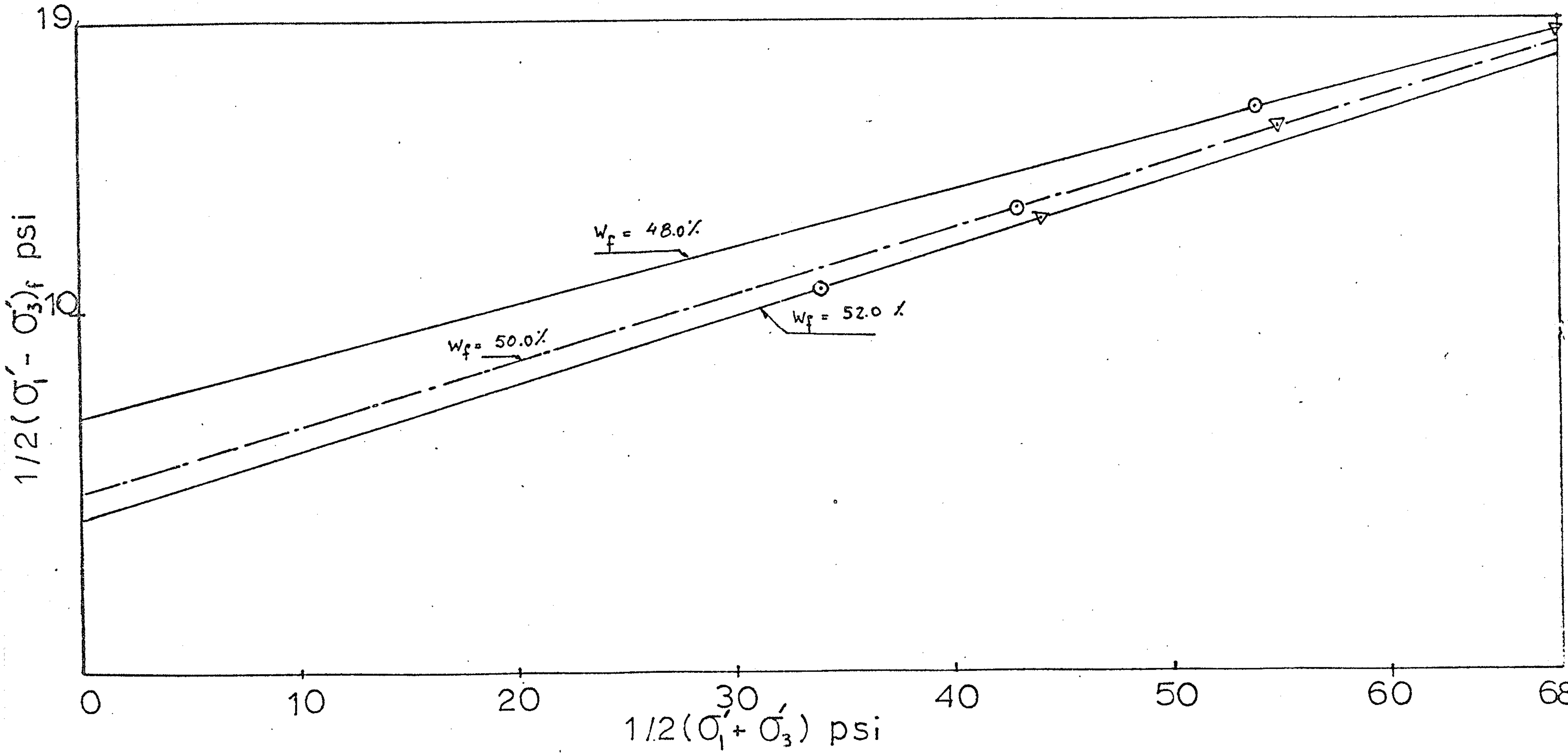

FIGURE 11 $1/2(\sigma_1' + \sigma_3')_f$ vs $1/2(\sigma_1' - \sigma_3')_f$; Method (1);
W_f = 48%, 50%, 52%

Table 5 Determination of c_e and ϕ_e by Method (1)

w %	Batch	σ'_c psi	$1/2\,(\sigma'_1 - \sigma'_3)_f$ psi	$1/2\,(\sigma'_1 + \sigma'_3)_f$ psi	σ'_{octf} psi	c_e psi	ϕ_e degree
65	1		3.15	7.90	7.10	1.2	14.6
	2		4.00	11.00	9.70		
64	1	10.6	3.42	8.80	8.00	1.2	14.6
	2	15.0	4.36	12.25	10.85		
62	1	12.2	4.15	11.00	10.00	1.5	14.0
	2	17.0	5.20	15.20	13.50		
60	1	15.2	5.00	13.80	12.60	1.7	13.5
	2	20.9	6.20	18.80	16.70		
57	1	21.4	6.60	18.70	17.60	2.5	12.8
	2	28.7	8.05	25.00	21.70		
55	1	26.7	8.00	24.20	21.00	3.2	11.8
	2	35.5	9.60	32.10	29.00		
53	1	33.2	9.60	30.50	28.00	4.0	10.7
	2	43.5	11.40	40.00	36.00		
52	1	37.2	10.60	34.00	31.20	4.3	10.6
	2	48.5	12.50	44.20	40.20		
50	1	46.6	12.80	43.00	39.00	5.1	10.6
	2	60.0	15.00	55.00	50.00		
48	1	58.1	15.50	54.00	58.10	7.3	9.1
	2	74.0	17.70	68.00	64.00		

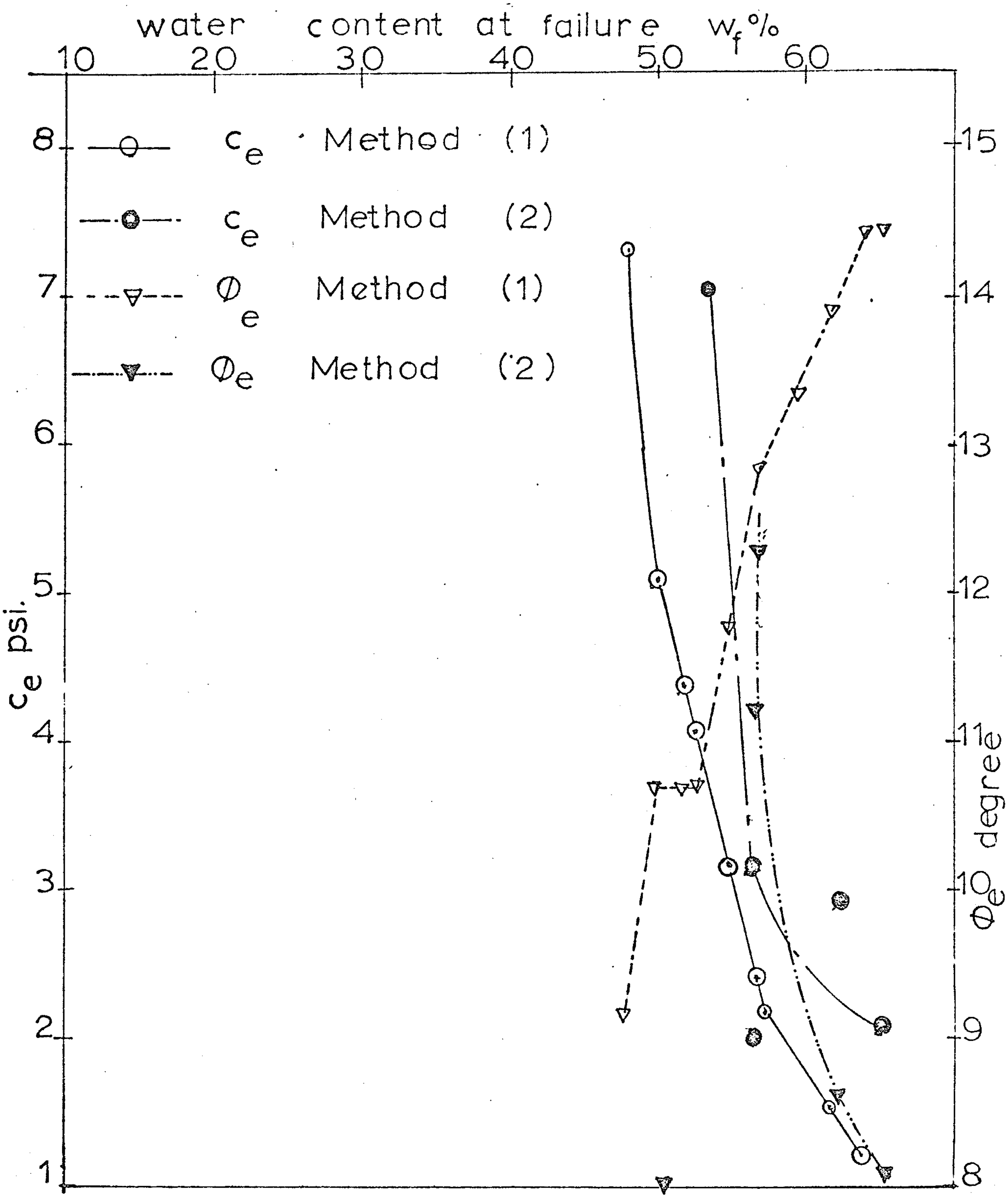

FIGURE 12 Water content at failure vs $\emptyset_e$ & c_e by Methods(1)&(2)

values of water content at failure, w_f, whereas ϕ_e, contrary to Hvorslev assumptions, was not constant, but increased with increasing values of water content at failure, w_f. The values of ϕ_e ranged from 9 to 14.5 degree for the range of water contents used in this study.

In Table 5, the effective octahedral normal stress at failure, $\sigma'_{octf} = 1/3\ (\sigma'_1 + 2\ \sigma'_3)$ obtained from Figure C-1 in Appendix C, and the effective consolidation pressure, σ'_c obtained from Figure 7 are also included. These results will be discussed in a subsequent section.

4.4.2 Determination of c_e and ϕ_e by Method (2)

Table 6 shows the cell pressure, the effective consolidation pressure of the consolidated-undrained samples tested. The cell pressure, the effective consolidation pressure before reducing the cell pressure, and the reduced cell pressure of the samples tested according to Method (2), and used in conjunction with the consolidated-undrained samples in the determination of the shear strength parameters c_e and ϕ_e are also shown in the table.

Plots of the pore pressure and the corresponding effective consolidation stresses versus time, after

Table 6 Cell pressure and consolidation pressure of tests used in Method (2)

Batch	Test * number	Cell pressure* psi.	σ'_c * psi.	Test number	Cell pressure before reduction psi.	σ'_c psi	Cell pressure after reduction psi
1	101.1	30.0	12.2	103.1	40.0	14.8	25.0
	101.2	40.0	21.5	103.2	50.0	24.7	24.5
	101.3	60.0	41,1	103.3	70.0	41.6	40.9
1	102.1	40.0	21.4	103.2	40.0	24.7	24.5
	102.2	50.0	31.0	103.3	60.0	41.6	40.9
2	201.1	30.0	12.2	203.1	30.0	12.2	13.1
	201.2	40.0	21.5	203.2	40.0	21.3	23.0
	201.3	60.0	41.2	203.3	60.0	40.2	44.3
2	202.1	35.0	17.6	204.1	35.0	17.6	19.0
	202.2	50.0	31.5	204.2	50.0	31.2	33.7

* Consolidated-undrained tests.

reducing the cell pressure are shown in Figures D-1 through D-8 in Appendix .

Figures 13 to 15 shows the water content at failure, w_f, plotted against $1/2(\sigma'_1-\sigma'_3)$ and $1/2(\sigma'_1+\sigma'_3)$ obtained from Tables 3 and 4. Each figure shows the results of two corresponding samples, one tested according to the consolidated-undrained test technique, and the other according to Method (2). The values of the stresses at failure used in the determination of c_e & ϕ_e were taken from the figures at the average water content at failure of the two corresponding tests. For example, with reference to Table 4, for test 201.1, w_f=64.7% and for the corresponding test 203.1 w_f=66.1%. Hence the average water content at failure of the two tests = 65.4%. The corresponding values of $1/2(\sigma'_1-\sigma'_3)$ & $1/2(\sigma'_1+\sigma'_3)$ were used in Figures 16 to 18 to obtain Hvorslev's parameters, and are shown in Table 7.

In Table 7, some of the values of c_e and ϕ_e were negative. This could be due to experimental errors, such as the incomplete dissipation of the pore pressure after the release of the cell pressure.

Because of the discrepancy and insufficient data obtained from tests by Method (2), no specific conclusions should be drawn from the results obtained by

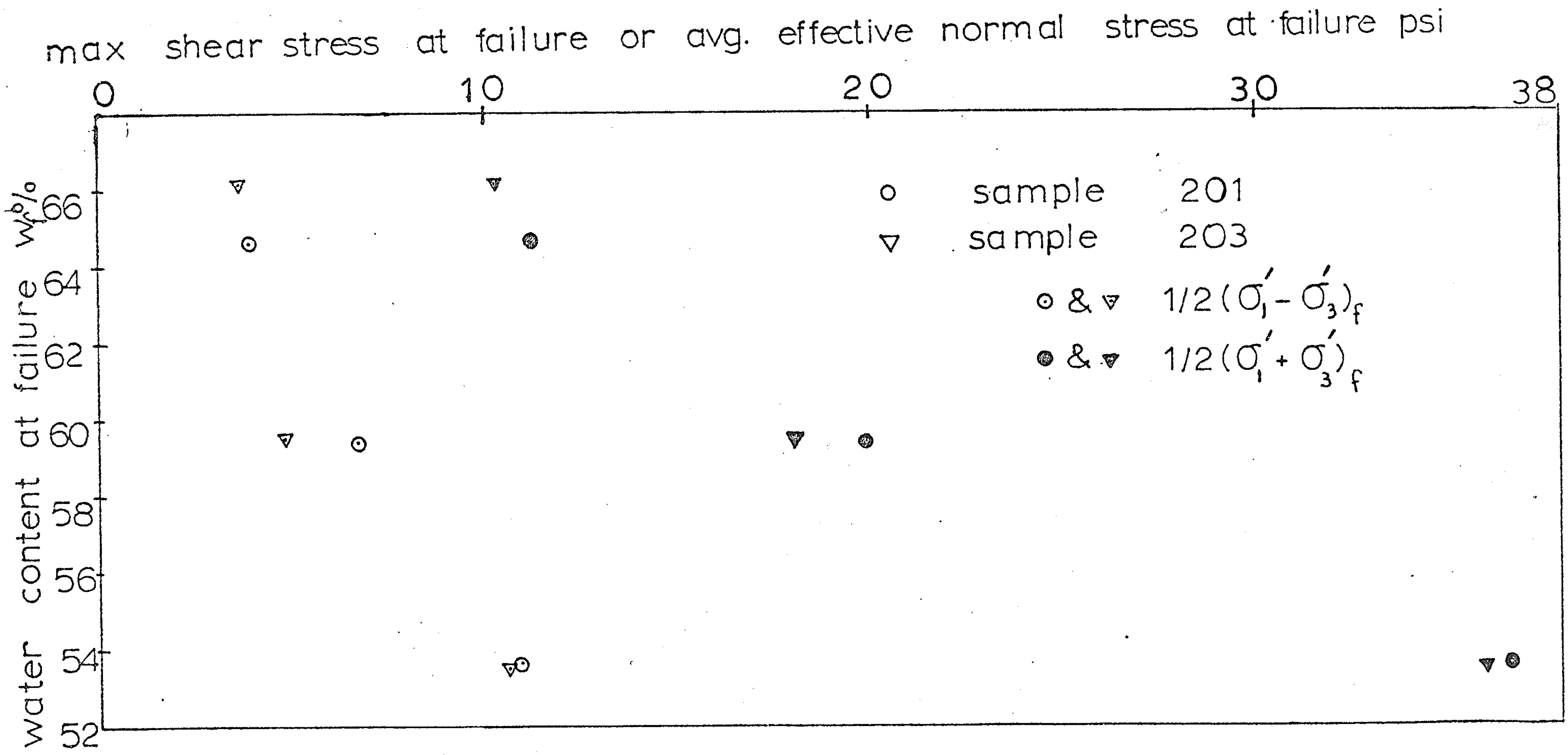

FIGURE 13 Water content at failure vs $1/2(\sigma_1' + \sigma_3')_f$ & $1/2(\sigma_1' - \sigma_3')_f$; Method (2); samples 201, 203

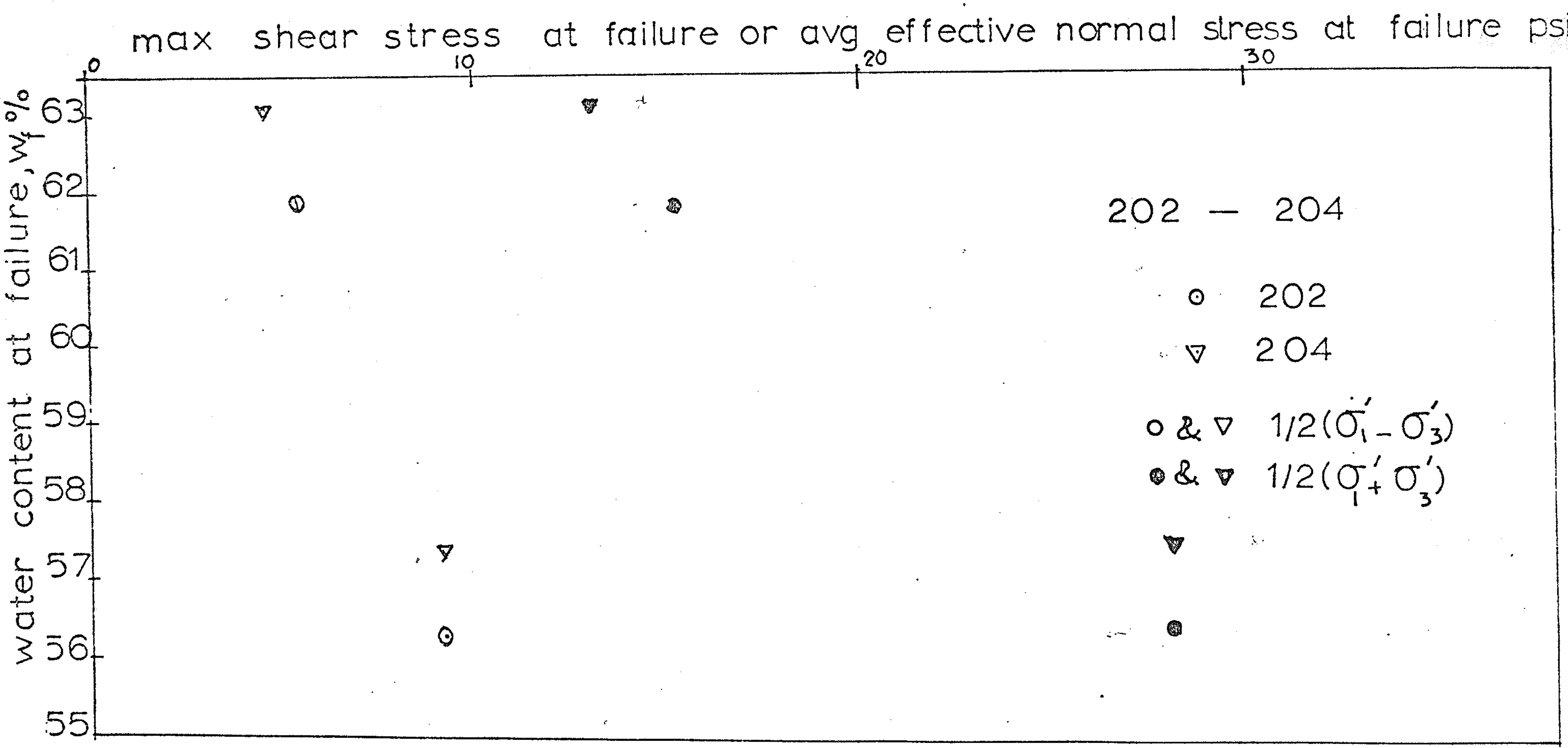

FIGURE 14 Water content at failure vs $1/2(\sigma_1' + \sigma_3')_f$ & $1/2(\sigma_1' - \sigma_3')_f$; Method (2) ; samples 202, 204 .

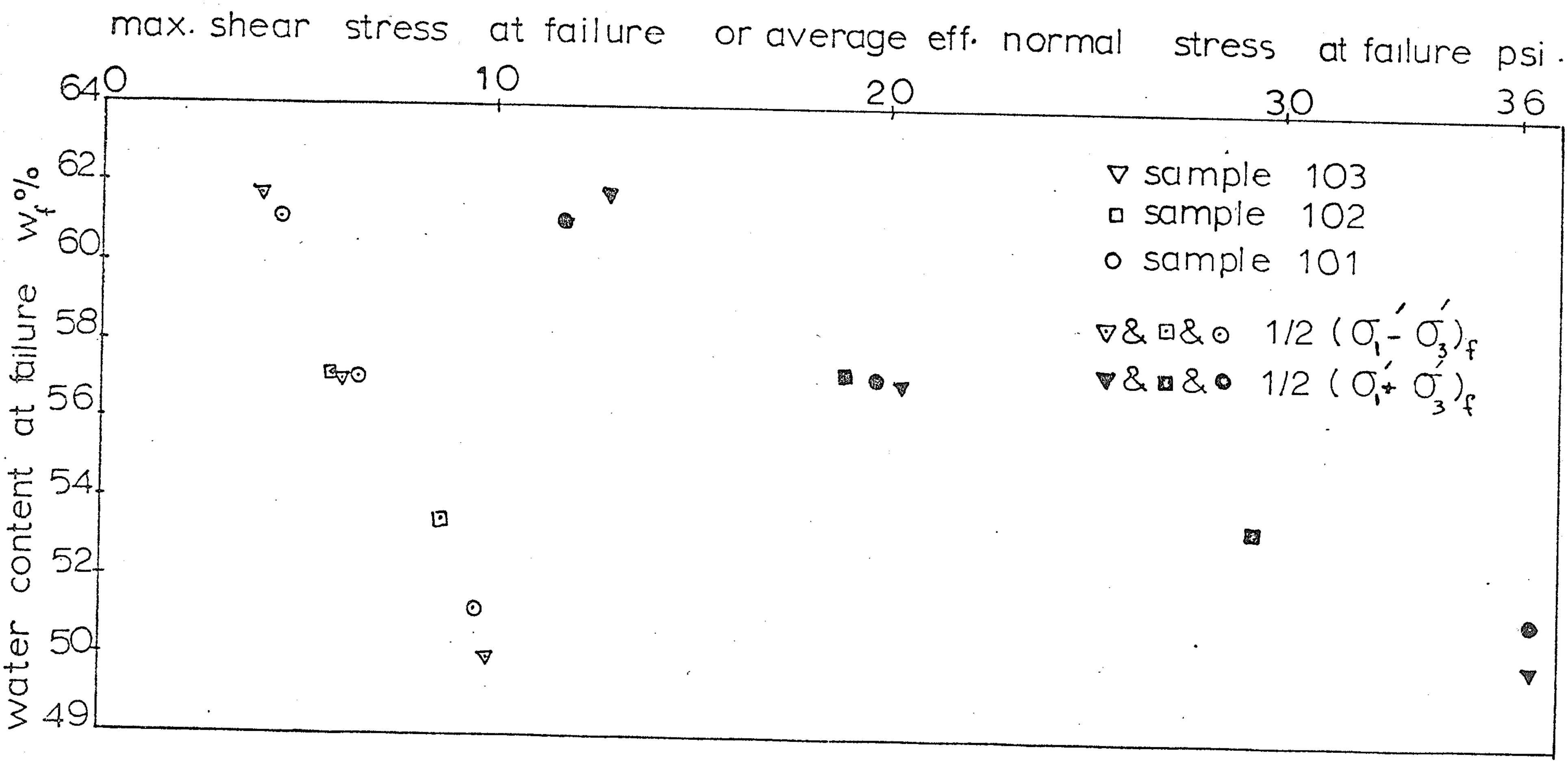

FIGURE 15. Water content at failure vs $1/2(\sigma_1' + \sigma_3')_f$ & $1/2(\sigma_1' - \sigma_3')_f$; Method (2); samples 101, 102, 103

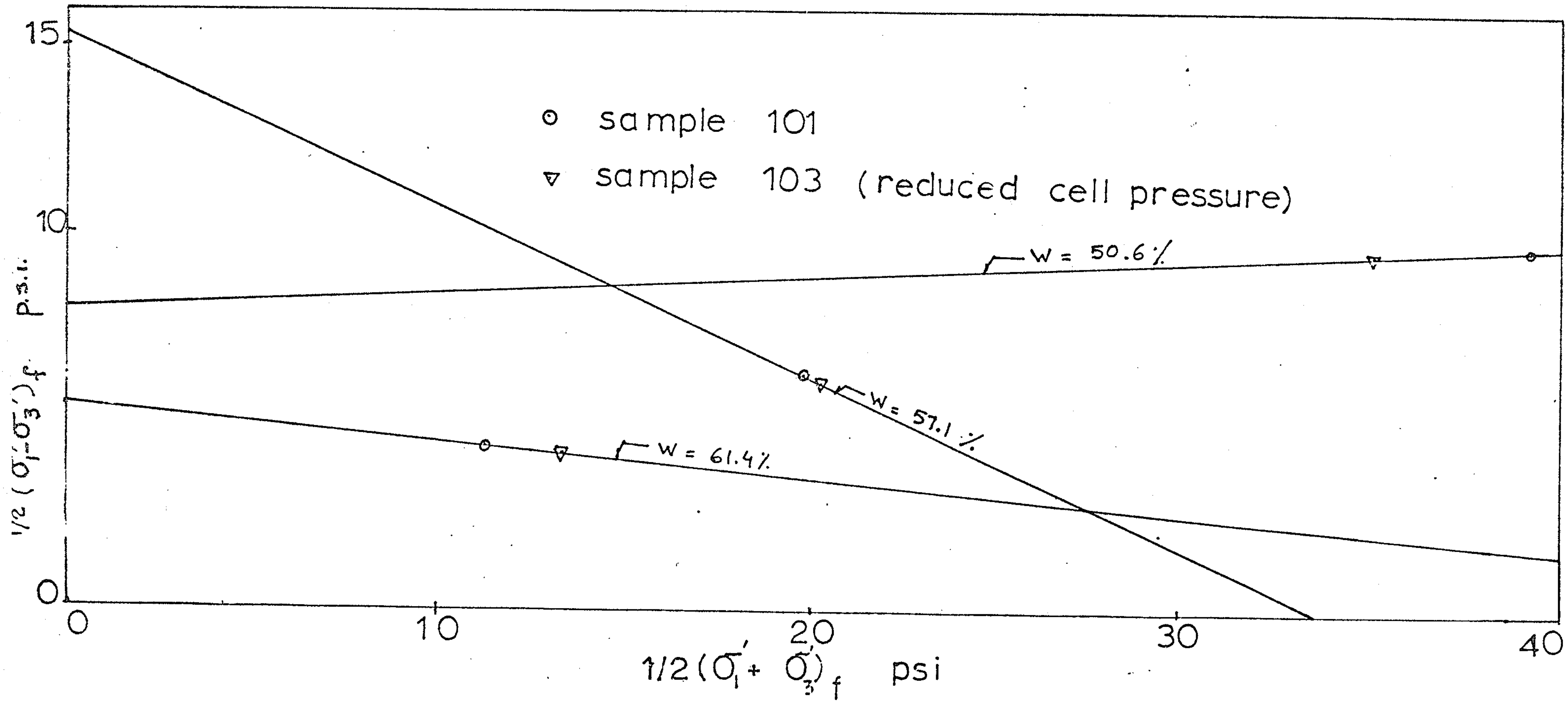

FIGURE 16 1/2 $(\sigma_1' + \sigma_3')_f$ vs 1/2 $(\sigma_1' - \sigma_3')_f$; Method (2); samples 101 , 103

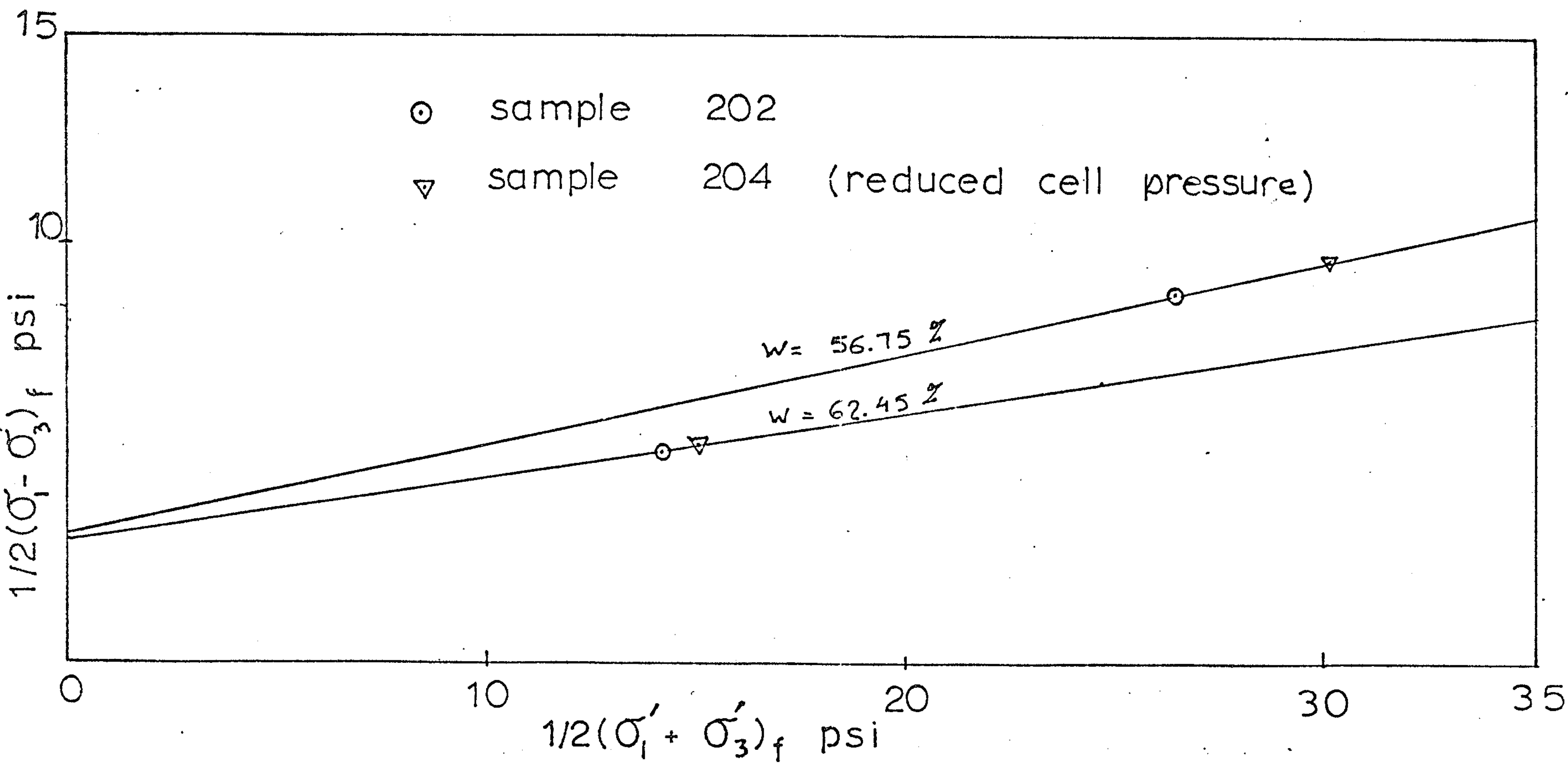

FIGURE 17 $1/2(\sigma_1' + \sigma_3')_f$ vs $1/2(\sigma_1' - \sigma_3')_f$; Method (2); samples 202 , 204

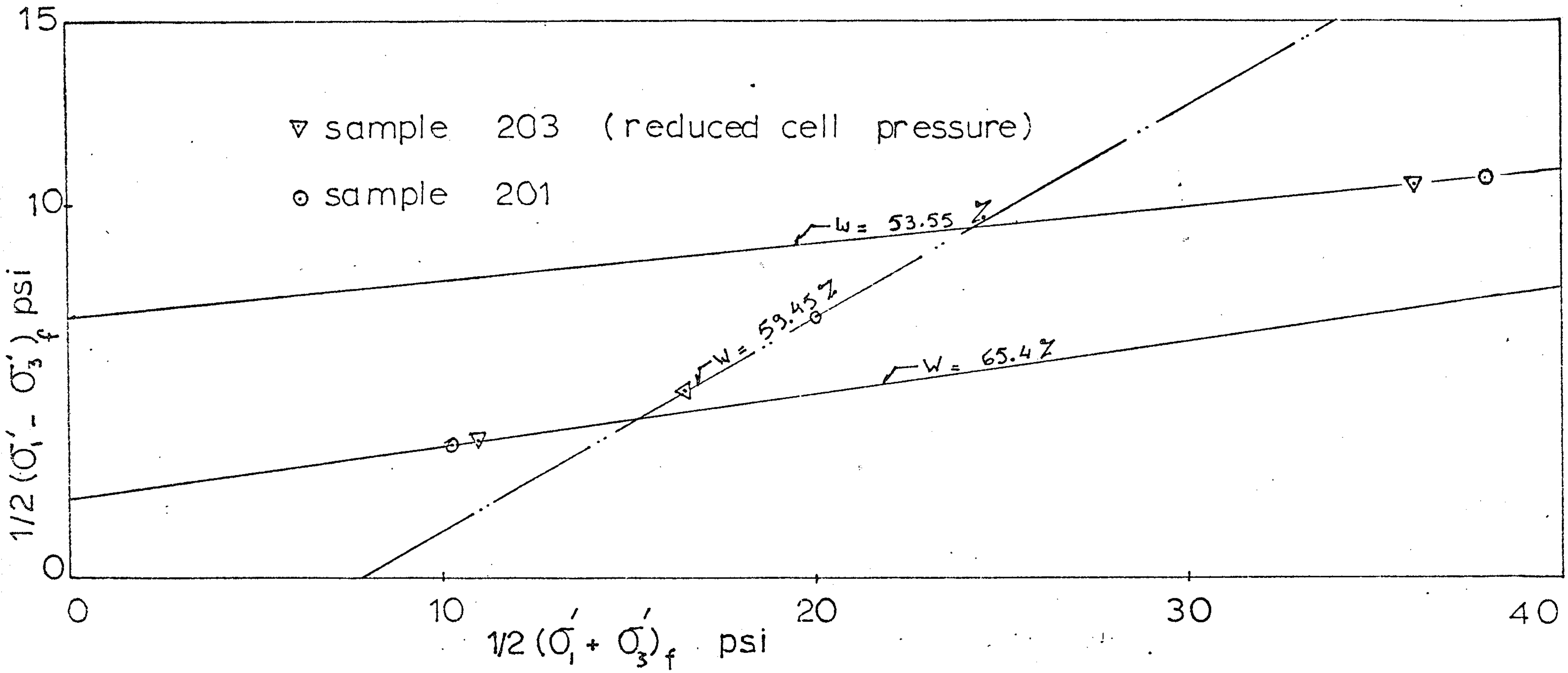

FIGURE 18 . $1/2(\sigma_1'+\sigma_3')_f$ vs. $1/2(\sigma_1'-\sigma_3')_f$; Method (2) ; samples 203 , 201

Table 7 Determination of c_e and ϕ_e by Method (2)

Batch	Test number	w_f %	σ'_c psi	$1/2(\sigma'_1-\sigma'_3)_f$ psi	$1/2(\sigma'_1+\sigma'_3)_f$ psi	σ'_{octf} psi	c_e psi	ϕ_e degree
1	101.1	61.4	12.2	4.40	11.30	7.60	5.40	-6.00
	103.1		14.8	4.20	13.30	10.00		
1	101.2	57.1	21.5	6.30	19.80	17.80	17.20	-24.0
	103.2		20.5	6.05	20.20	17.40		
1	102.1	57.0	21.4	5.89	19.20	16.93	2.00	12.3
	103.2		20.5	6.11	20.27	18.27		
1	101.3	50.6	41.1	9.80	39.20	34.40	8.05	2.5
	103.3		41.6	9.60	35.00	33.80		
2	201.1	65.4	12.2	3.60	10.30	9.10	2.12	8.1
	203.1		12.2	3.65	10.90	9.80		
2	202.1	62.4	17.6	5.10	14.20	12.40	2.94	8.6
	204.1		17.6	5.20	15.10	13.20		
2	201.2	59.4	21.5	6.80	19.90	17.70	-4.00	25.00
	203.2		21.3	4.90	18.10	16.50		
2	202.2	56.7	31.5	8.80	27.20	23.70	3.16	11.22
	204.2		31.2	9.60	30.20	26.10		

this method. In the subsequent section, only the positive values of c_e and ϕ_e will be used in comparison of the results obtained by Methods (1) and (2).

4.2.3. Comparison of values of c_e and ϕ_e obtained by Method (1) and (2)

Values of c_e obtained by Methods (1) and (2) as summarized respectively in Tables 5 and 7 are presented in Figures 19 ,20 and 21. The logarithm of c_e and (c_e) was plotted against the water content at failure, w_f , in Figure 19, against the logarithm of σ'_c in Figure 20, and against the octahedral normal stress at failure, $(\sigma_{oct})_f$ in Figure 21. From these figures, the following relationships can be derived :

For Method (1)

$$c_e = e^{11.0(0.655 - w_f)} \quad \text{..................(20)}$$

$$c_e = 0.11\ (\sigma'_c\ )^{0.98} \quad \text{..................(21)}$$

$$c_e = 0.135(\sigma'_{oct})_f^{0.975} \quad \text{..................(22)}$$

and for Method (2)

$$c_e = e^{11.0(0.73\ -\ w_f)} \quad \text{..................(23)}$$

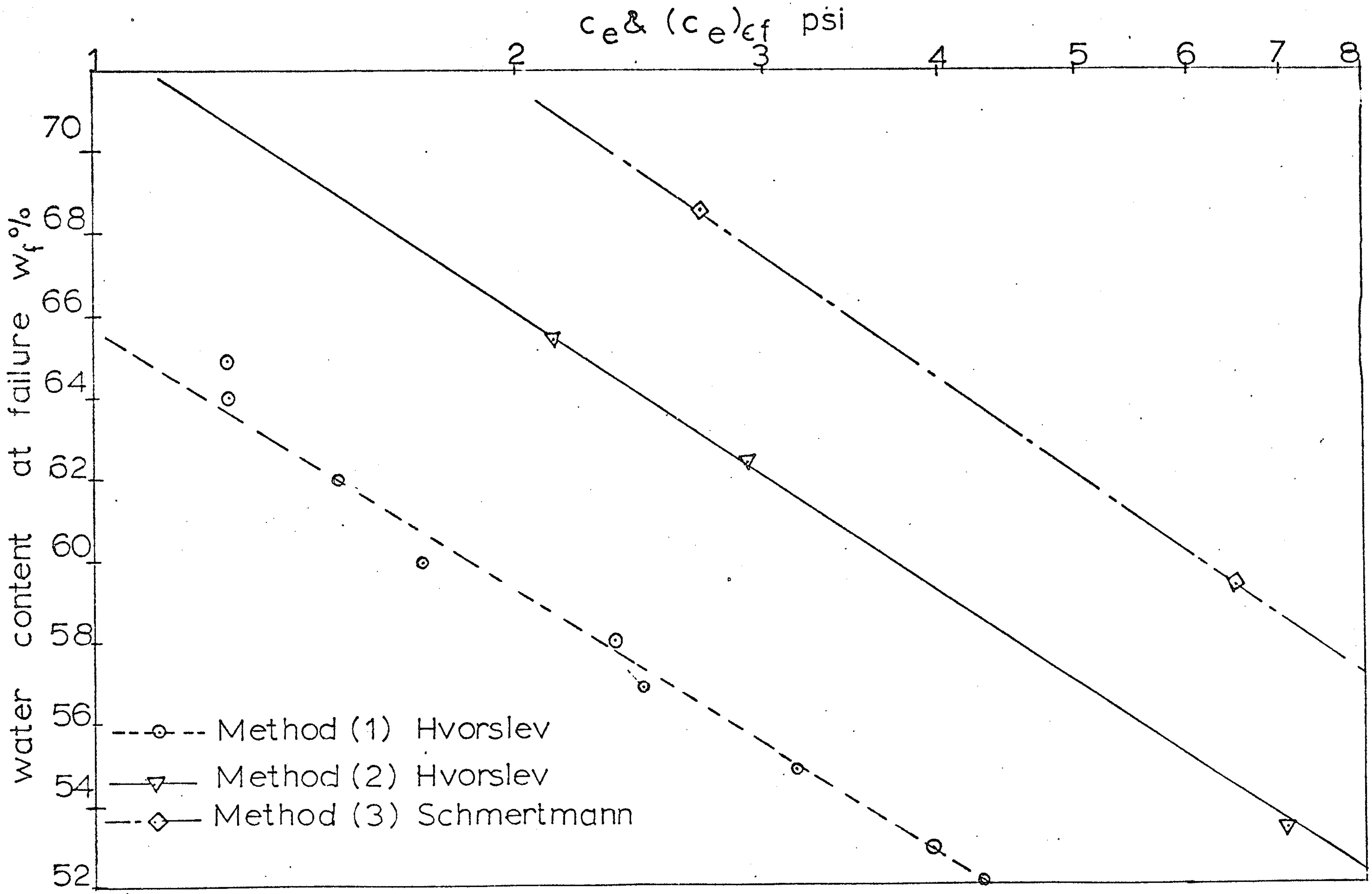

FIGURE 19 water content at failure versus c_e & $(c_e)_\epsilon$

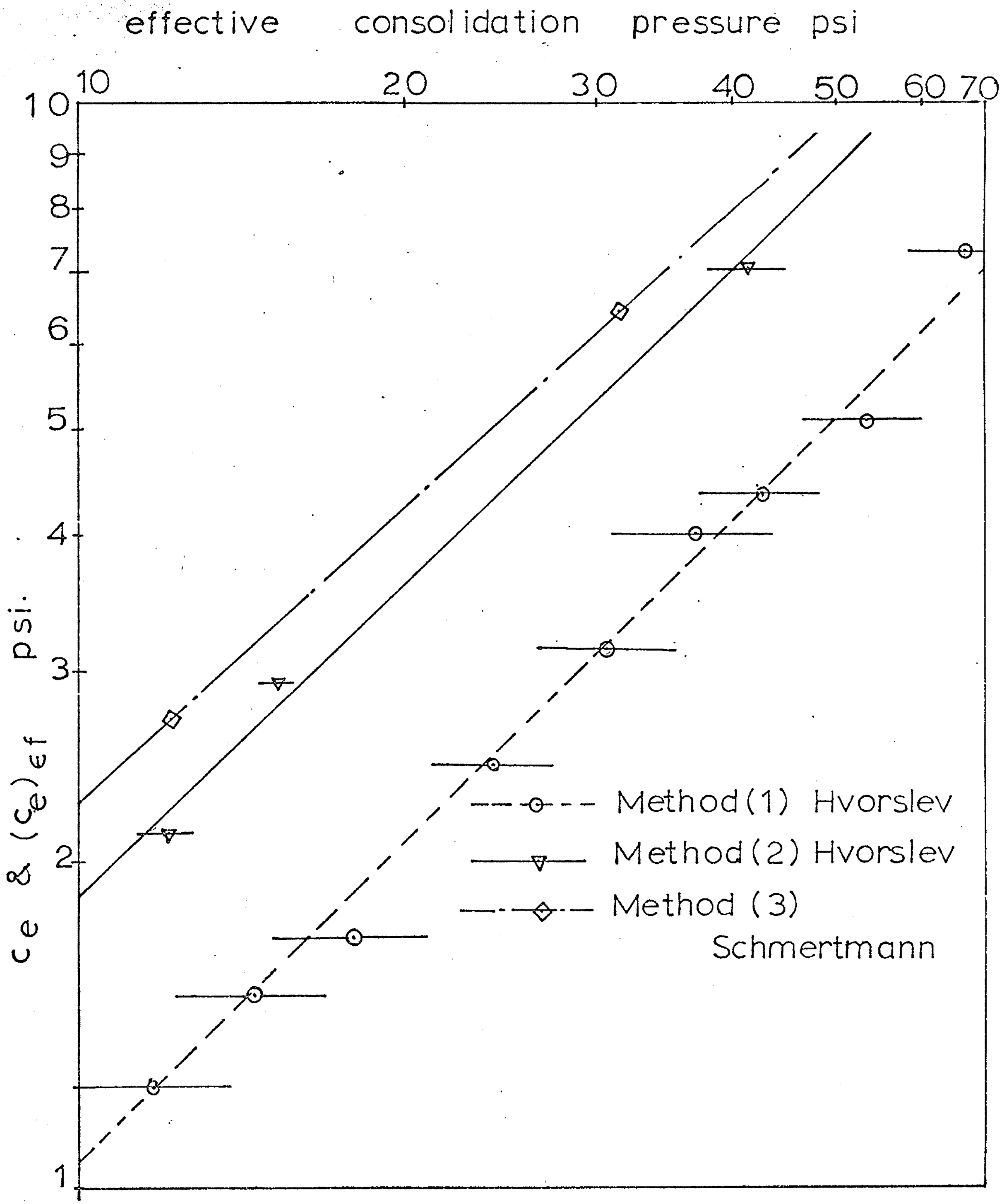

FIGURE 20 c_e & $(c_e)_{\epsilon f}$ vs. Effective consolidation pressure

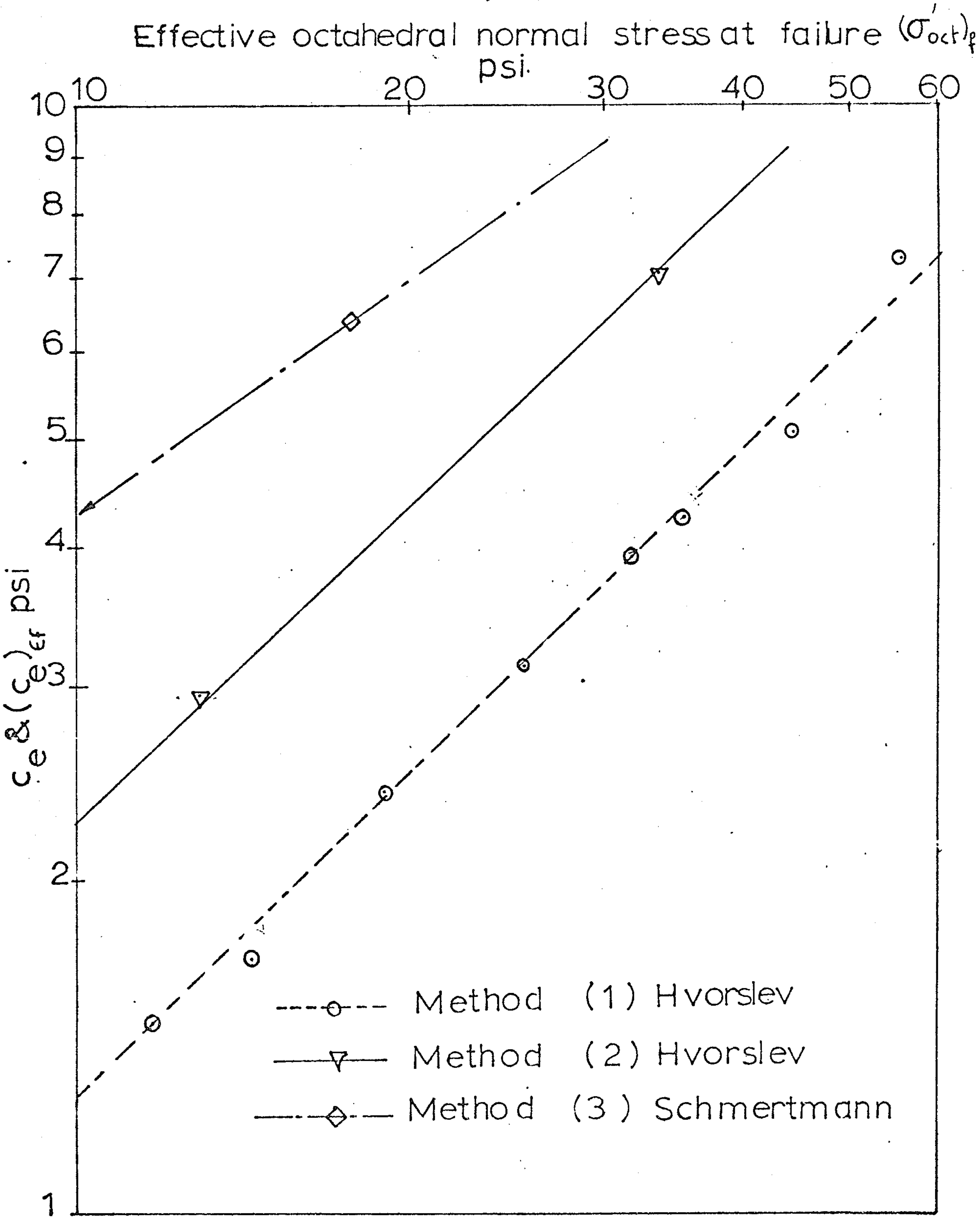

FIGURE 21 c_e & (c_e) versus effective octahedral normal stress at failure

$$c_e = 0.203((\sigma'_c)^{0.96} \quad \ldots\ldots\ldots\ldots\ldots\ldots(24)$$

$$c_e = 0.247\ (\sigma'_{oct})_f^{0.96} \quad \ldots\ldots\ldots\ldots\ldots\ldots(25)$$

where:

c_e is the effective cohesion,

σ'_c is the effective consolidation pressure,

σ'_{octf} is the effective octahedral normal stress at failure.

It can be seen from these equations that c_e is related to the water content at failure, w_f, or the effective consolidation pressure, σ'_c, as well as to the effective octahedral normal stress at failure, σ'_{octf}. The relationships obtained by Method (1) take the same functional forms as those obtained by Method (2). It appears, therefore, that the stress history plays an important role in the determination of c_e for the remoulded Winnipeg clay.

Contrary to Hvorslev assumption, ϕ_e was found to vary with w_f or σ'_c by Method (1). In Figure 22 where ϕ_e was plotted against the logarithm of $(\sigma'_{oct})_f$, ϕ_e appeared to vary linearly with the logarithm of $(\sigma'_{oct})_f$ for Method (1). No conclusion can be drawn regarding the results obtained by Method (2) because of the short-comings of the test procedure which yielded negative

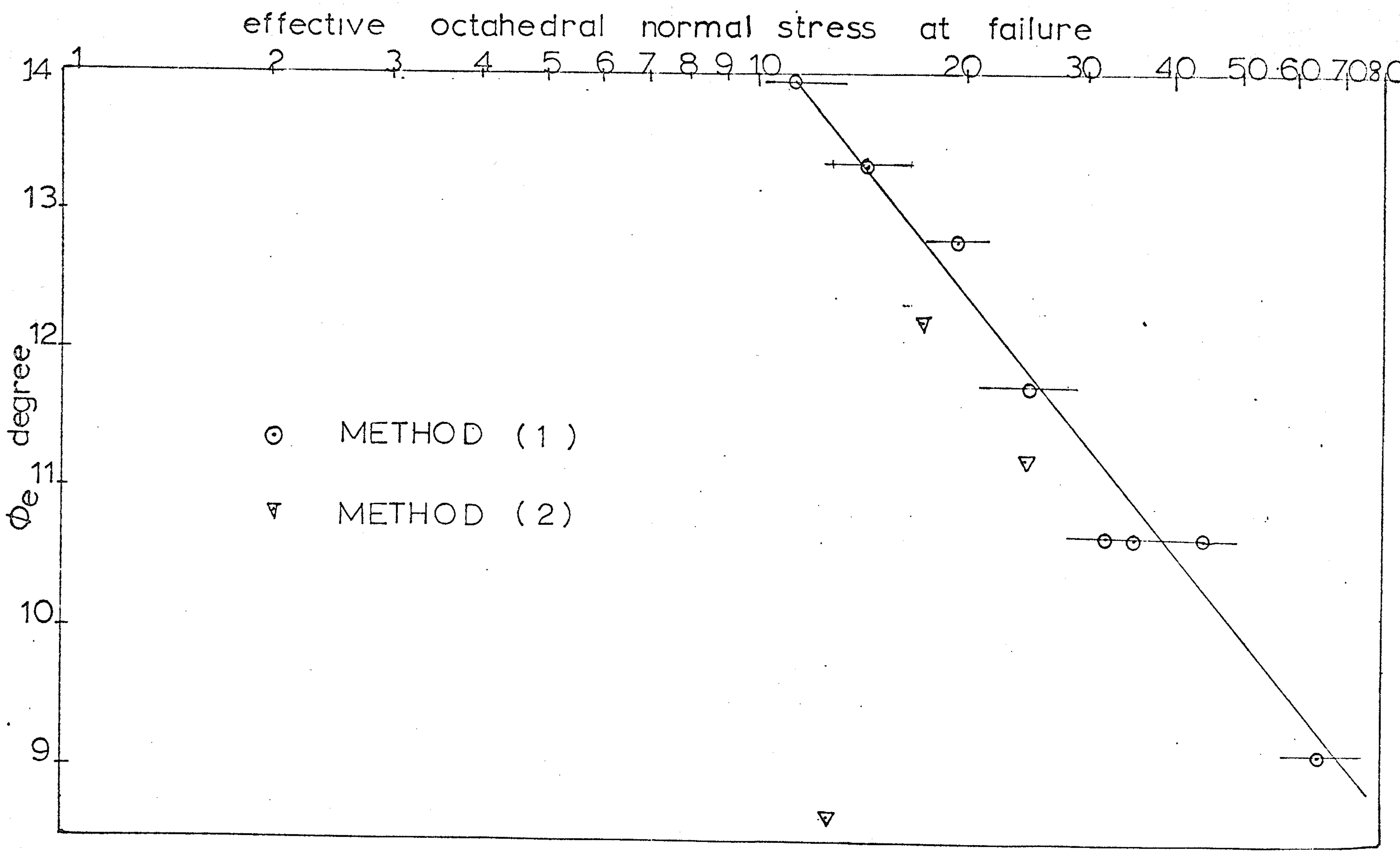

FIGURE 22 ϕ_e vs effective octahedral normal stress at failure values of c_e and ϕ_e in some instances. In Figure 23, where ϕ_e was plotted against the logarithm of σ'_e, a straight line was obtained for Method (1). It appears that ϕ_e may be related to the water content at failure, w_f, to the effective consolidation pressure, σ'_c, to the effective octahedral normal stress at failure, σ'_{octf}, and stress history. The data obtained in the present investigation were insufficient to draw any conclusion with respect to the factors that could influence ϕ_e. Much more research is needed before any strong assertion can be made.

4.3 Schmertmann's Parameters

Test data for samples 301 are shown in Figure A-32 A-33 and A-34 in Appendix A. It can be seen from these figures that the volume change resulting from curve hopping in order to maintain two different stress levels of σ'_1 during the test was less than 1 cc. The effect of this small volume change on the interpretation of results is not known since the clay used is of swelling character. Results are shown in Figures 24 and 25, where (c_e) and (ϕ_e) were plotted against the axial strain. It may be observed from the figures that despite the

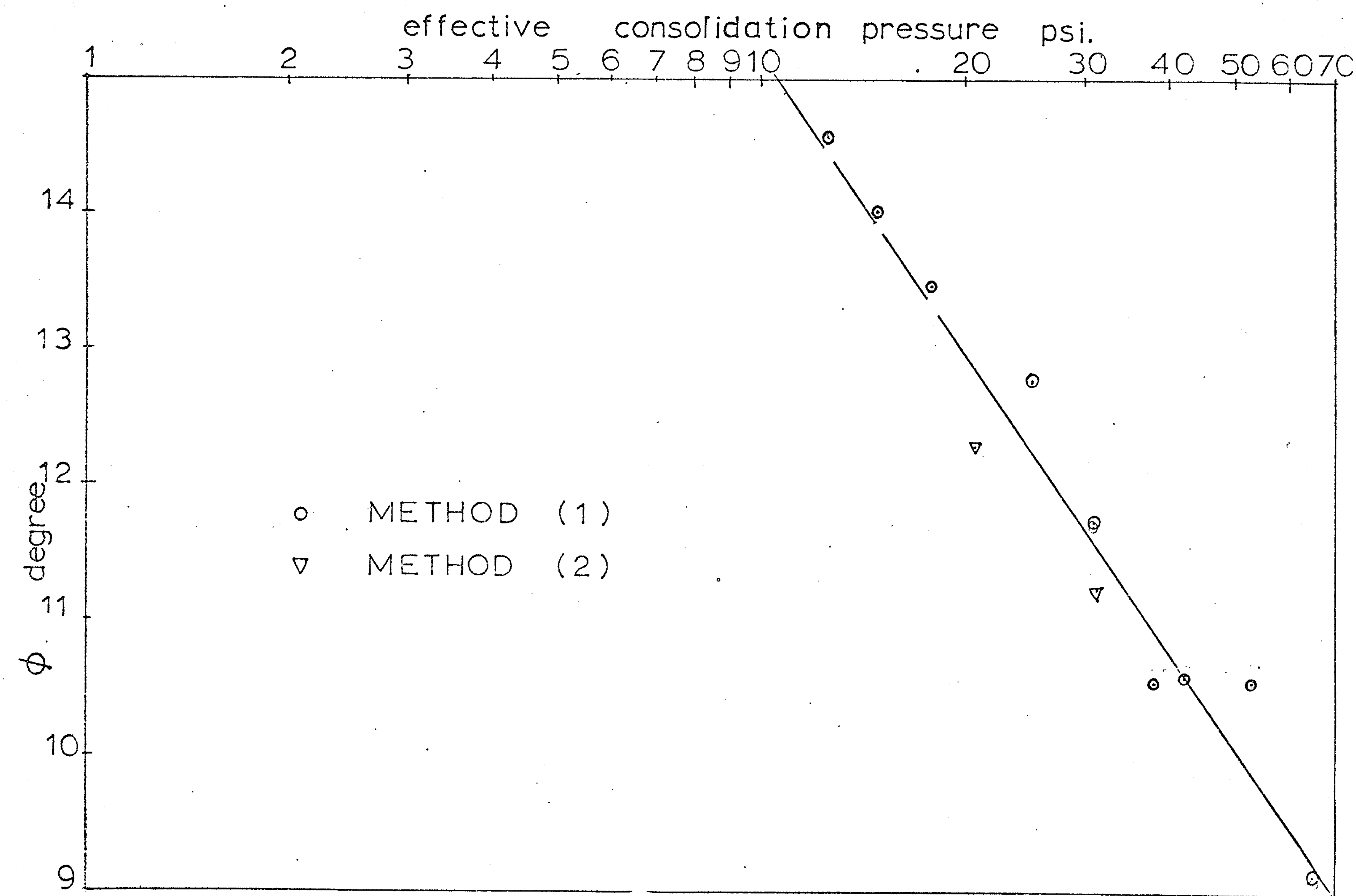

FIGURE 23 ϕ_e versus effective consolidation pressure

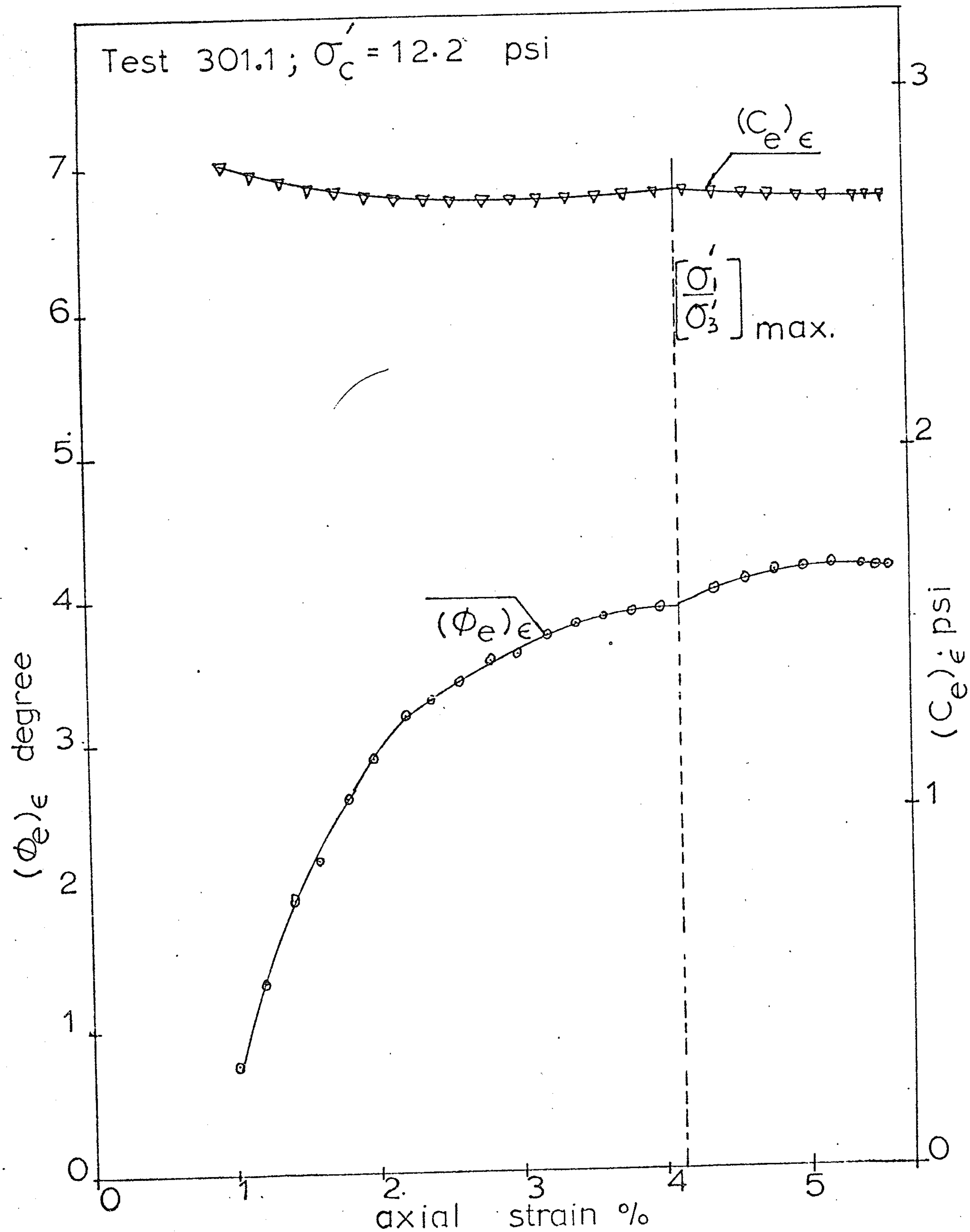

FIGURE 24 Schmertmann parameters

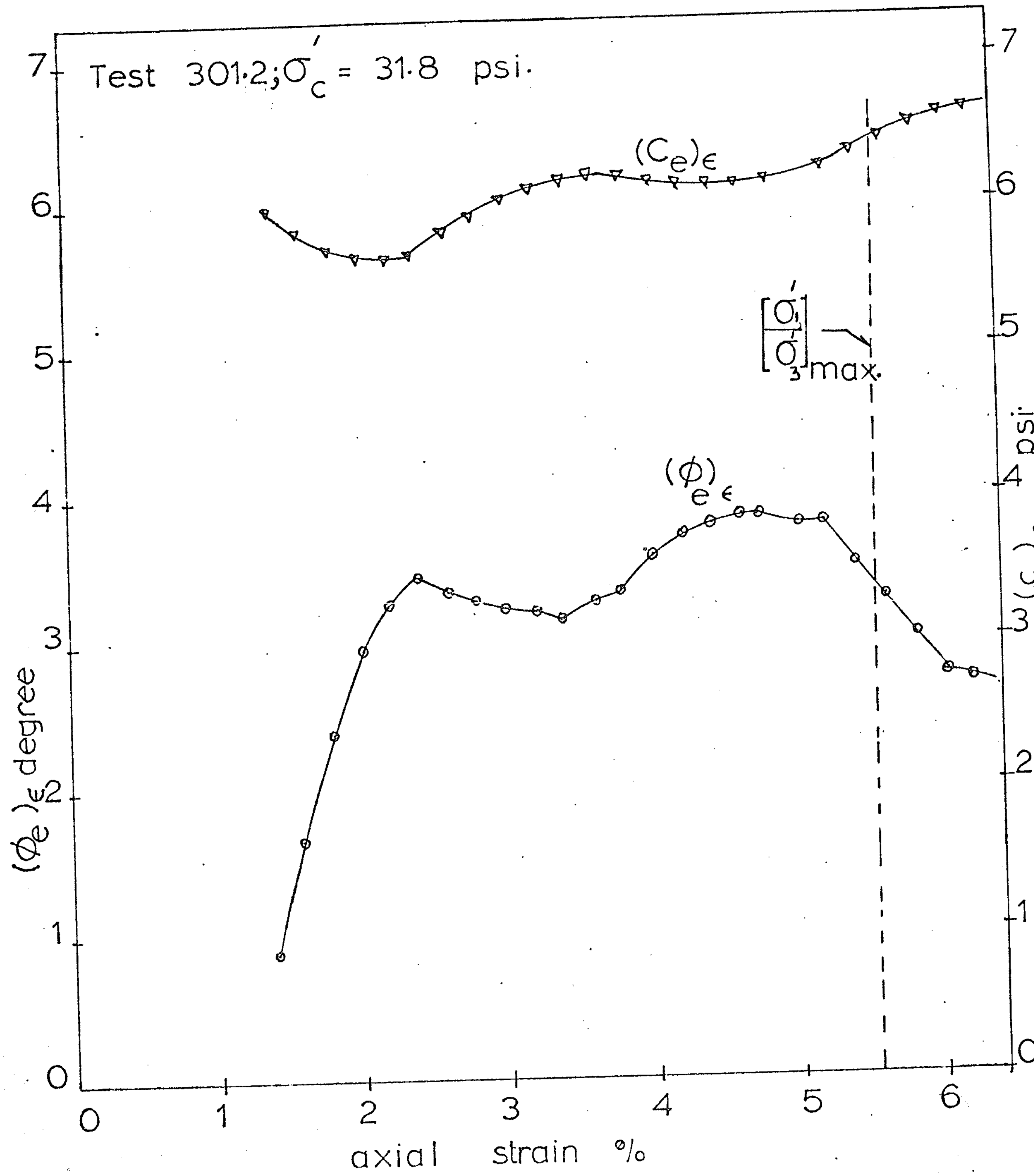

FIGURE 25 Schmertmann parameters

scatter due to extrapolation of results, there was little variation in (c_e), whereas (ϕ_e) increased with increasing values of strain ϵ. Furthermore (c_e) appeared to be affected by the effective consolidation pressure, σ'_c, or the water content at failure, w_f, while (ϕ_e) was virtually independent of the effective consolidation pressure, σ'_c, or the water content at failure, w_f.

4.4 Comparison of Hvorslev and Schmertmann Parameters

For comparison, results of (c_e), (ϕ_e) at failure obtained by Method (3) are presented in Figures 20, 21 and 22. From these figures, the following relationship can be obtained:

$$(c_e) = e^{11.0(0.787 - w_f)} \quad \ldots\ldots\ldots\ldots\ldots (26)$$

$$(c_e) = 0.267\ (\sigma'_c)^{0.925} \quad \ldots\ldots\ldots\ldots\ldots (27)$$

$$(c_e) = 0.86\ (\sigma'_{oct})_f^{0.70} \quad \ldots\ldots\ldots\ldots\ldots (28)$$

The functional forms of these equations are seen to be the same as those of equations (20), (21) and (22) or (23), (24) and (25) obtained by Method (1) or Method (2). Apart from the difference in testing procedures of the methods, a small volume change occured in the IDS tests of Method (3). It appears that (c_e) may be influenced by drainage conditions during tests, although the data was insufficient to explain why such a relatively small change could have affected (c_e). It is significant, however, that both c_e and (c_e) relate to the water content at failure, w_f, to the effective consolidation pressure σ'_c or to the effective octahedral normal stress at failure, σ'_{octf} in similar functional form.

It may be noted from Figure 12 and from the other values of Hvorslev's or Schmertmann's parameters that the value of ϕ' was always higher than that of ϕ_e or (ϕ_e). Although commonly used in practical work because of the relative simplicity, the conventional strength parameters c' and ϕ' are unable to explain the fundamental nature of shear strength of clays.

CONCLUSIONS

The conclusions summarized below reflect the findings of this investigation and are limited to the soil used,the methods of sample preparation and the testing procedure employed :

1-Hvorslev's or Schmertmann's (c_e) is exponentially related to :the water content at failure,the effective consolidation pressure,and the effective octahedral normal stress at failure. c_e appears to be stress history dependent.

2-Hvorslev's ϕ_e is not constant but appears to vary with the water content at failure,the effective consolidation pressure and the effective octahedral normal stress at failure.

3-Schmertmann's (ϕ_e) at failure,however is virtually independent of water content at failure or effective consolidation pressure. Much more research is needed before any assertion can be made with respect to the nature of these parameters.

REFERENCES

1. Bishop, A.W.& Henkel, D.J. (1957) " The measurement of soil properties in the triaxial test". Edward Arnold Ltd. London.

2. Bjerrum, L. (1954) " Theoretical and experimental investigations on the shear strength of soil ". Norwegian Geotechnical Institute. Publication # 5, Oslo.

3. Hvorslev, M.J., (1960) " Physical components of the shear strength of saturated clays ". Research conference of shear strength of cohesive soils (A.S.C.E.), Boulder, Colorado, pp.169-273.

4. Kenney, T.C. & Watson, G.H. (1961) " Multiple stage triaxial test for determining c' & Ø' of saturated soils" Proceding of the Fifth International conference on Soil Mechanics and Foundation Engineering, Paris.

5. Kenney, T.C. (1967) " Shear strength of soft clay". Proceeding of the Geotechnical Conference, Oslo, Volume 2, pp. 45-59.

6. Lambe, T.W. (1960) " A mechanistic picture of shear strength of clays ". Research conference of shear strength

of cohesive soil (A.S.C.E.) Boulder,Colorado,pp.550-580.

7. Noorany,I.& Seed,B. (1965) " A new experimental method for the determination of Hvorslev strength parameters for sensitive clays ".Proceeding of the sixth international conference on Soil Mechanics and Foundation Engineering, Canada,Volume 1,pp.318-322.

8. Schmertmann,H.J.& Osterberg J. (1960) " An experimental study of the development of cohesion and friction with axial strain in saturated cohesive soils ".Research conference of shear strength of cohesive soils (A.S.C.E.) Boulder,Colorado,pp. 643-694.

9. Schmertmann H.J.(1962) " Comparison of one and two specimen CFS tests" .Journal of the Soil Mechanics and Foundation division,ASCE,Vol.88,No SM 6,December 1962. pp.169-205.

10. Schmertmann,H.J. (1963) "Generalizing and measuring the Hvorslev effective components of shear resistance". Laboratory shear testing of soils,A.S.T.M. Special technical publication # 361.pp. 147-157.

11. Terzaghi,K.(1938) " Die Coulobshe gleinchung für den scherwiderstrand bindiger böden ".Bautechnik Vol.16,pp. 343-346.

12. Whitman, V.R. (1960) " Some considerations and data regarding the shear strength of clay ". Research conference of shear strength of cohesive soils (A.S.C.E.), Boulder, Colorado, pp.581-614.

13. Wu, T.H., Douglas, A.G. & Goughnour R.D. (1962), " Friction and cohesion of saturated clays ". Journal of the Soil Mechanics and Foundation Division, ASCE, Vol. 88, No SM 3, June 1962, pp.1-32.

VIII NOTATIONS

a intecept on the $1/2(\sigma_1' - \sigma_3')$ axis.

$\bar{A}_f$ Skempton pore pressure parameter at failure.

α angle between plane of failure and major principal stress.

b intercept on the σ_1' axis.

$(b_n)_\epsilon$ bond strength at strain ϵ

β angle of inclination of the common straight line drawn through the top points of the Mohr circle at failure.

c cohesion

c' effective cohesion.

c_e Hvorslev's effective cohesion parameter.

$(c_e)_\epsilon$ Schmertmann's effective cohesion parameter, at axial strain ϵ.

c_o initial cohesion.

c_c compression index.

D_ϵ mobilized component of shearing resistance independent of effective stress at a given strain on a given plane

e void ratio.

f subscript indicating failure.

G specific gravity of soil solids.

I_ϵ mobilized component of shearing resistance depending on effective stress at a given strain on a given plane.

K coefficient of cohesion.

K' coefficient of cohesion for clays remoulded at low water content.

ϕ angle of friction.

ϕ' angle of shearing resistance based on effective stress.

ϕ_e effective angle of friction

$(\phi_e)_\epsilon$ Schmertmann's angle of friction at axial strain ϵ.

σ_n total normal stress on the plane of failure.

σ'_n effective normal stress on the plane of failure.

σ_e equivalent consolidation pressure.

σ'_{ci} effective consolidation pressure before reducing the cell pressure.

σ'_{ca} effective consolidation pressure after reducing the cell pressure.

σ'_1 effective major principal stress.

σ'_3 effective minor principal stress.

σ'_{oct} effective octahedral normal stress = $1/3\ (\sigma'_1 + 2\sigma'_3)$

s shear strength at failure on the failure plane.

s_ϵ total shearing resistance mobilized at a given strain on a given plane.

S degree of saturation.

u pore water pressure.

Δu pore water pressure change .

w water content.

APPENDICES

Appendix A

Stress -pore pressure-volume change versus strain datas.

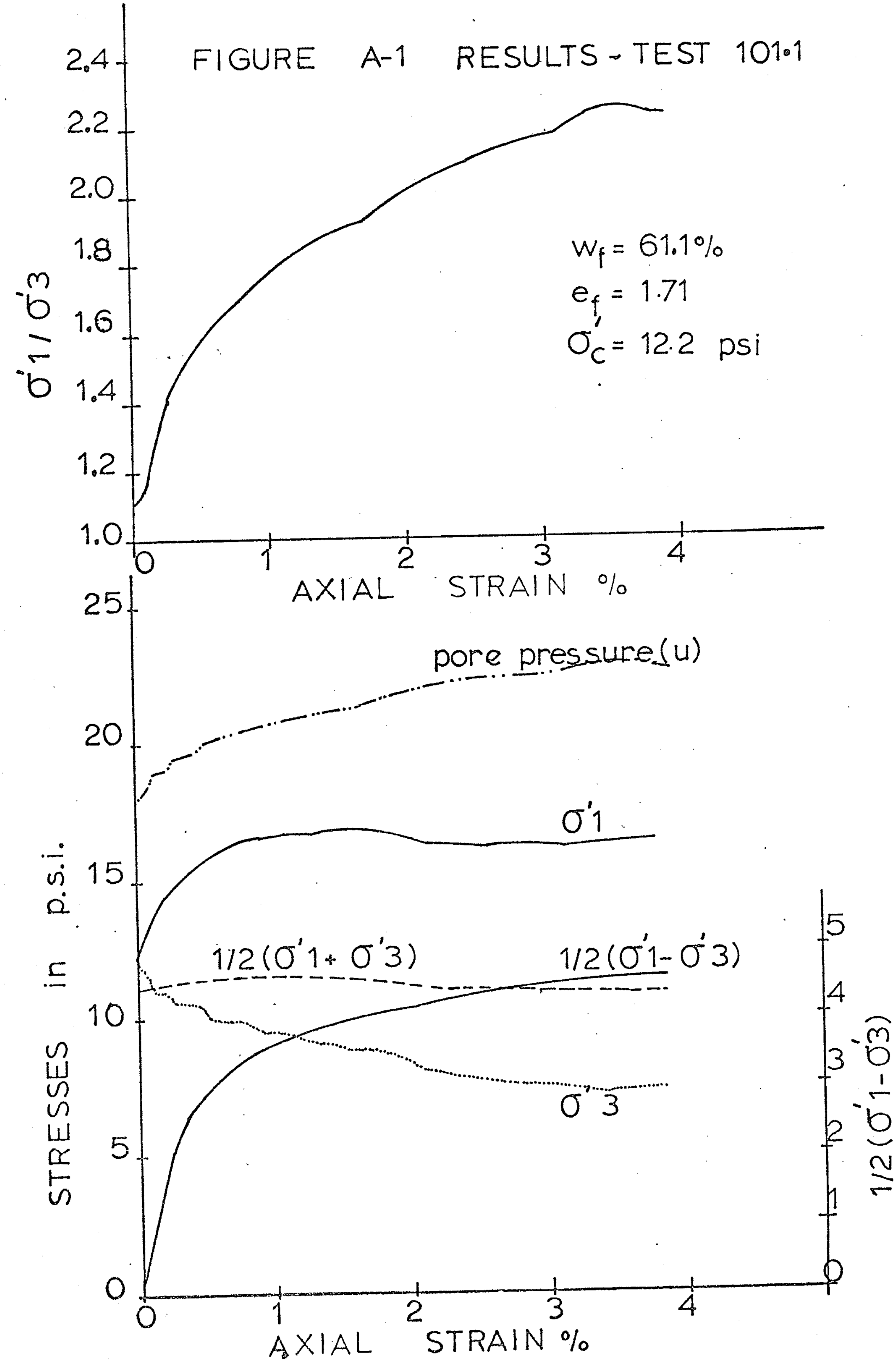
FIGURE A-1 RESULTS - TEST 101.1
W_f = 61.1%
e_f = 1.71
σ'_c = 12.2 psi
$\sigma'1 / \sigma'3$
2.4
2.2
2.0
1.8
1.6
1.4
1.2
1.0
0
1
2
3
4
AXIAL STRAIN %
25
20
15
10
5
0
pore pressure (u)
$\sigma'1$
1/2($\sigma'1$ + $\sigma'3$)
1/2($\sigma'1$ - $\sigma'3$)
$\sigma'3$
STRESSES in p.s.i.
1/2($\sigma'1$-$\sigma'3$)
AXIAL STRAIN %

FIGURE A-2 RESULTS - TEST 101.2

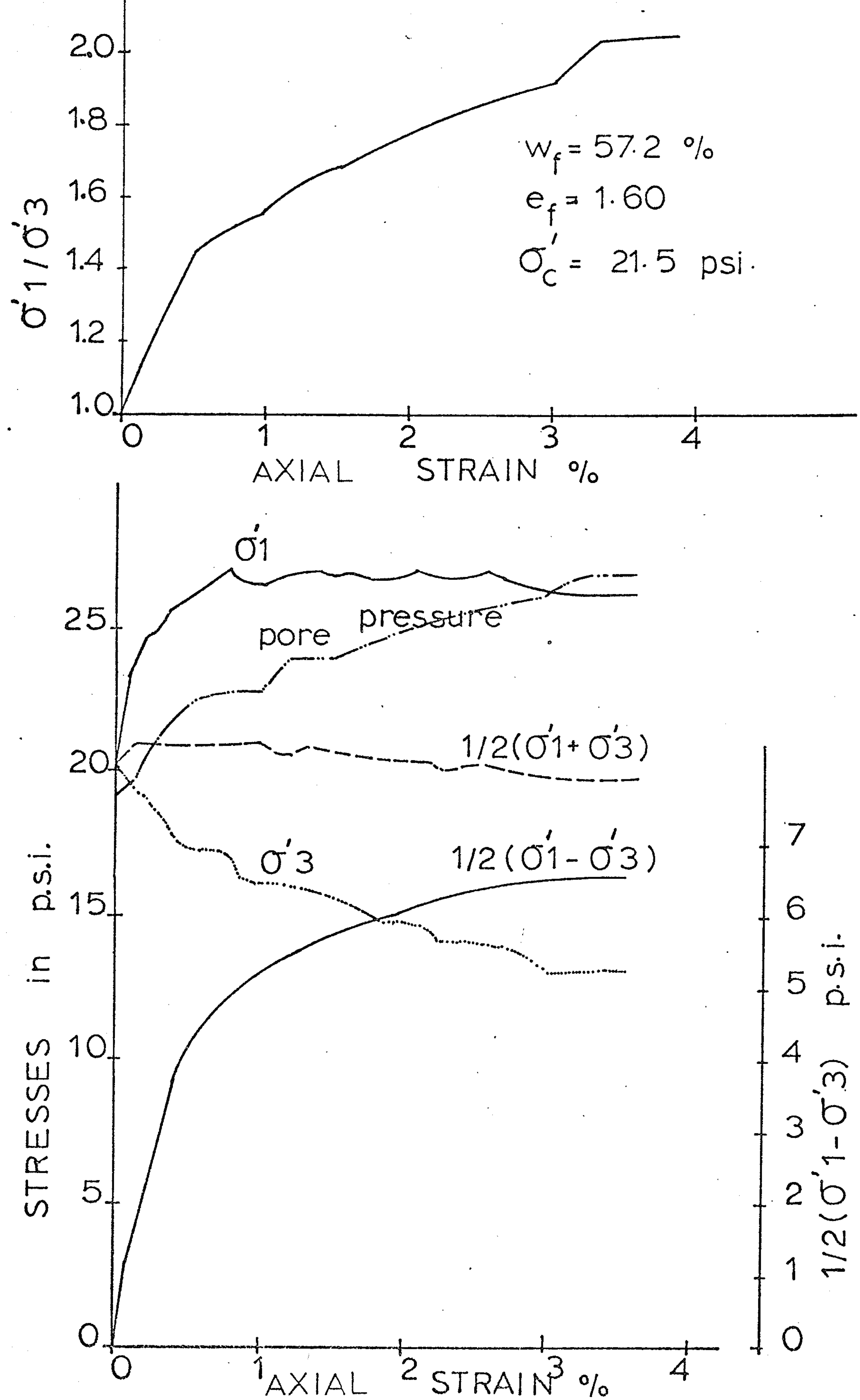

FIGURE A-3 RESULTS - TEST 101.3

$w_f = 51.2\%$ $e_f = 1.44$ $\sigma_c' = 411$ psi

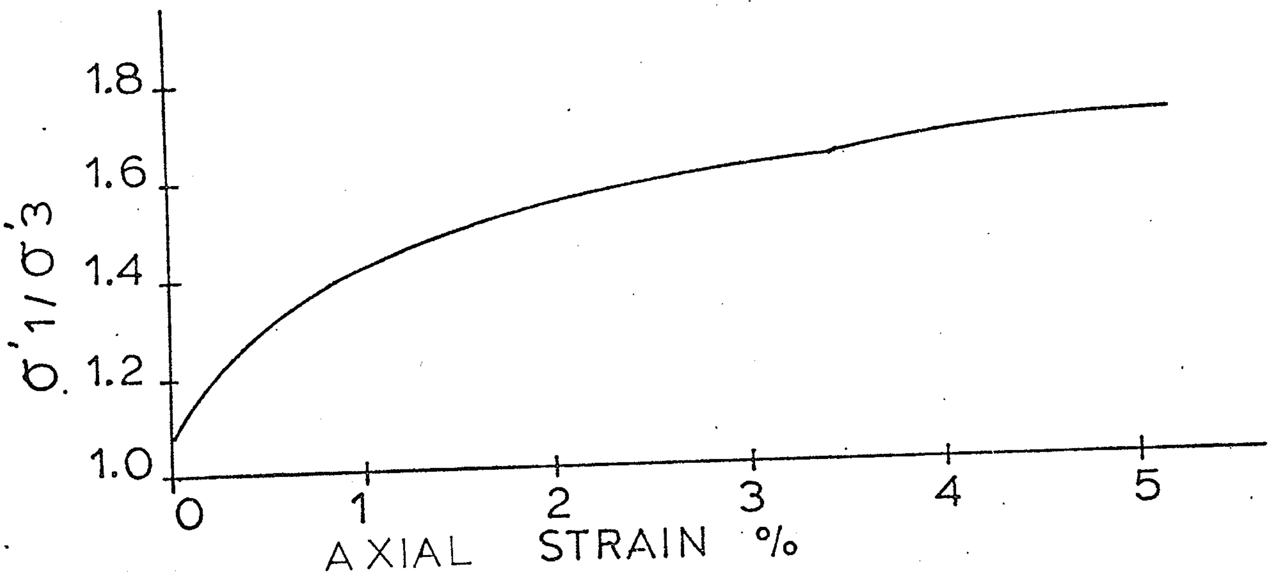

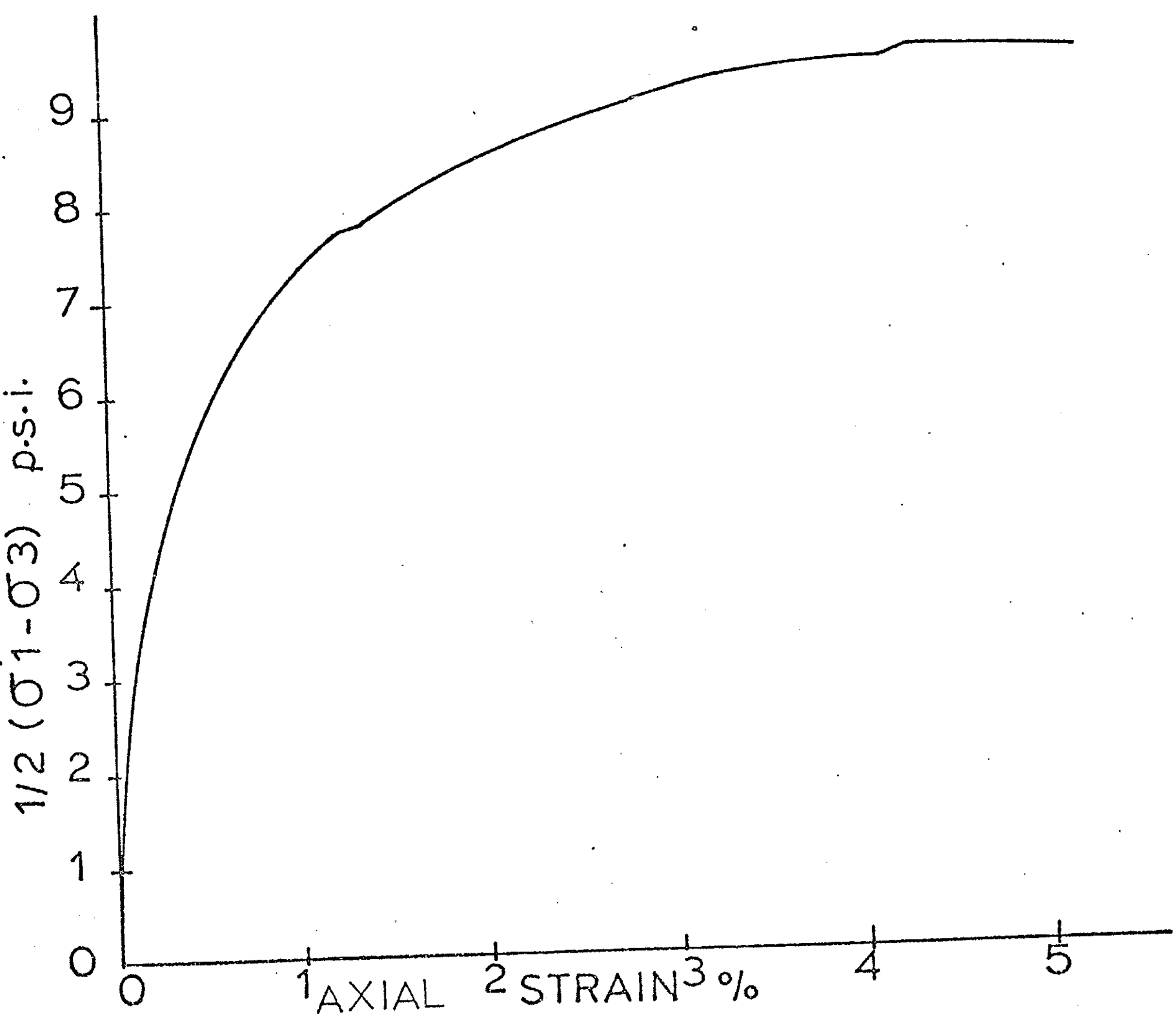

FIGURE A-4 RESULTS - TEST 101-3

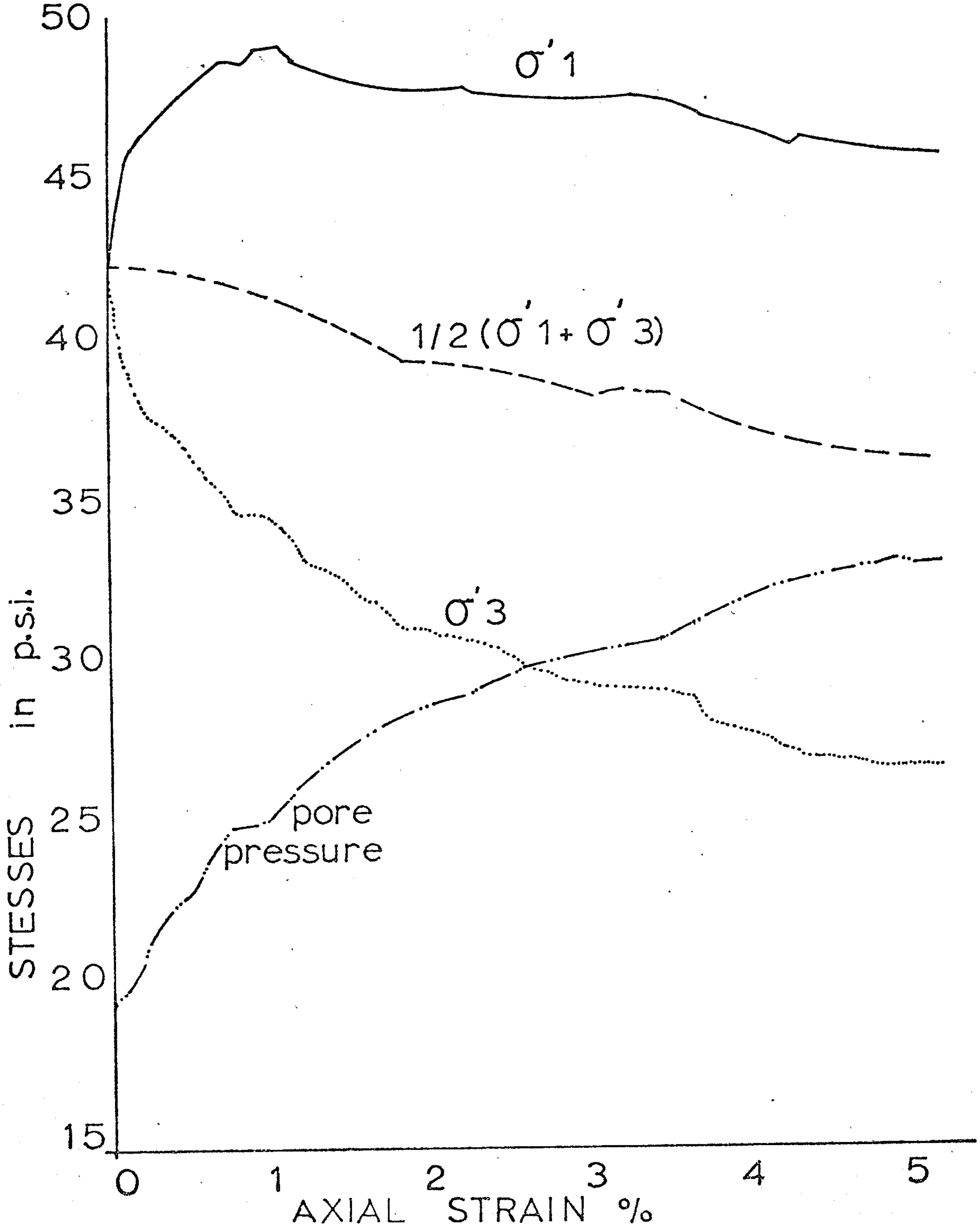

FIGURE A-5 RESULTS - TEST 102.1

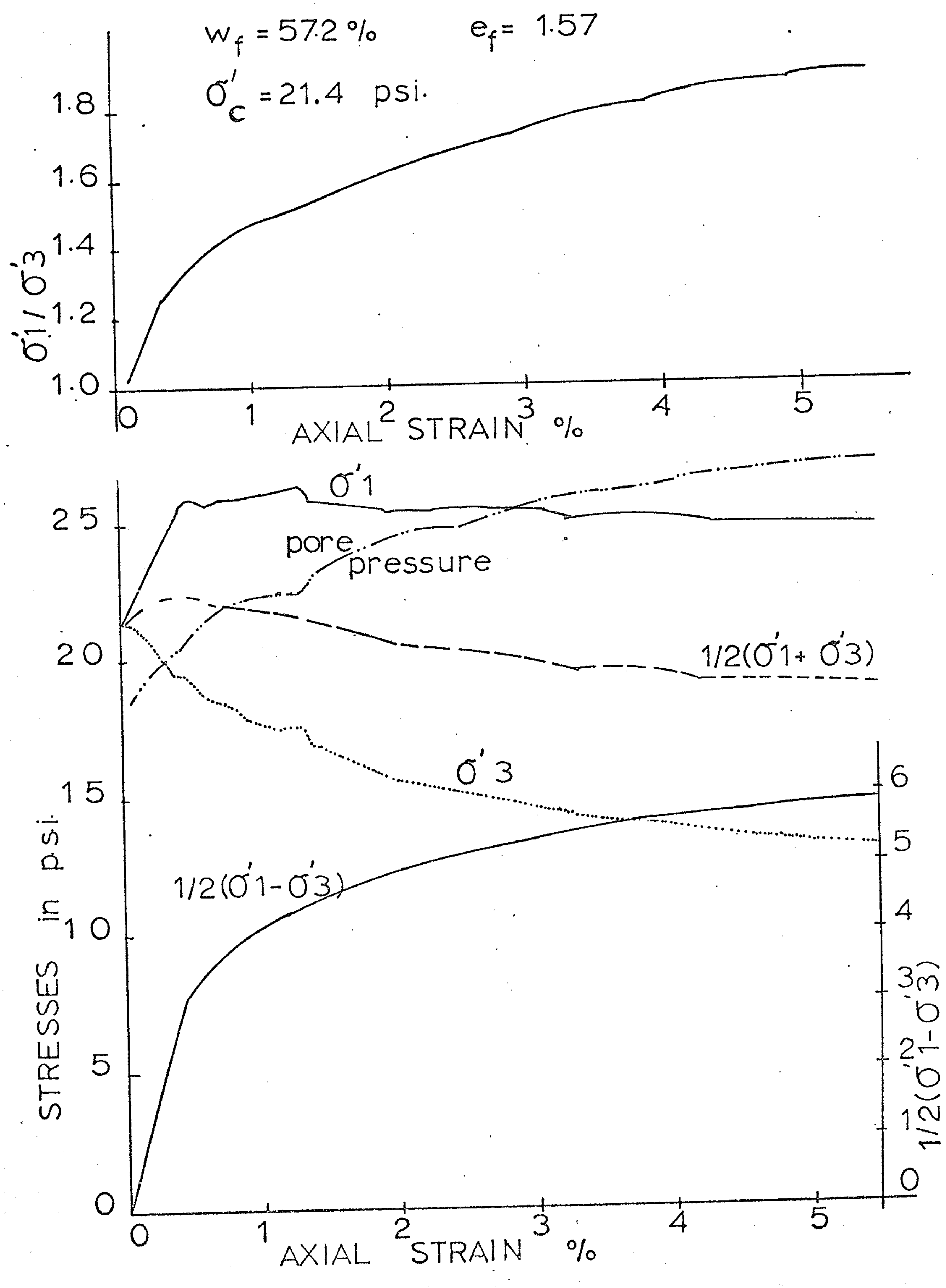

FIGURE A-6 RESULTS - TEST 102.2

$w_f = 53.5\%$ $e_f = 1.47$ $\sigma'_c = 31.0$ psi.

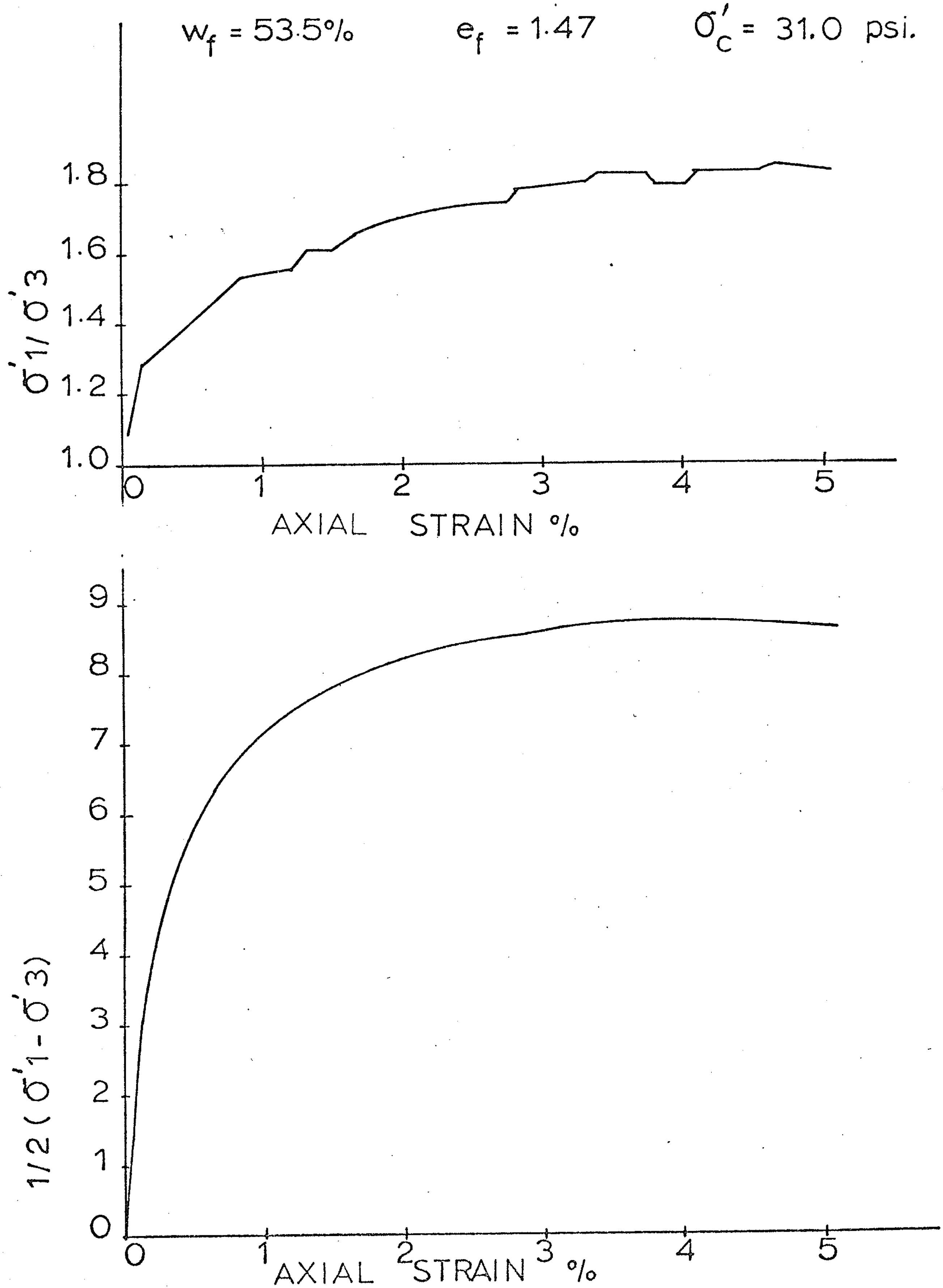

FIGURE A-7 RESULTS - TEST 102.2

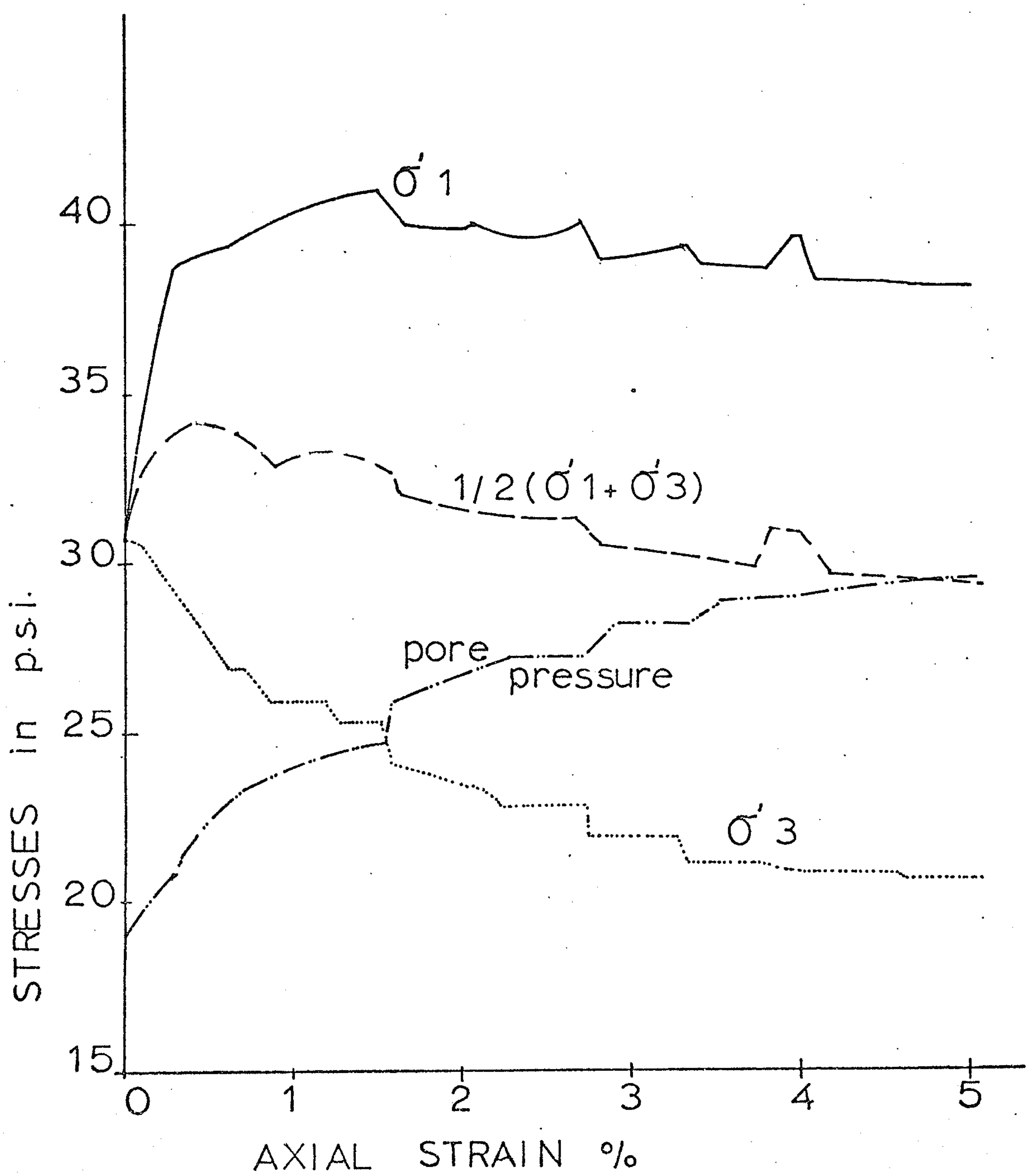

FIGURE A-8 RESULTS-TEST 103.1

$w_f = 61.7\%$ $e_f = 1.71$ $\sigma'_c = 12.2$ p.s.i.

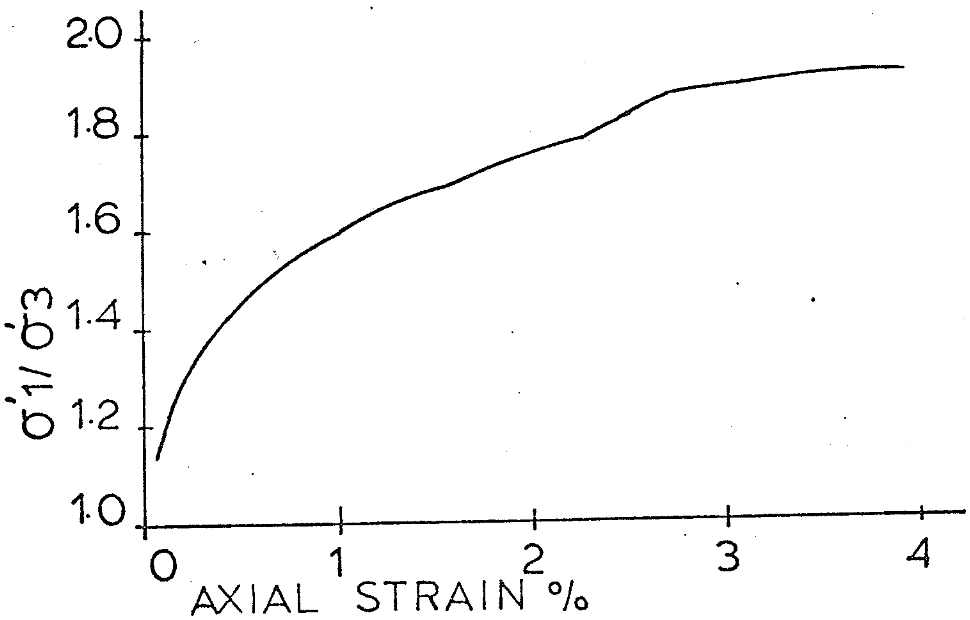

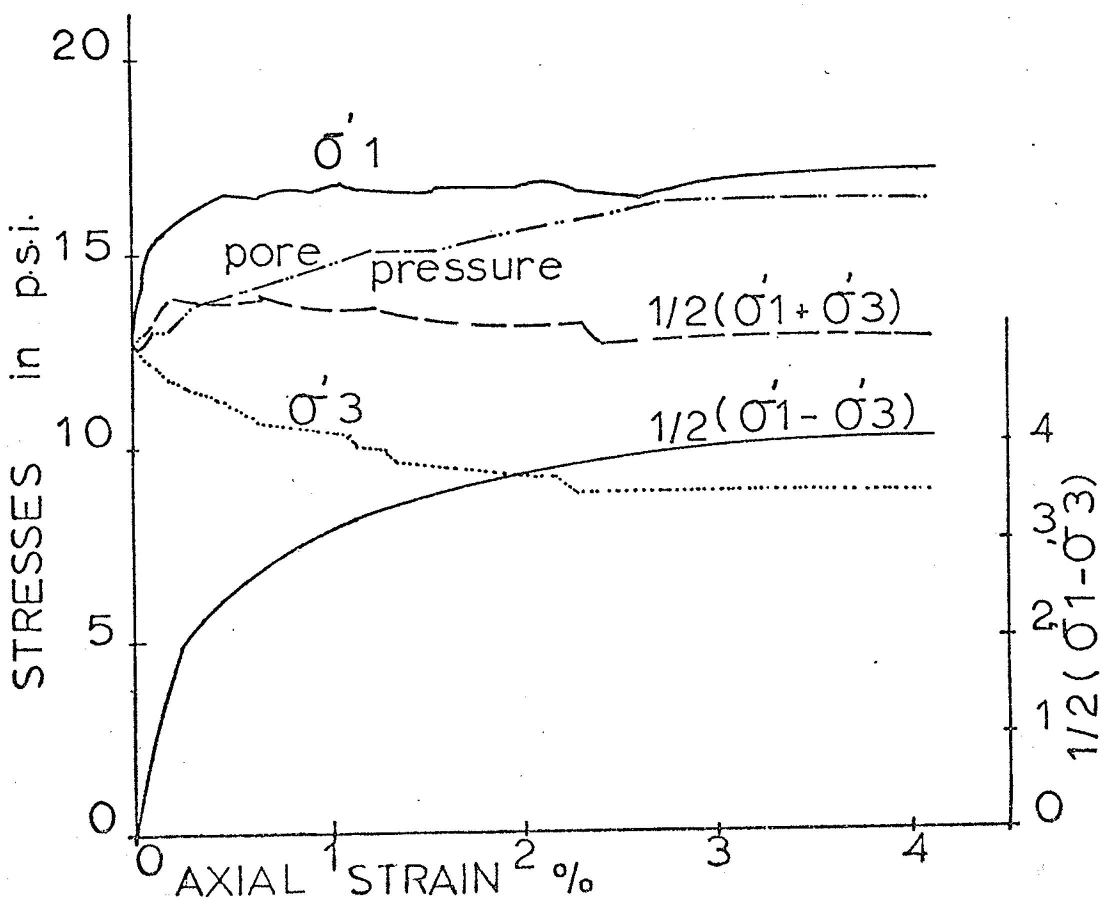

FIGURE A-9 RESULTS - TEST 103.2

$w_f = 57.0\%$ $e_f = 1.58$ $\sigma'_c = 24.7$ psi.

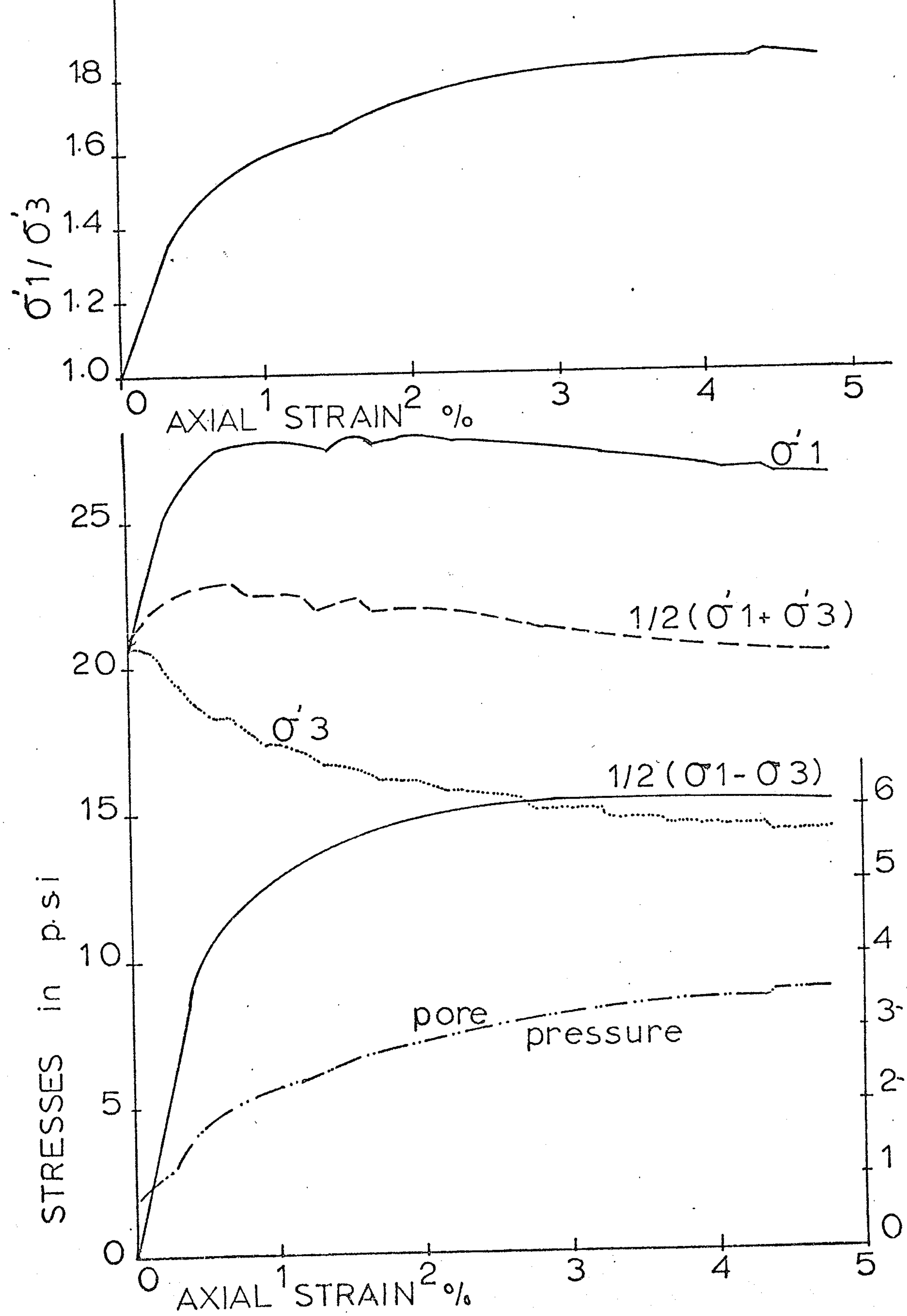

FIGURE A-10 RESULTS-TEST 103.3

$w_f = 50.0\%$ $e_f = 1.42$ $\sigma_c' = 41.6$ psi.

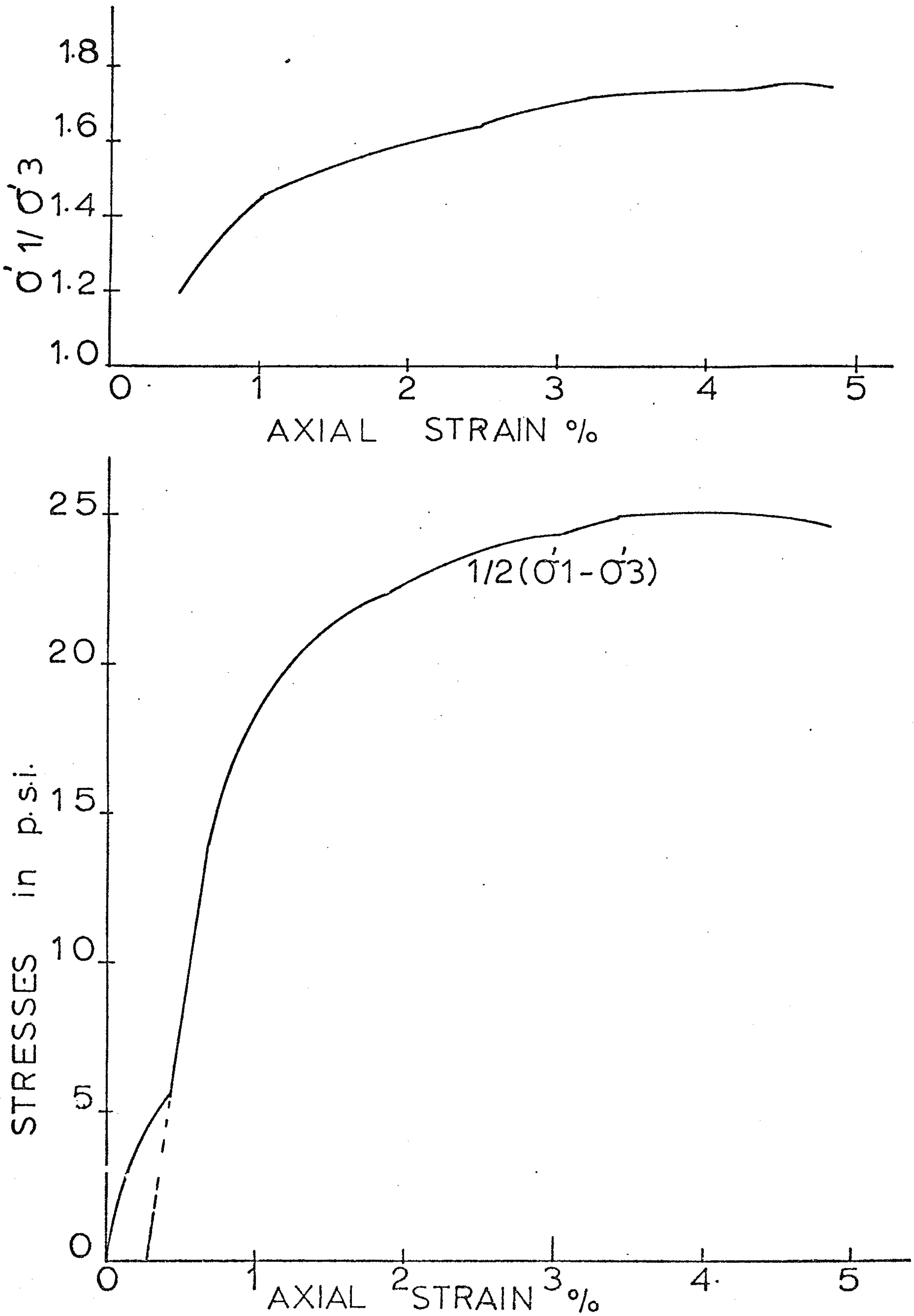

FIGURE A-11 RESULTS-TEST 103.3

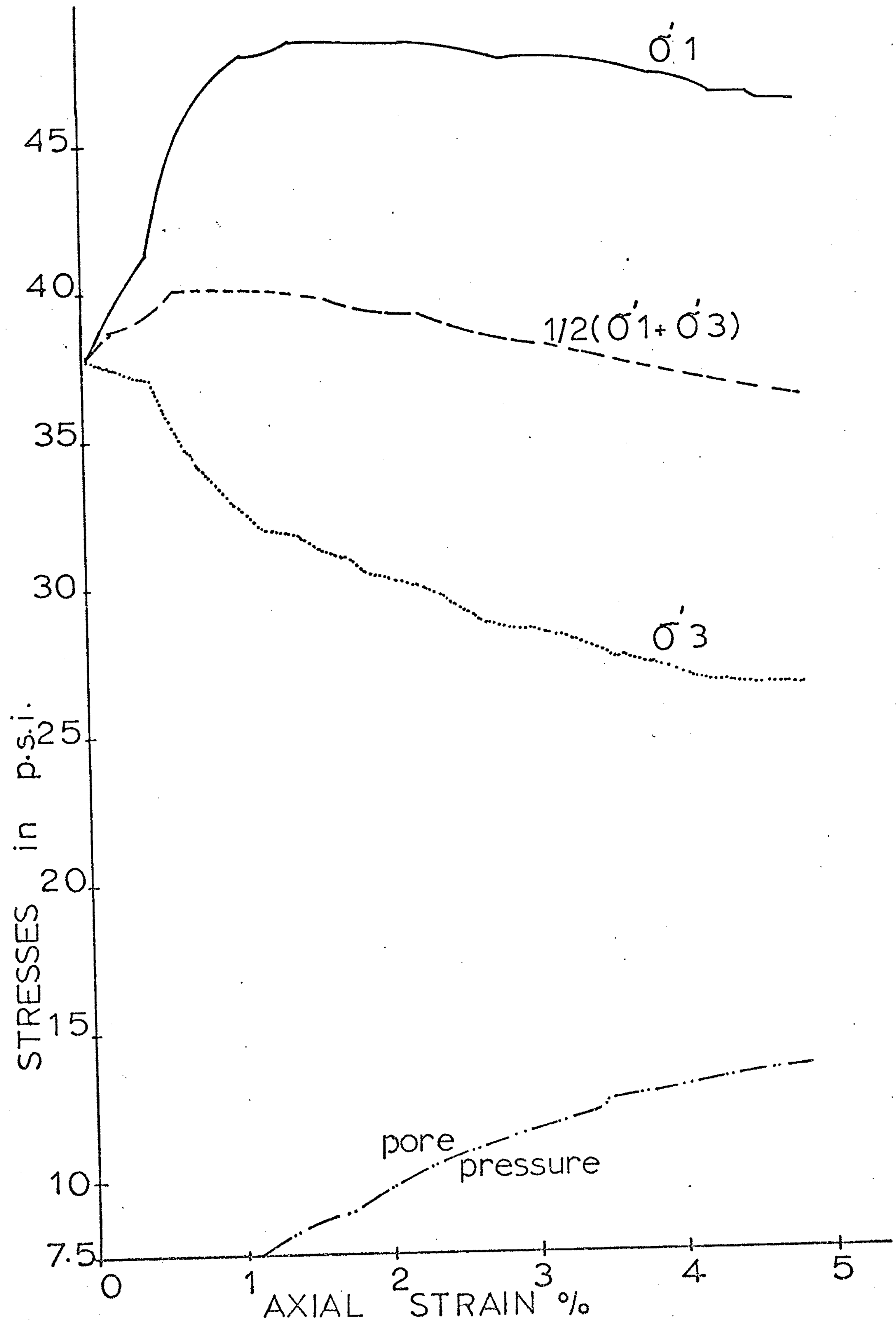

FIGURE A-12 RESULTS-TEST 104.1

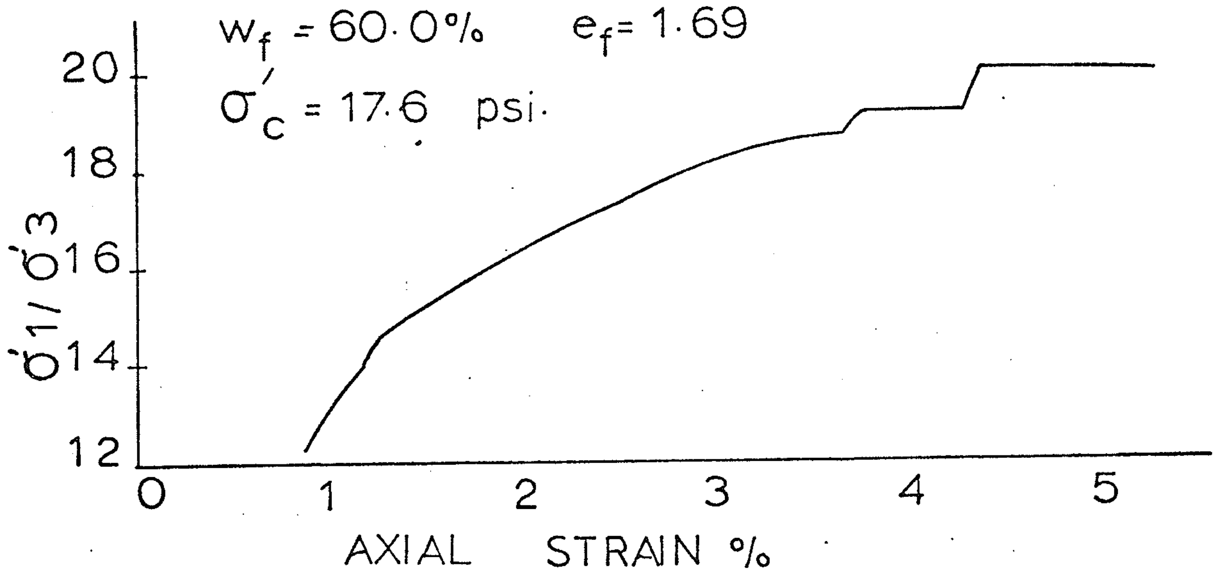

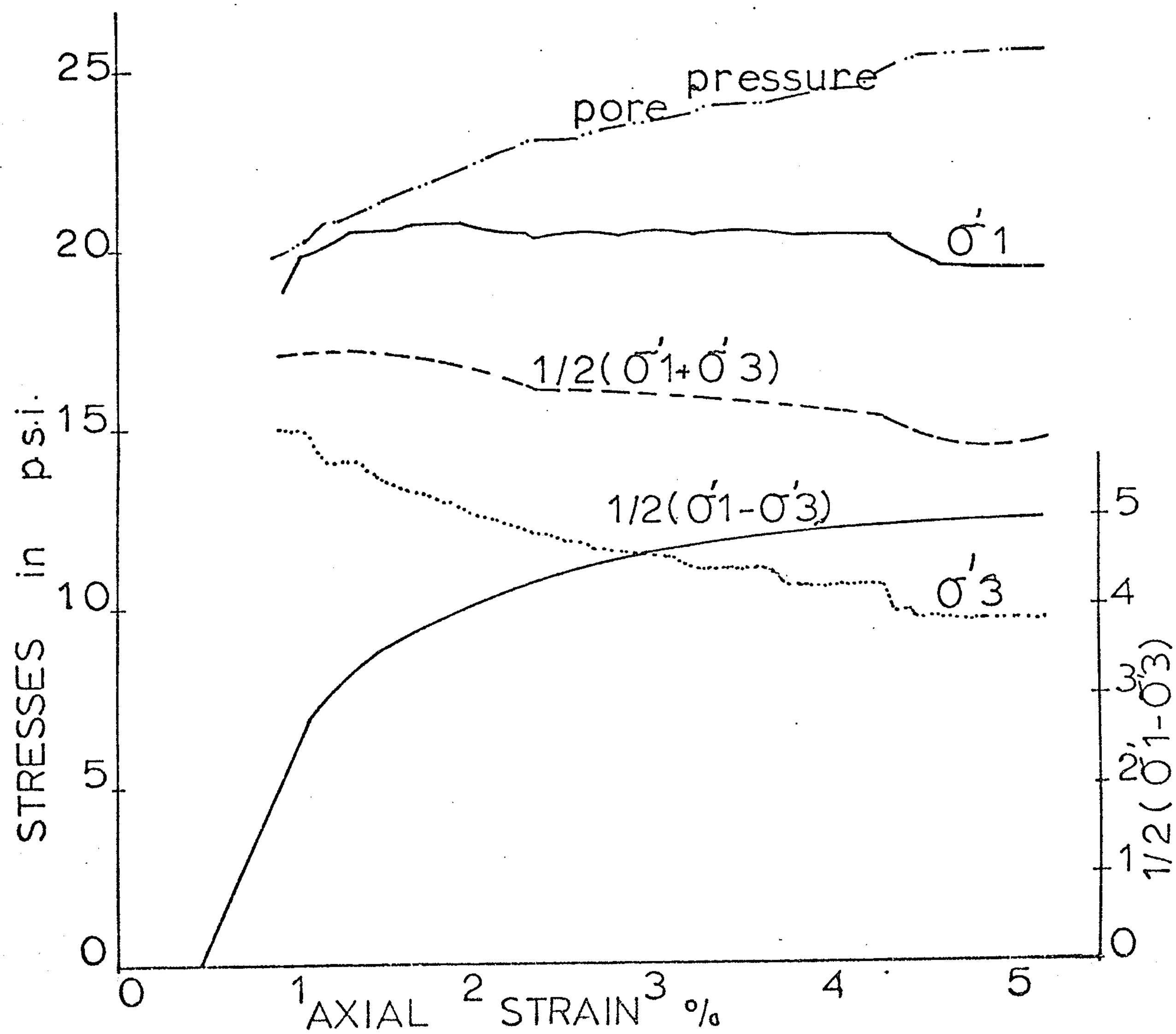

FIGURE A-13 RESULTS-TEST 104.2

$w_f = 53.5\%$ $e_f = 1.51$ $\sigma_c' = 31.0$ psi.

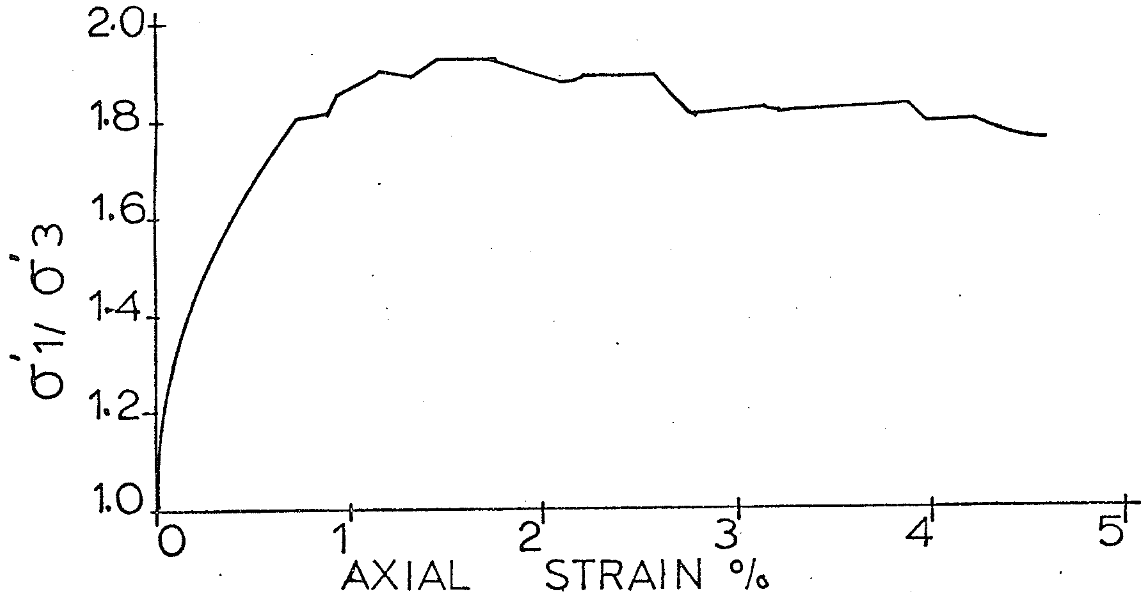

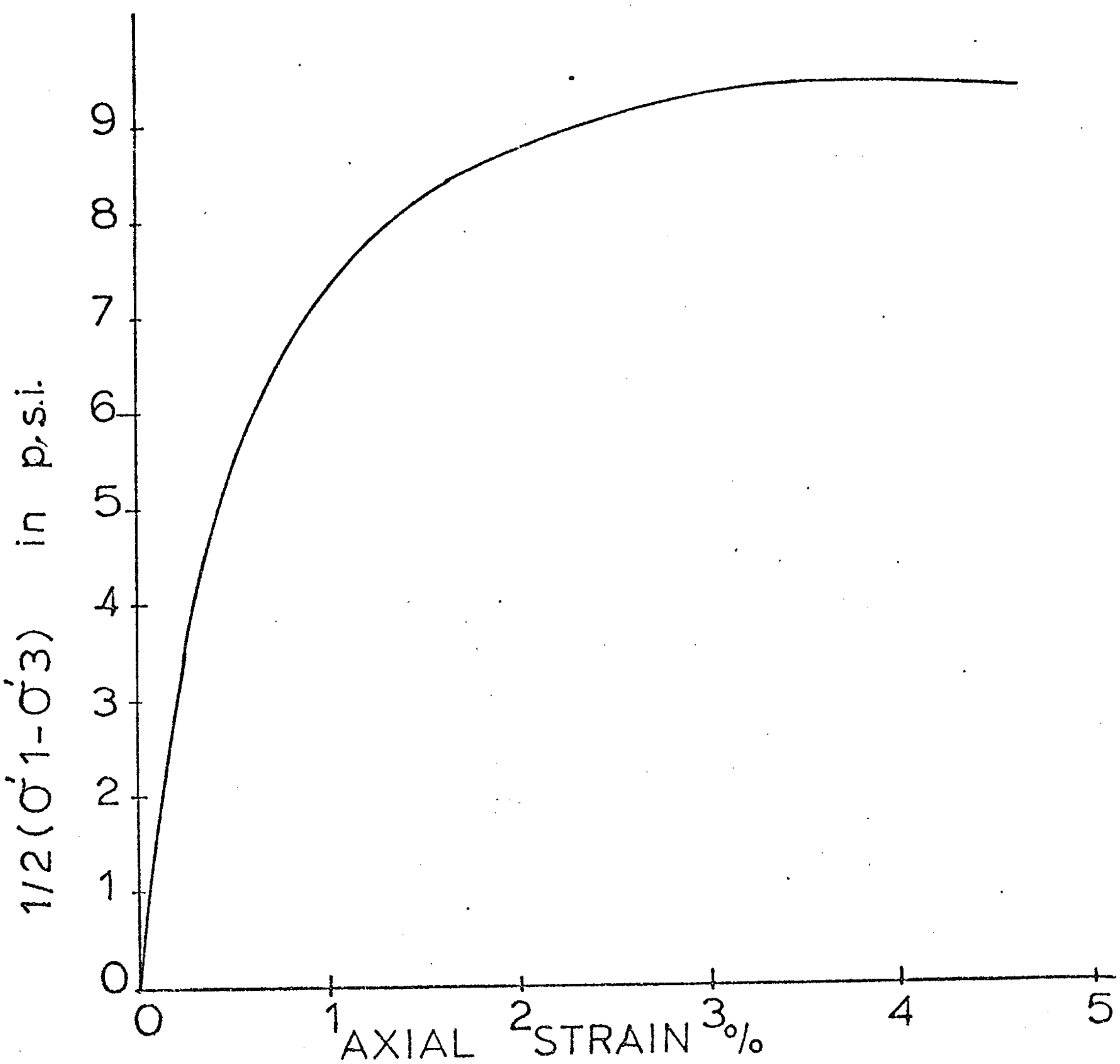

FIGURE A-14 RESULTS -TEST 1042

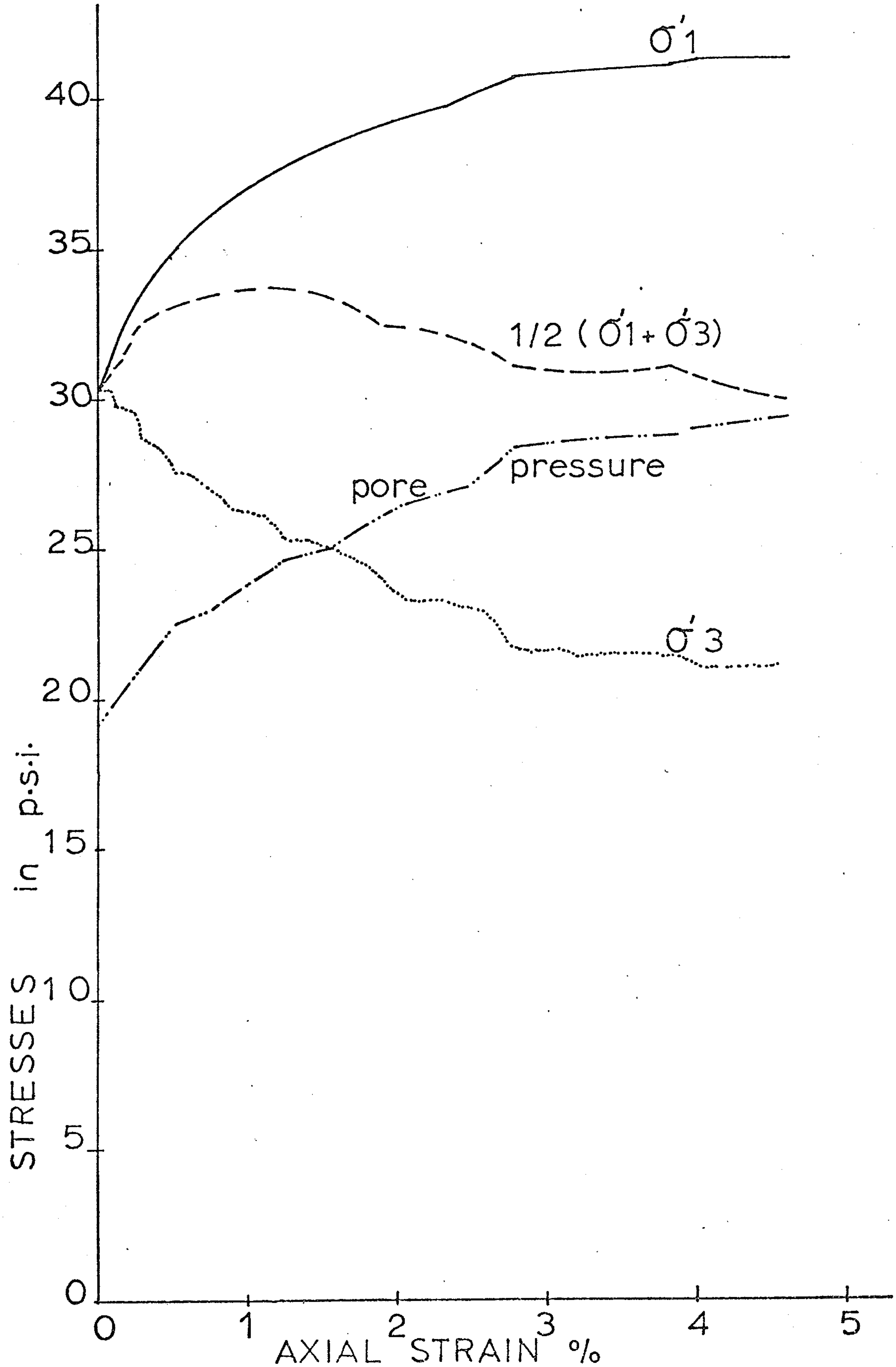

FIGURE A-15 RESULTS - TEST 104.3

$w_f = 47.41\%$ $e_f = 1337$ $\sigma'_c = 62.3$ psi.

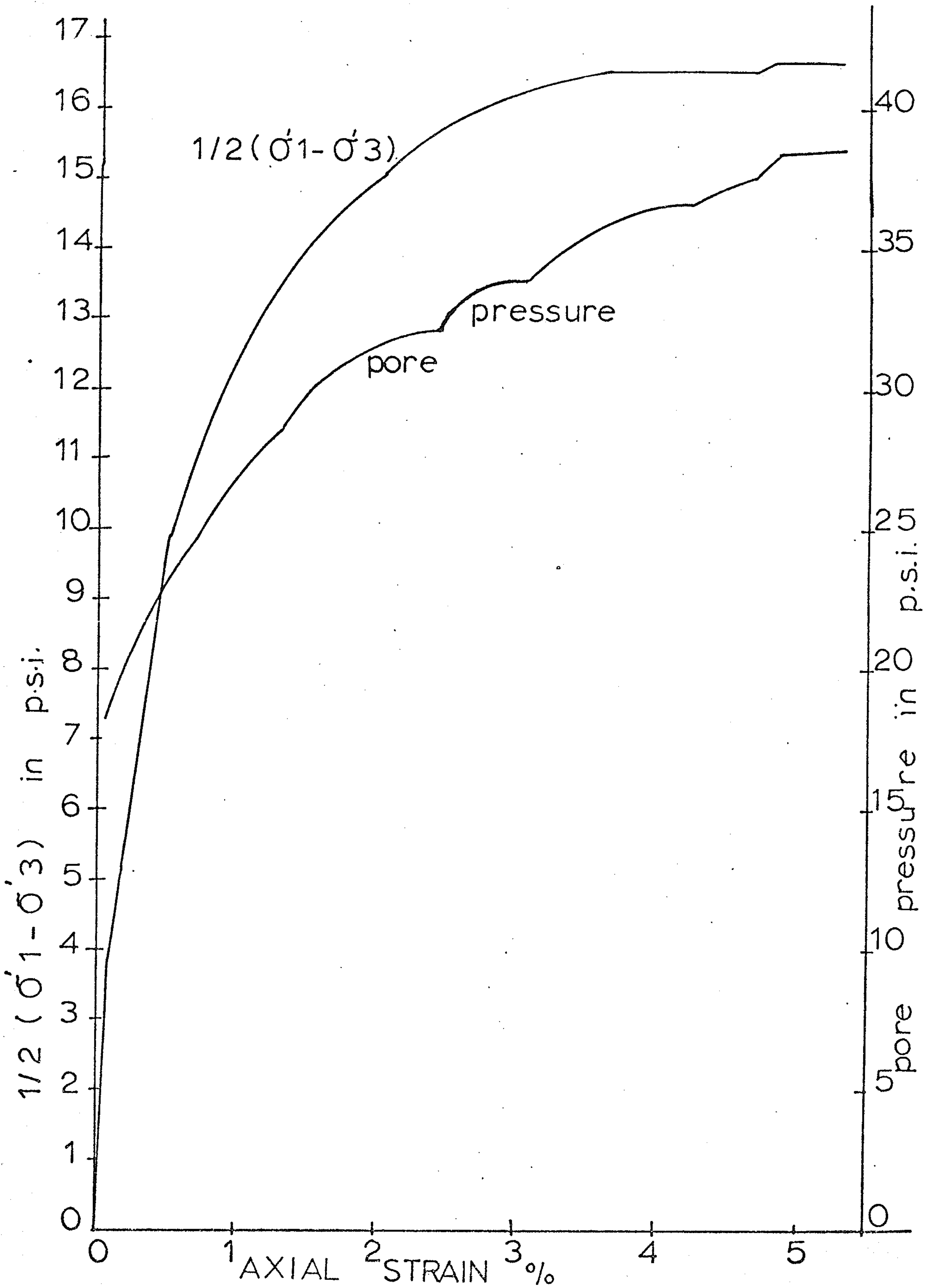

FIGURE A-16 RESULTS - TEST 104.3

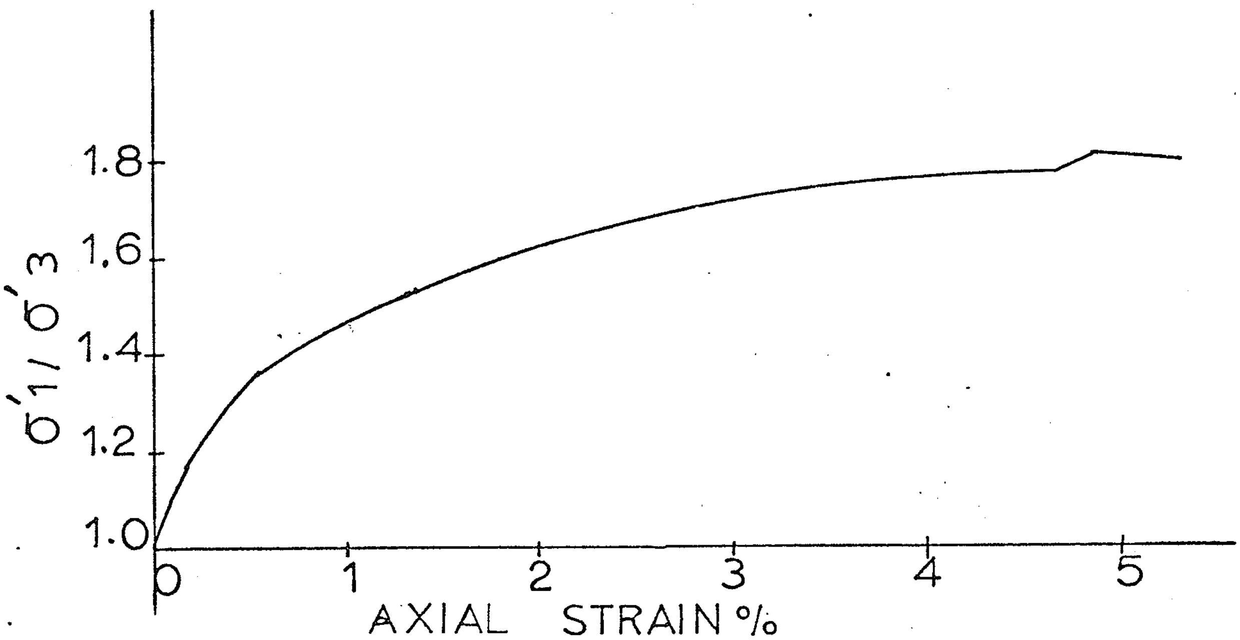

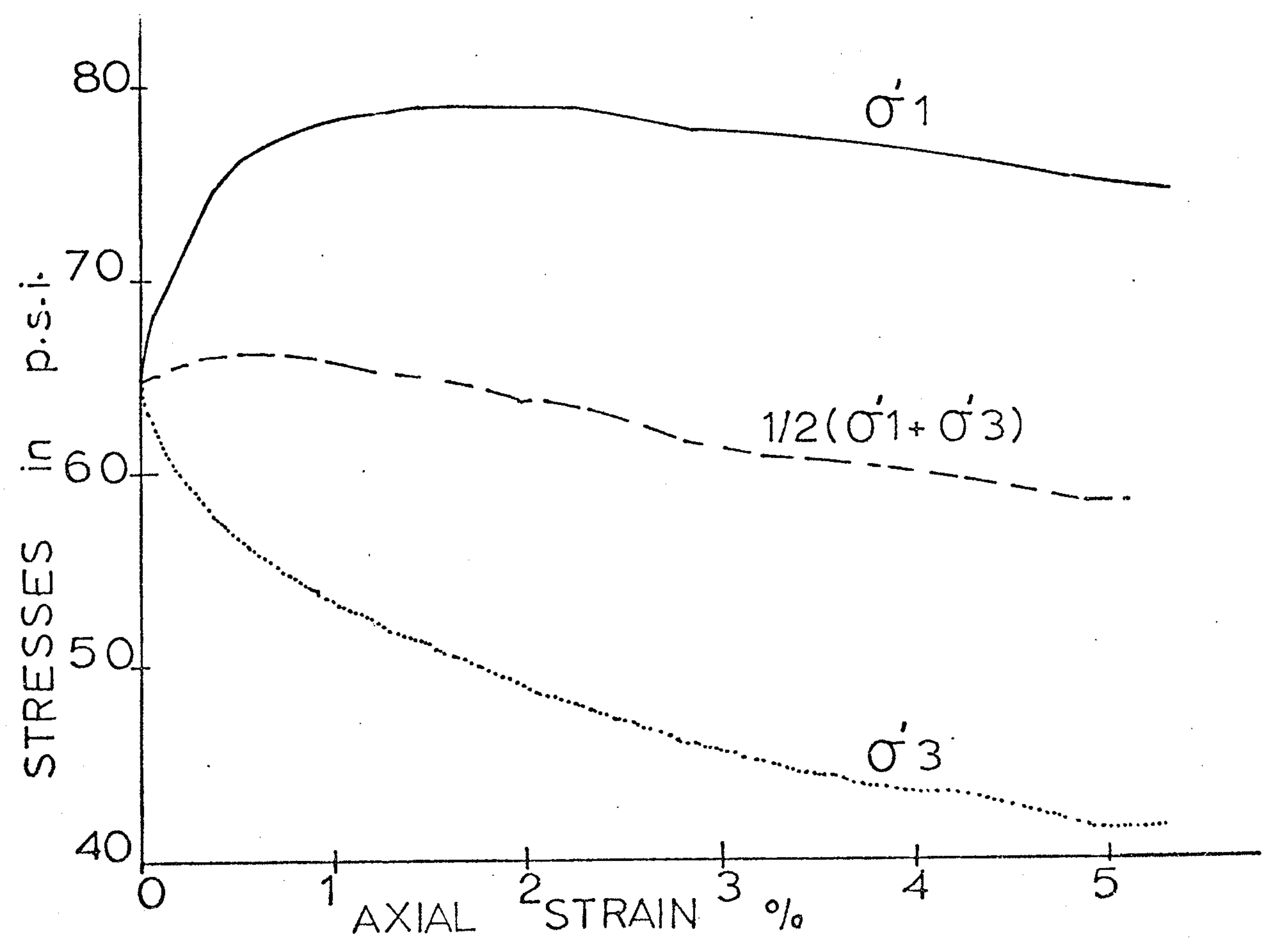

FIGURE A-17 RESULTS - TEST 201-1

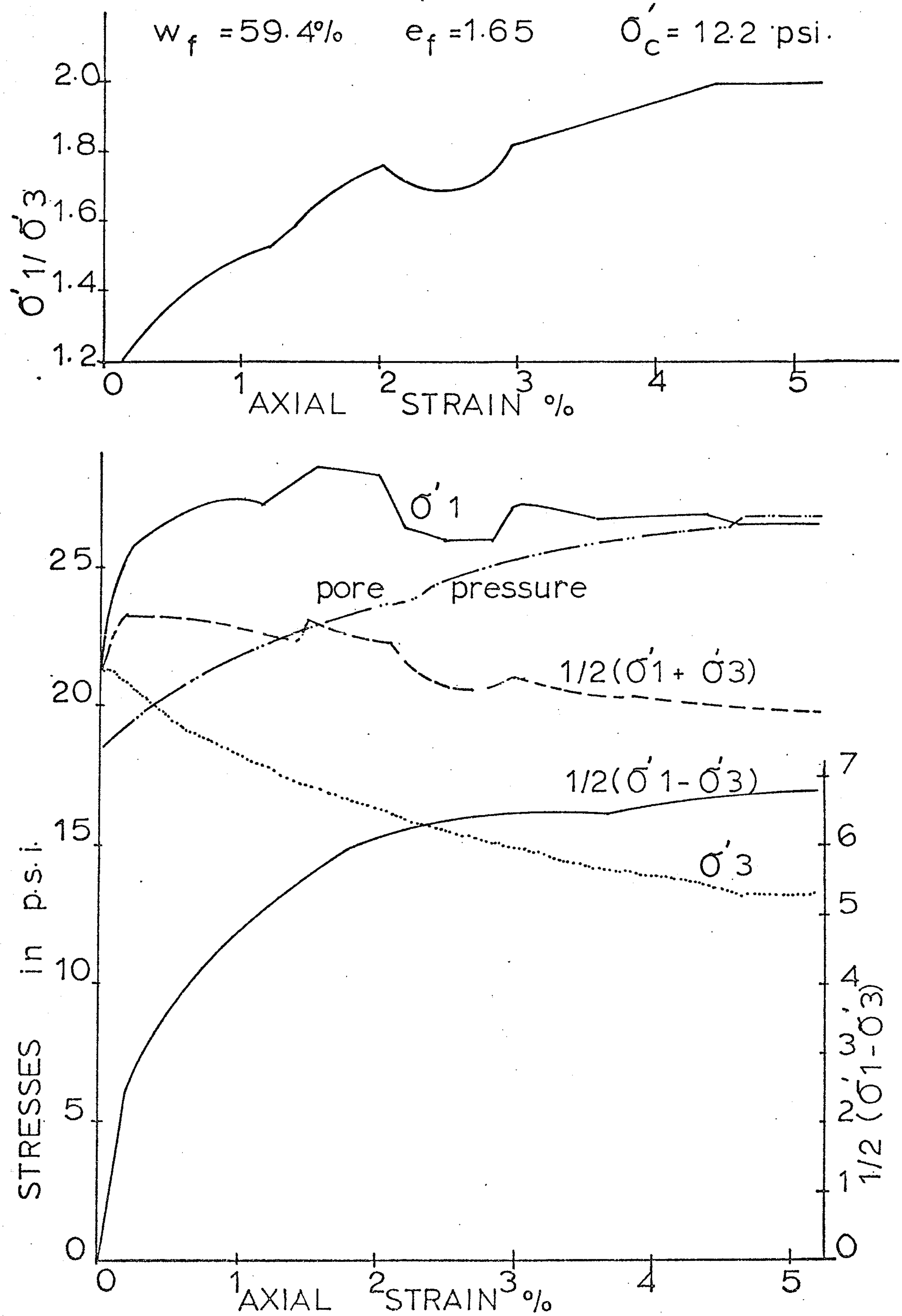

FIGURE A-18 RESULTS-TEST 201.2

$w_f = 64.7\%$ $e_f = 1.79$ $\sigma'_c = 21.5$ p.s.i.

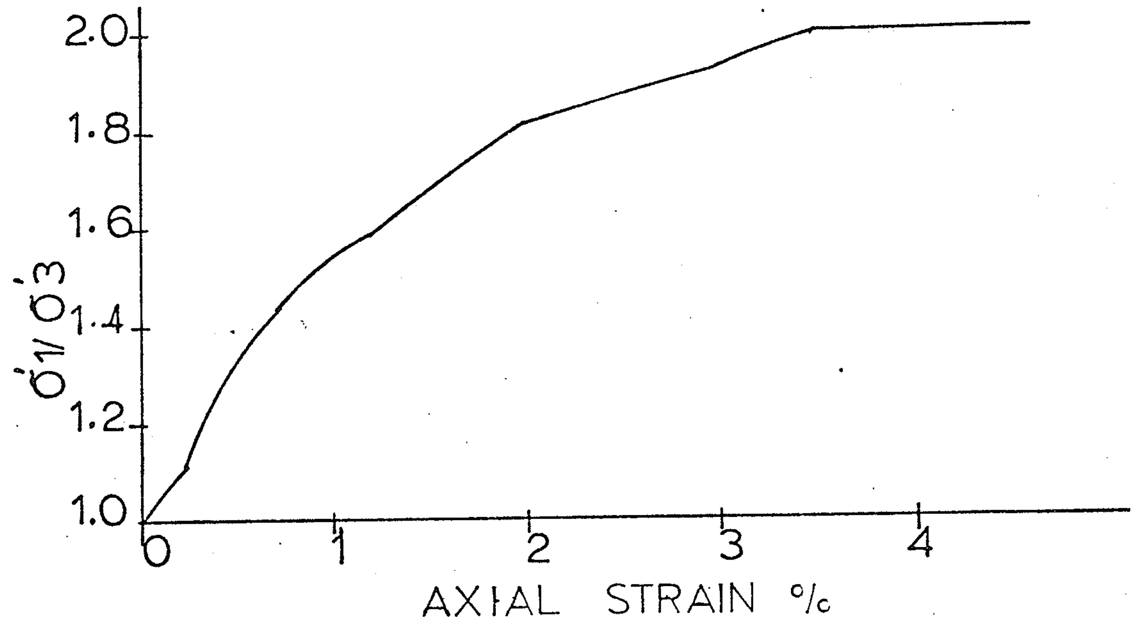

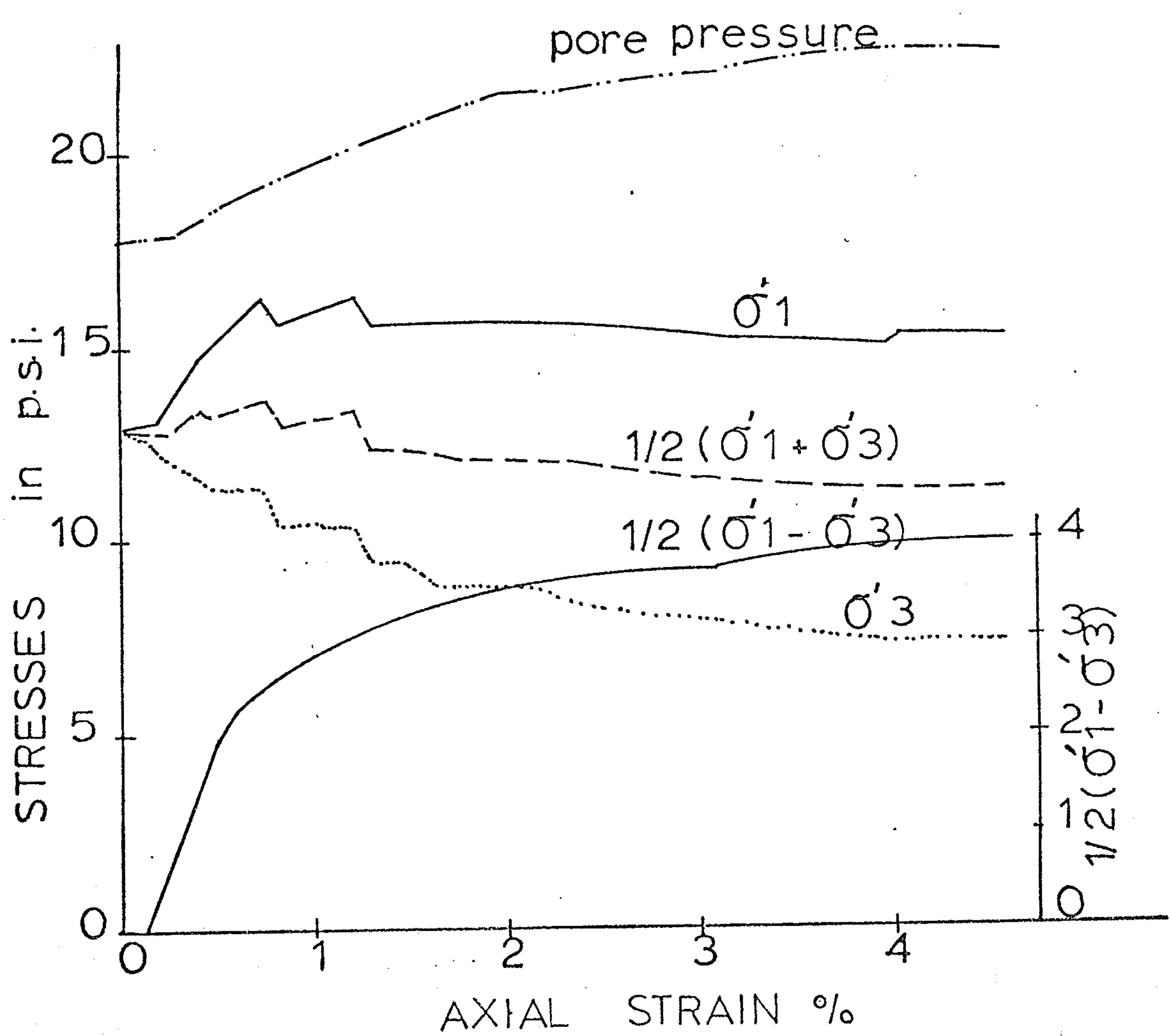

FIGURE 19 RESULTS TEST 201.3

w_f = 53.5% e_f = 1.49 σ'_c = 41.2 psi.

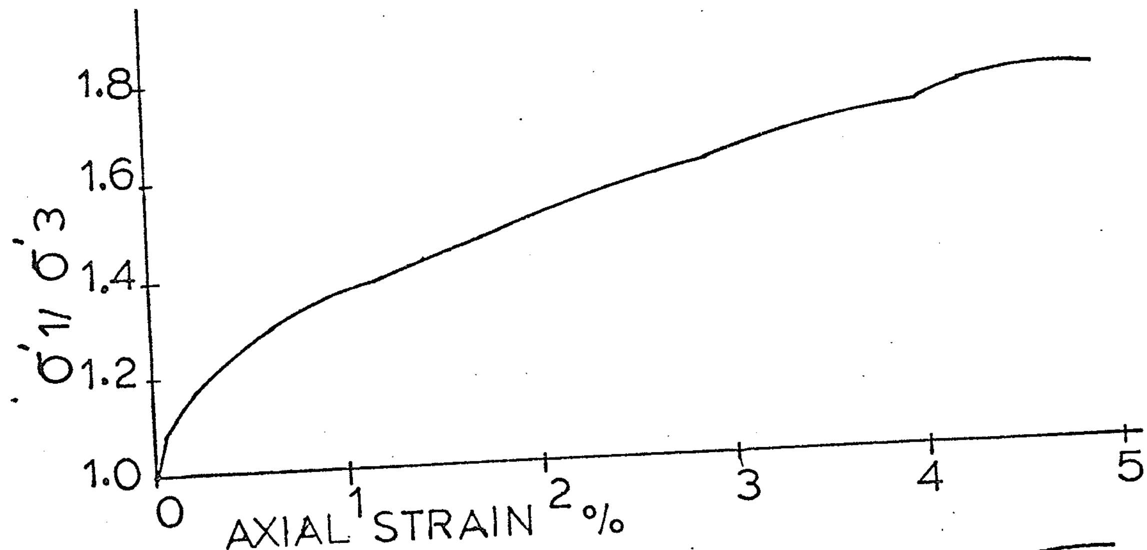

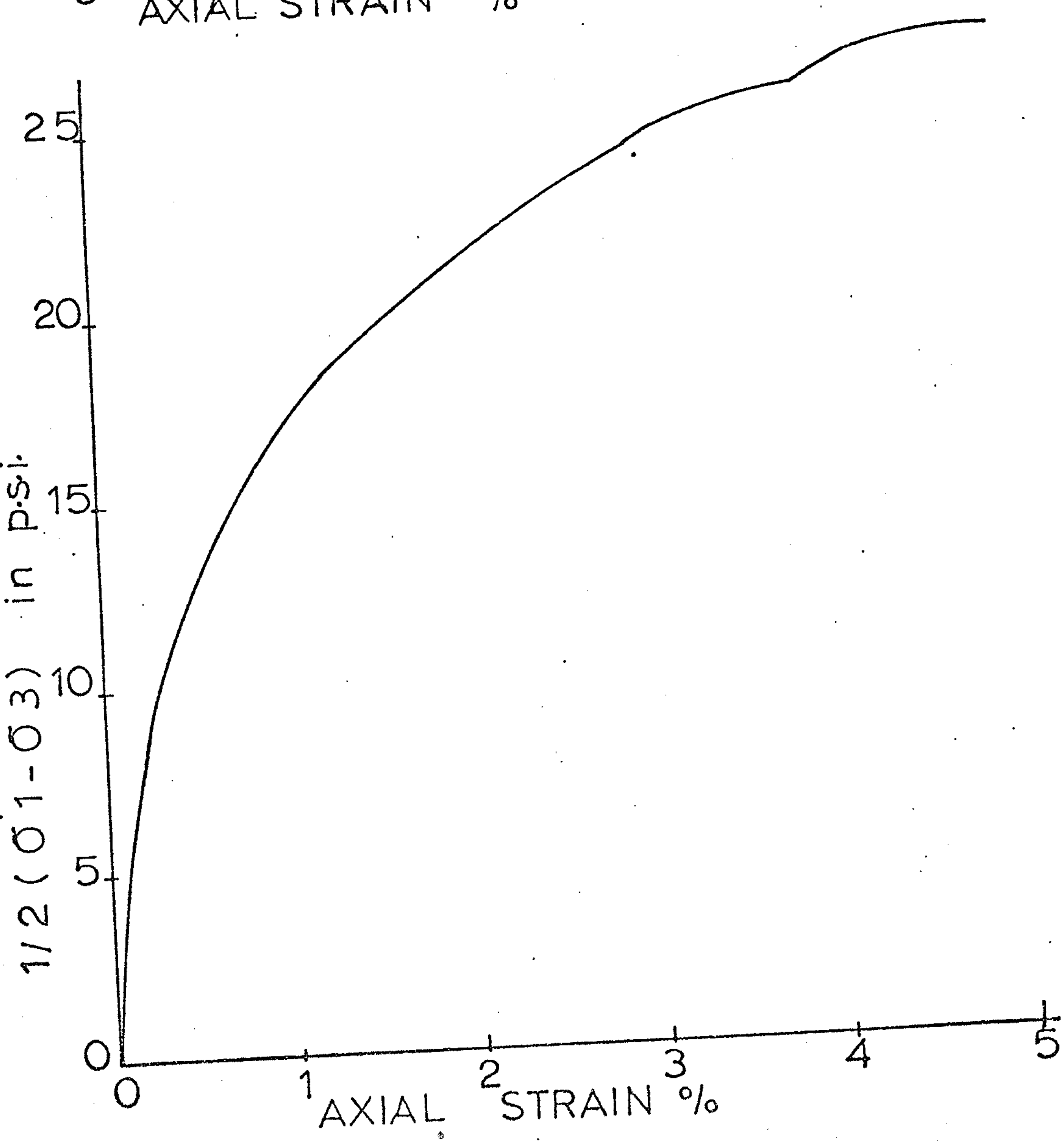

FIGURE A-20 RESULTS - TEST 201.3

$w_f = 53.5\%$ $e_f = 1.49$ $\sigma'_c = 41.2$ psi.

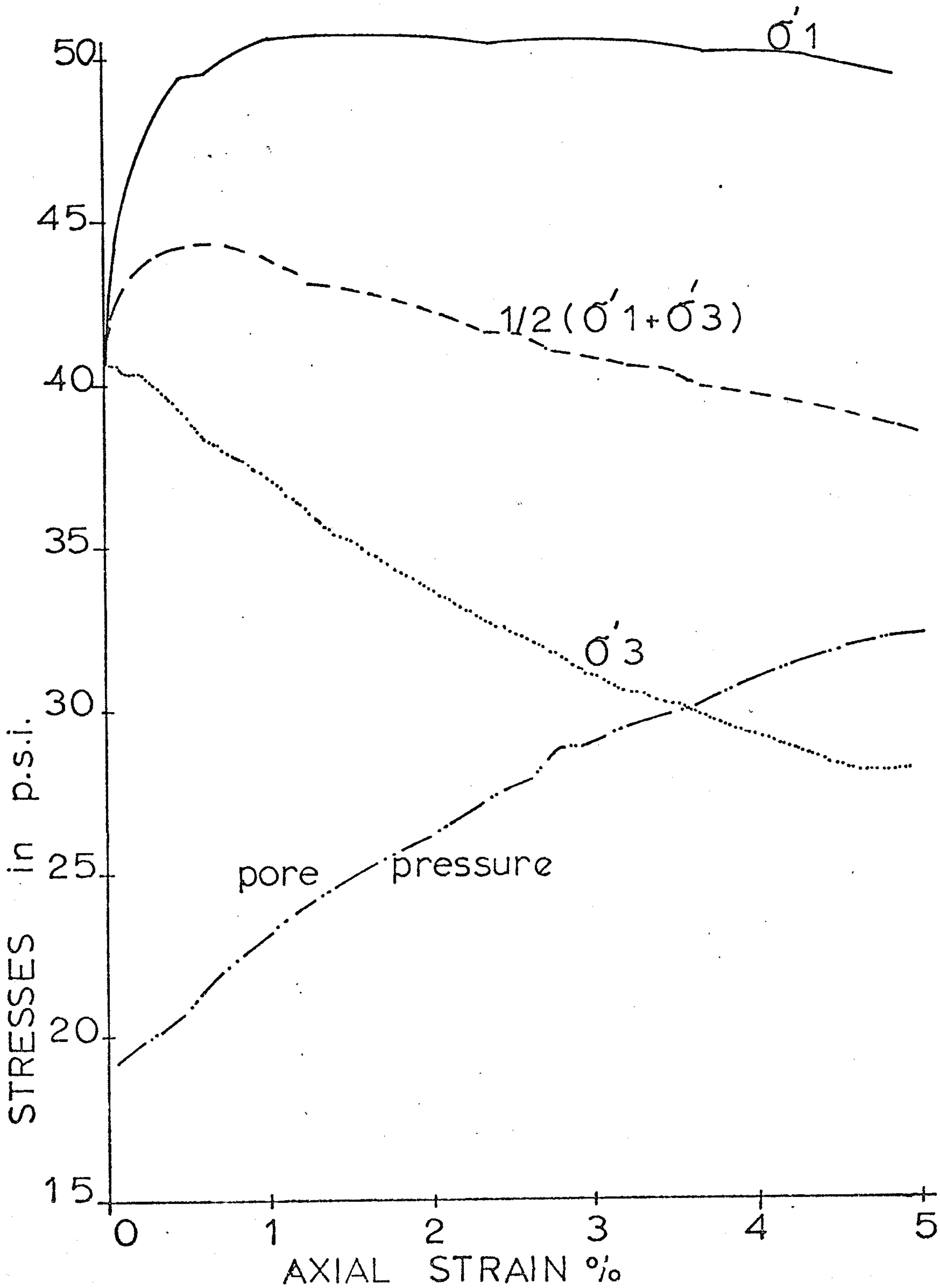

FIGURE A-21 RESULTS - TEST 2021

$w_f = 61.8\%$ $e_f = 1.72$ $\sigma'_c = 17.6$ psi.

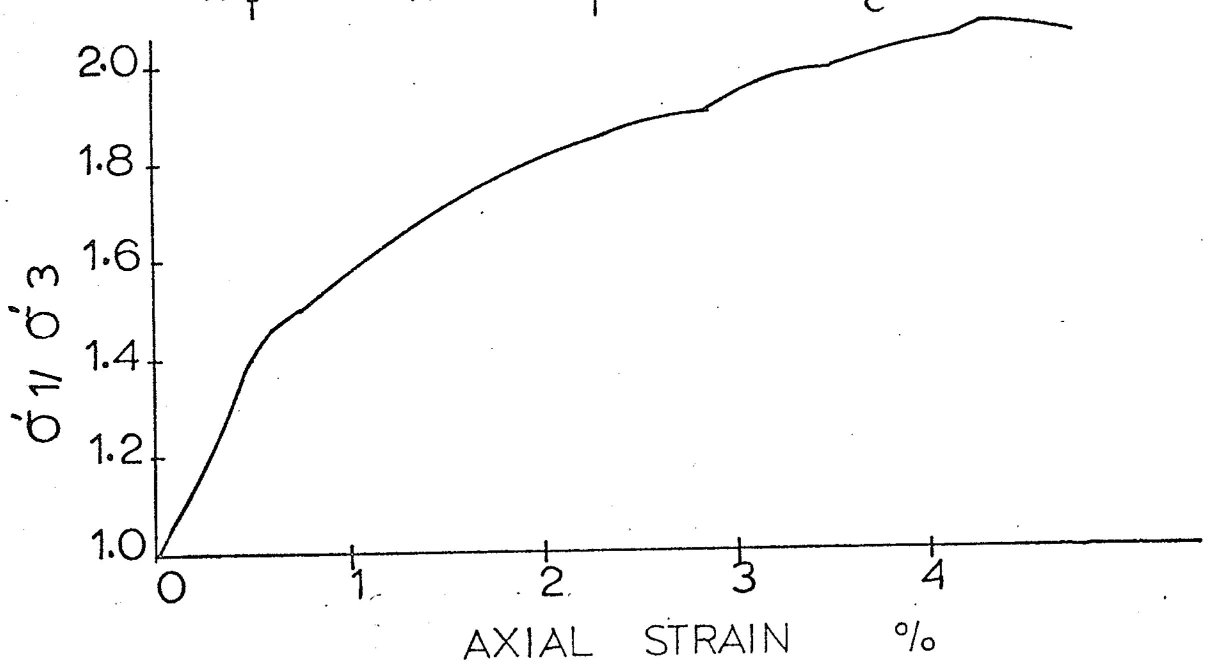

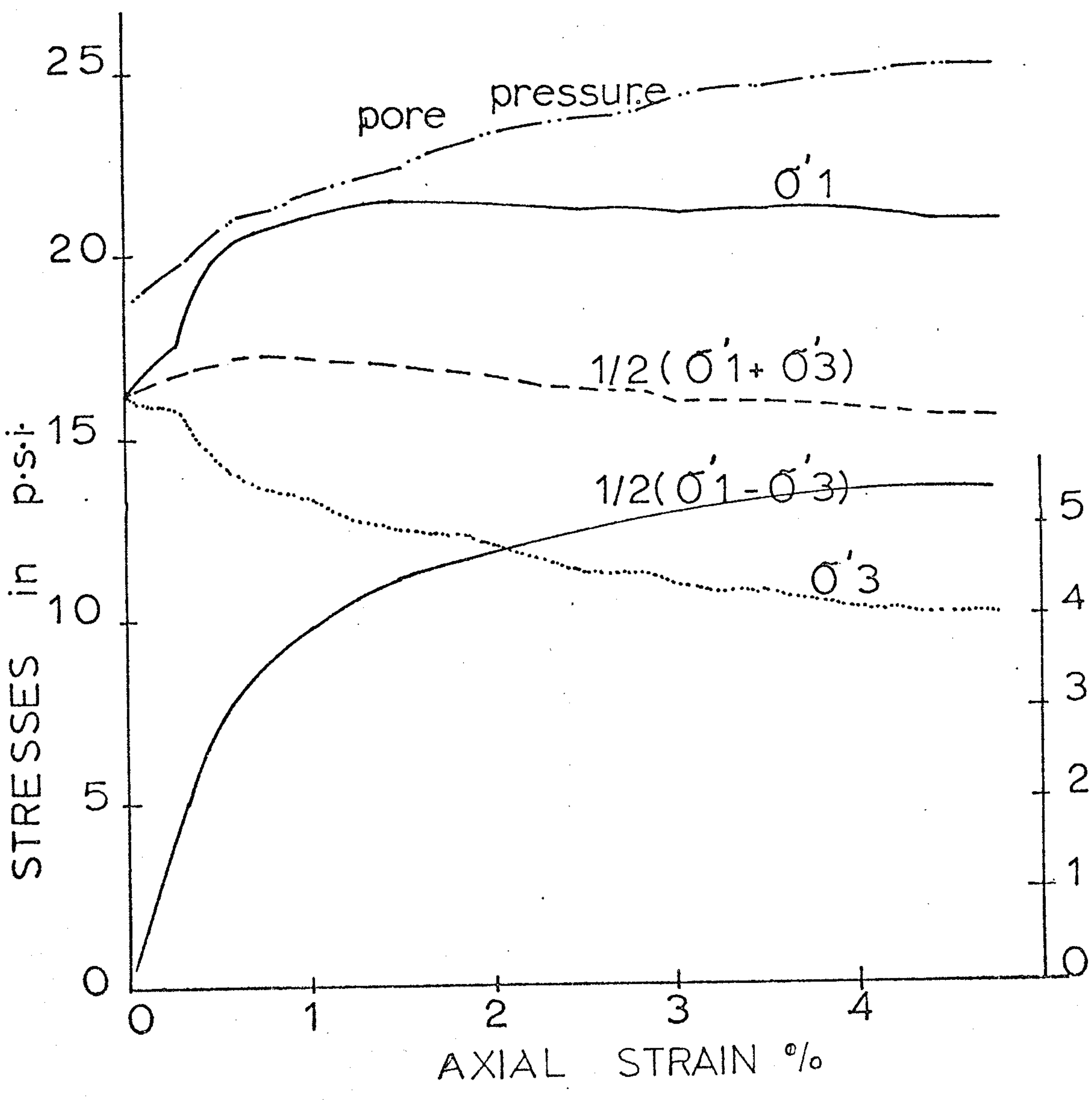

FIGURE A-22 RESULTS-TEST 202.2

$w_f = 56.2\%$ $e_f = 1.56$ $\sigma'_c = 31.5$ psi.

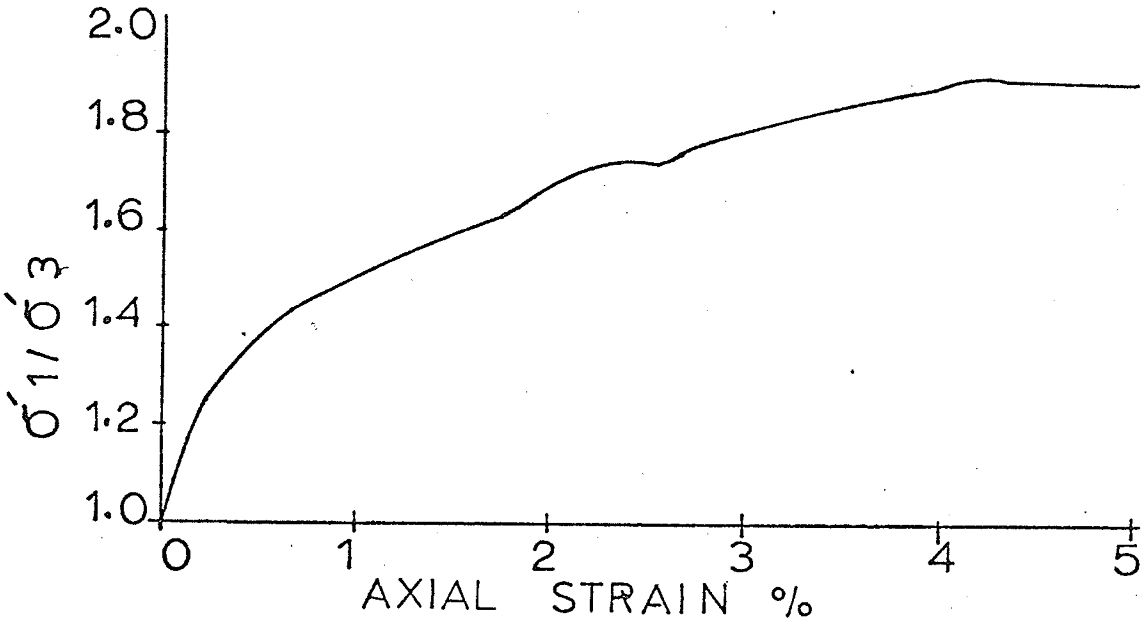

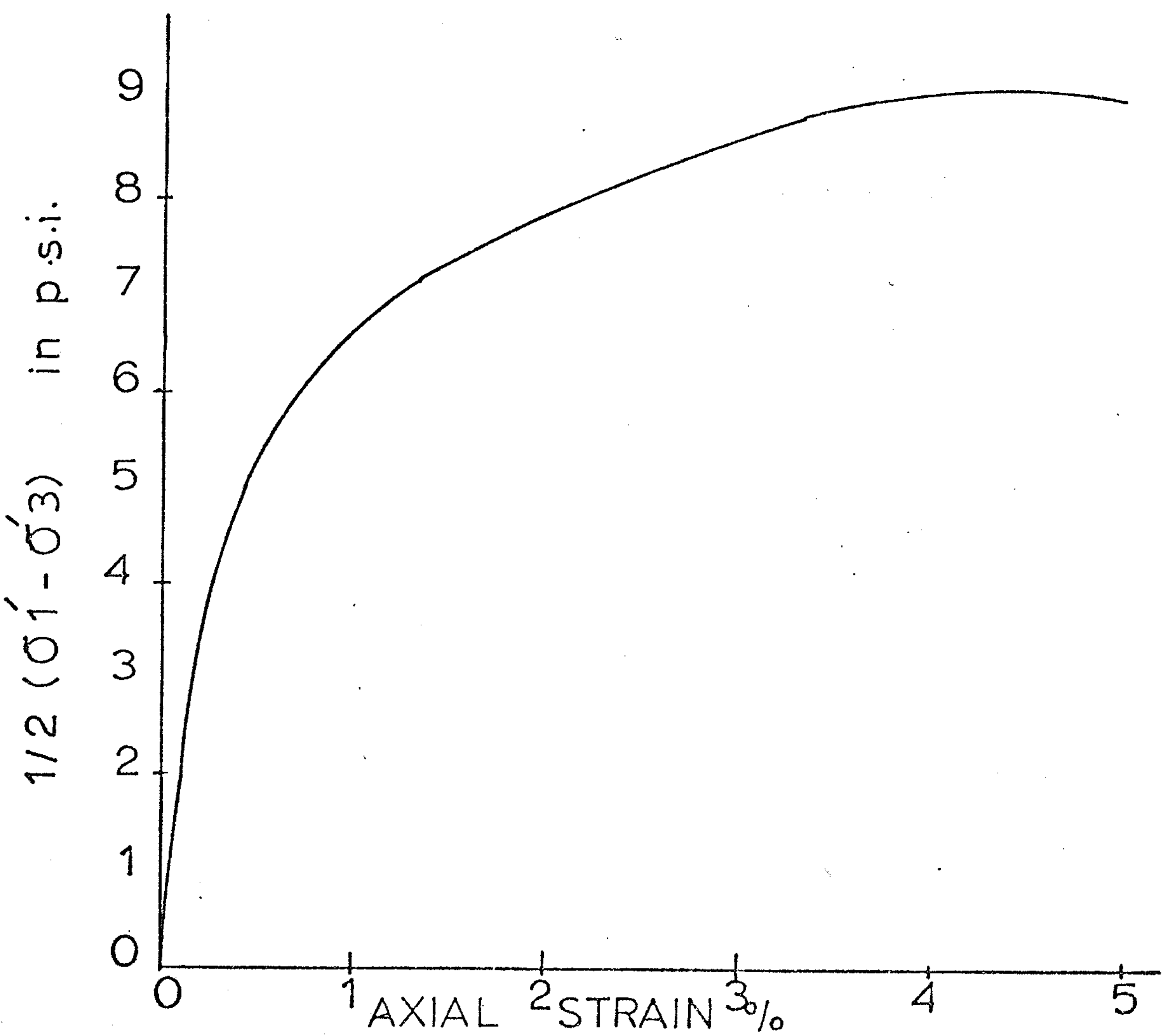

FIGURE A-23 RESULTS-TEST 202.2

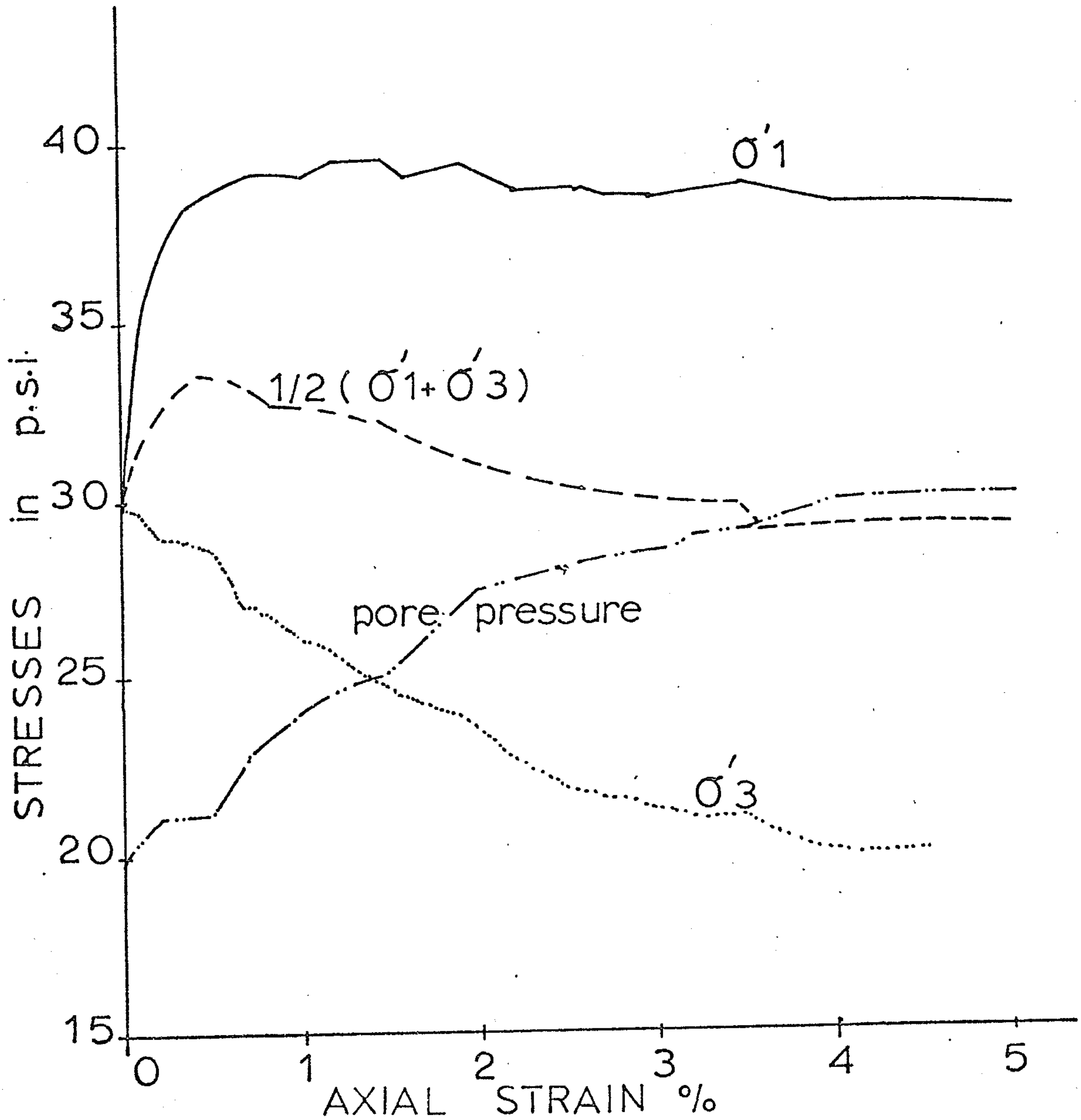

FIGURE A-24 RESULTS - TEST 202.3

$w_f = 49.3\%$ $e_f = 1.37$ $\sigma'_c = 61.5$ psi.

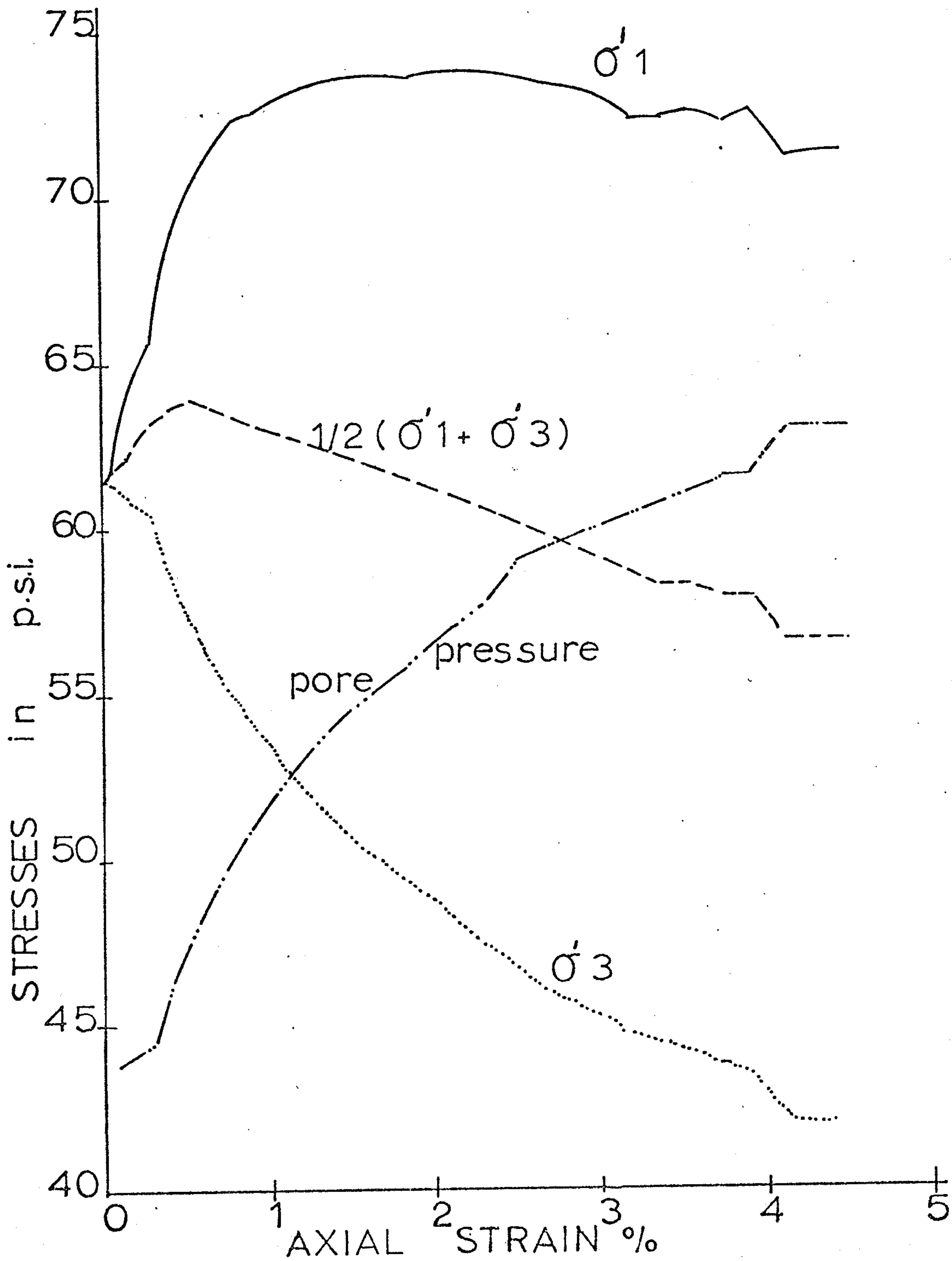

FIGURE A-25 RESULTS-TEST 202.3

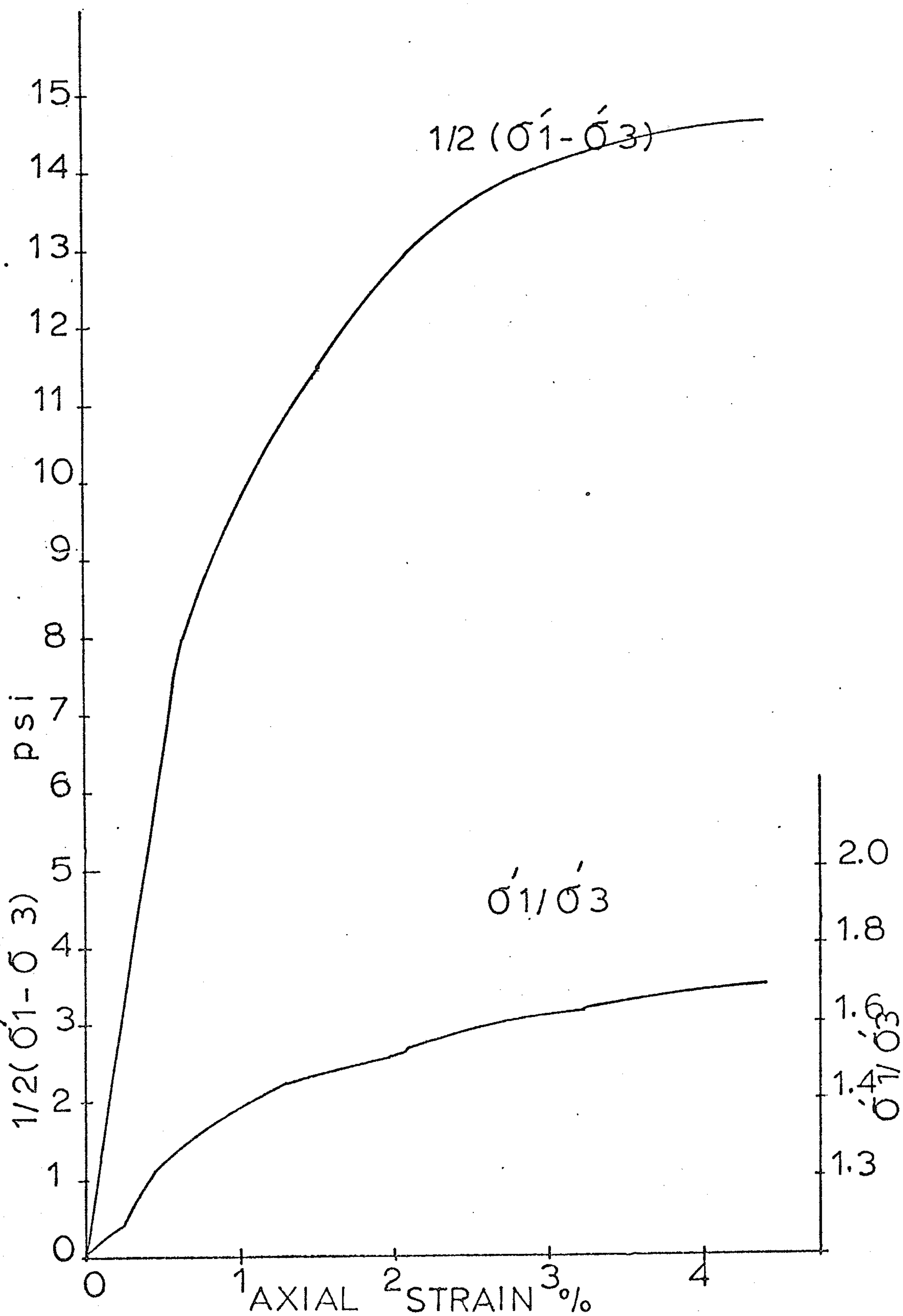

FIGURE A-26 RESULTS - TEST 203.1

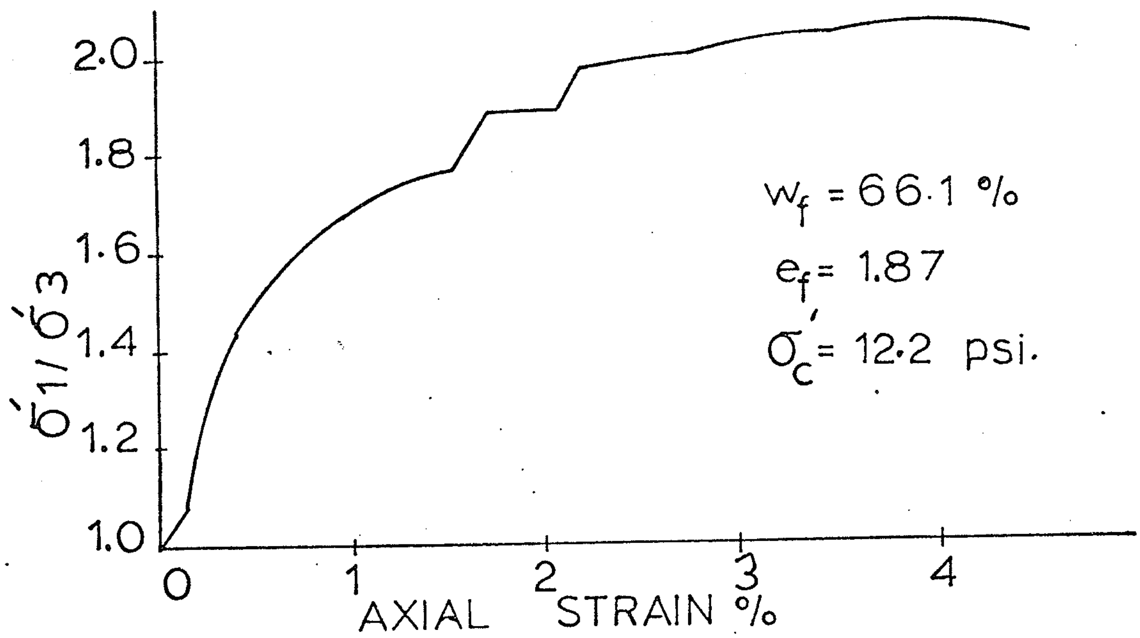

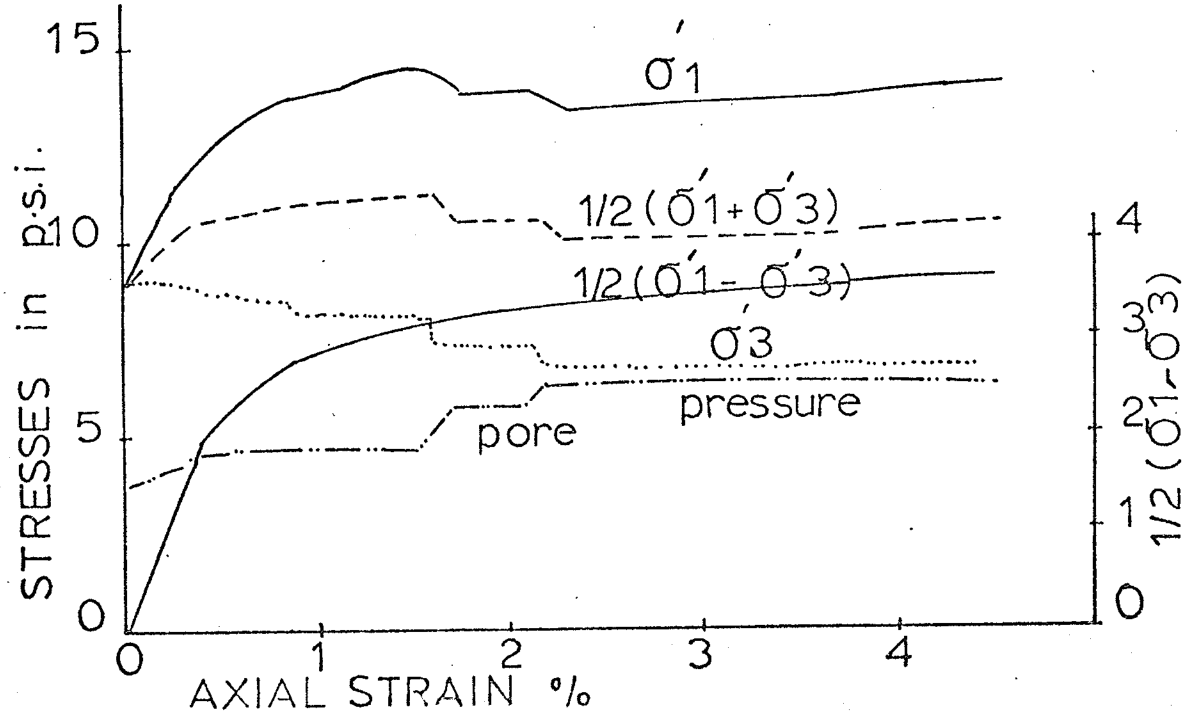

FIGURE A-27 RESULTS-TEST 203.2

$w_f = 59.5\%$ $e_f = 1.68$ $\sigma'_c = 21.3$ psi

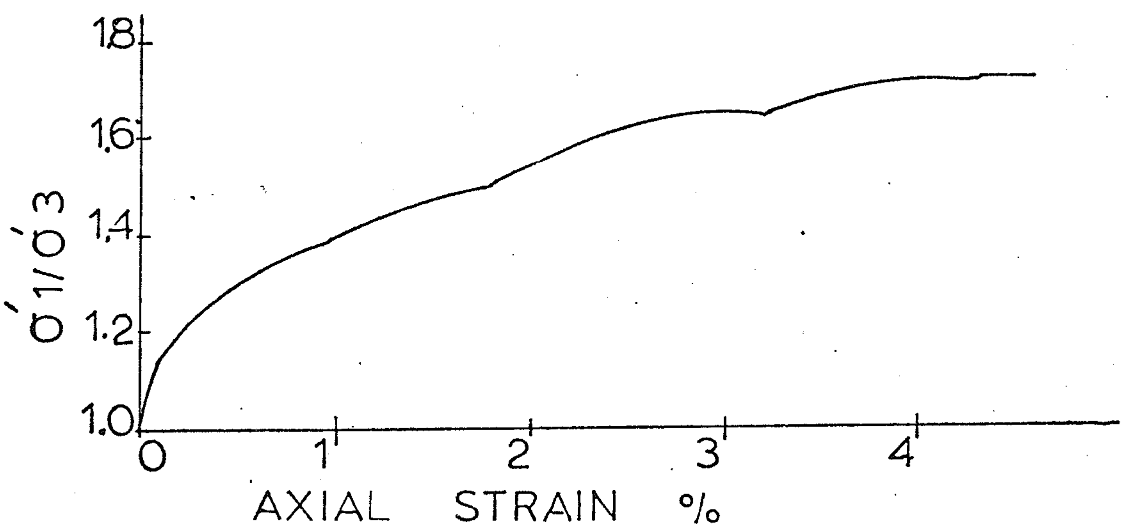

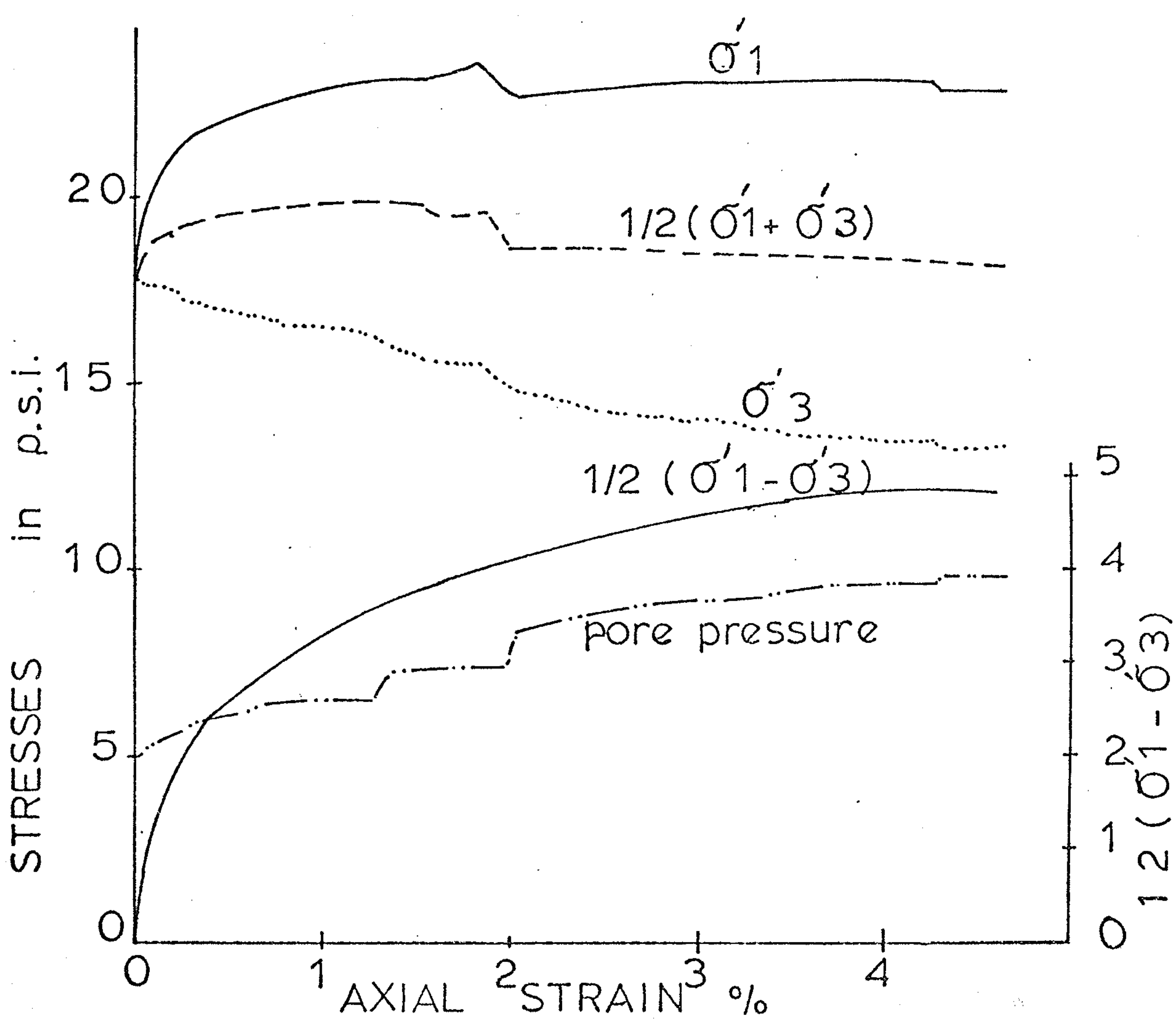

FIGURE A - 28 RESULTS-TEST 203.3

w_f = 53.6 % e_f = 1.49 σ_c' = 40.5 psi.

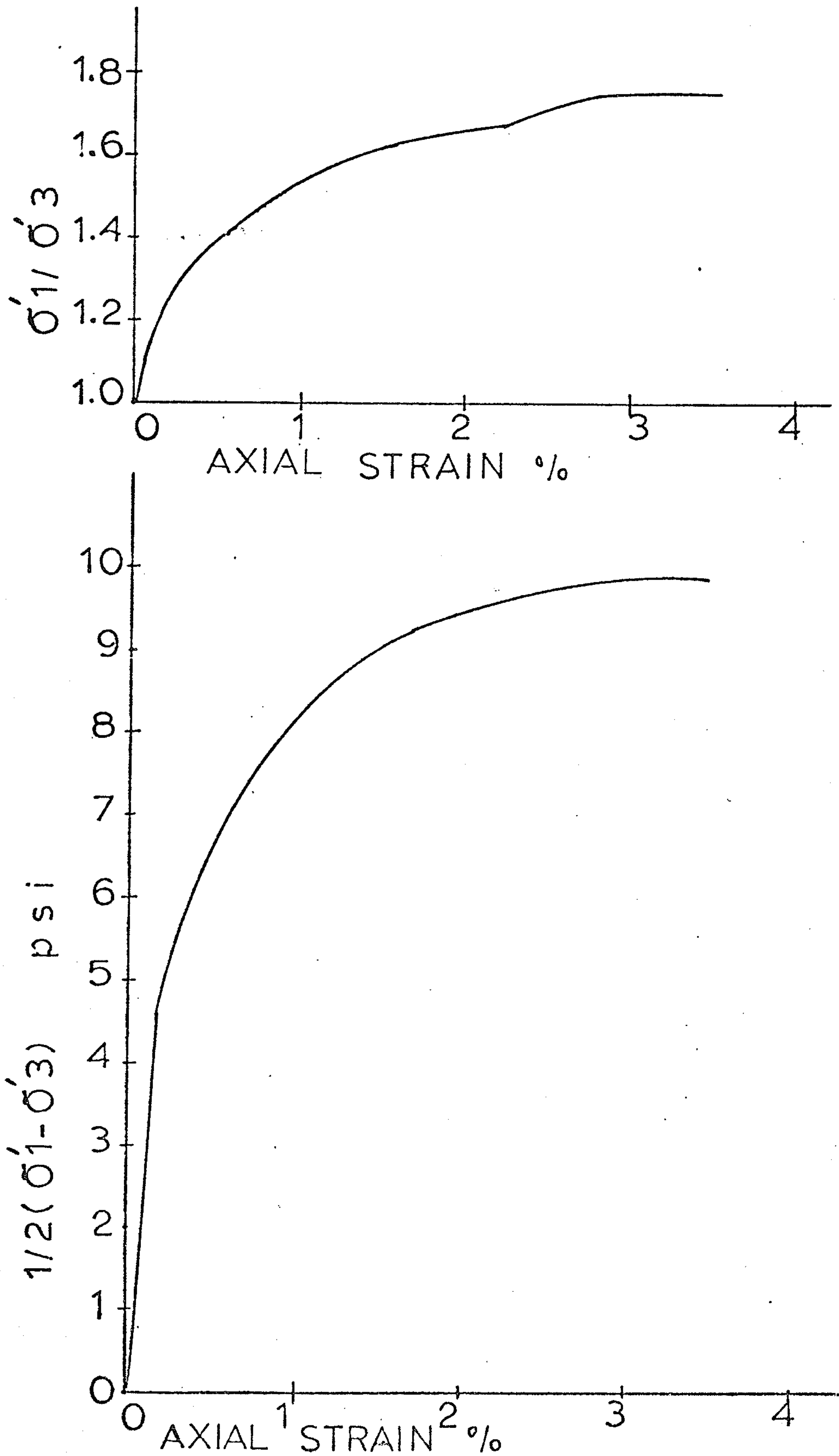

FIGURE A-29 RESULTS- TEST 203.3

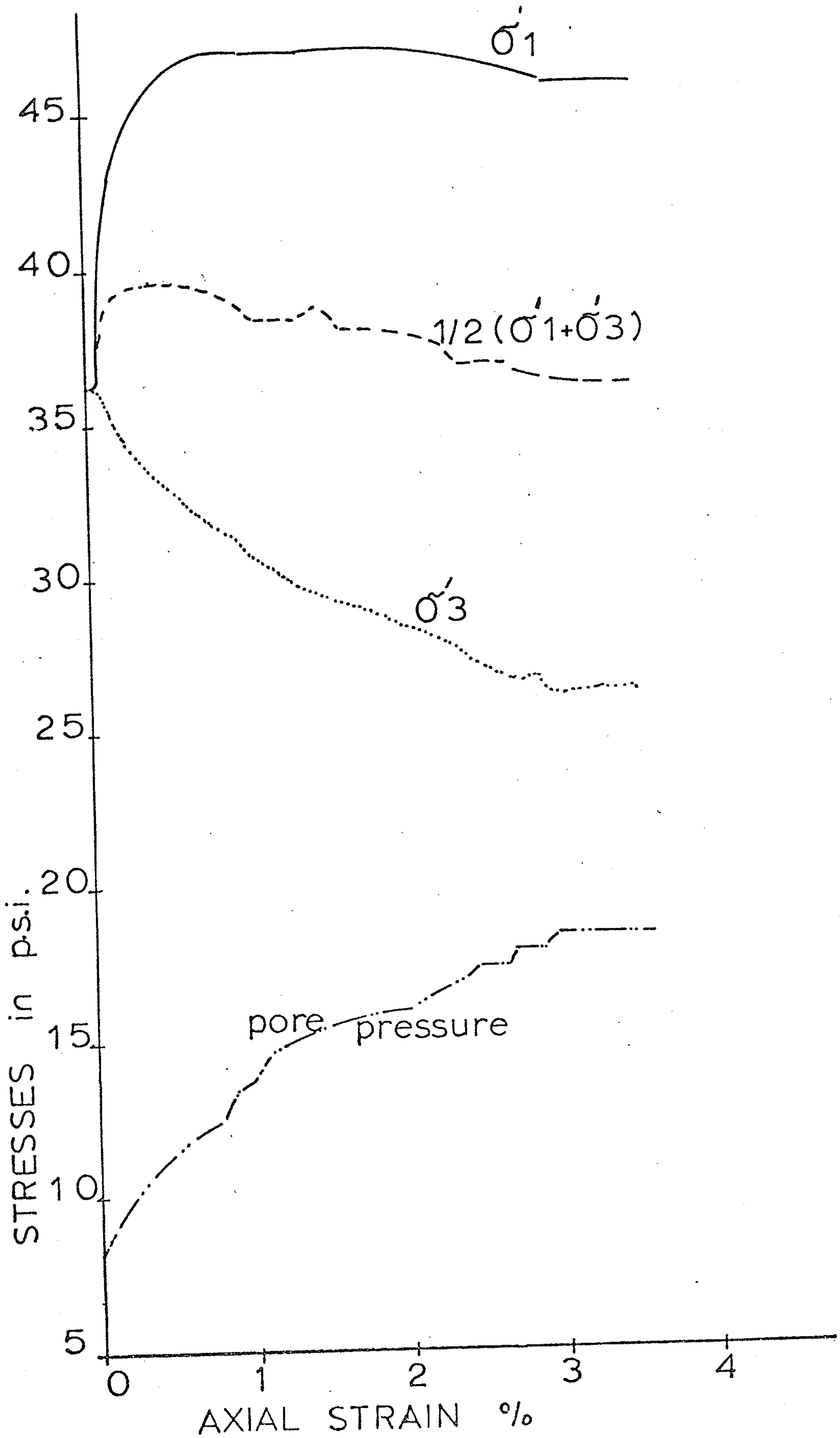

FIGURE A-30. RESULTS - TEST 204.1

$w_f = 63.1\%$ $e_f = 185$ $\sigma'_c = 17.6$ psi.

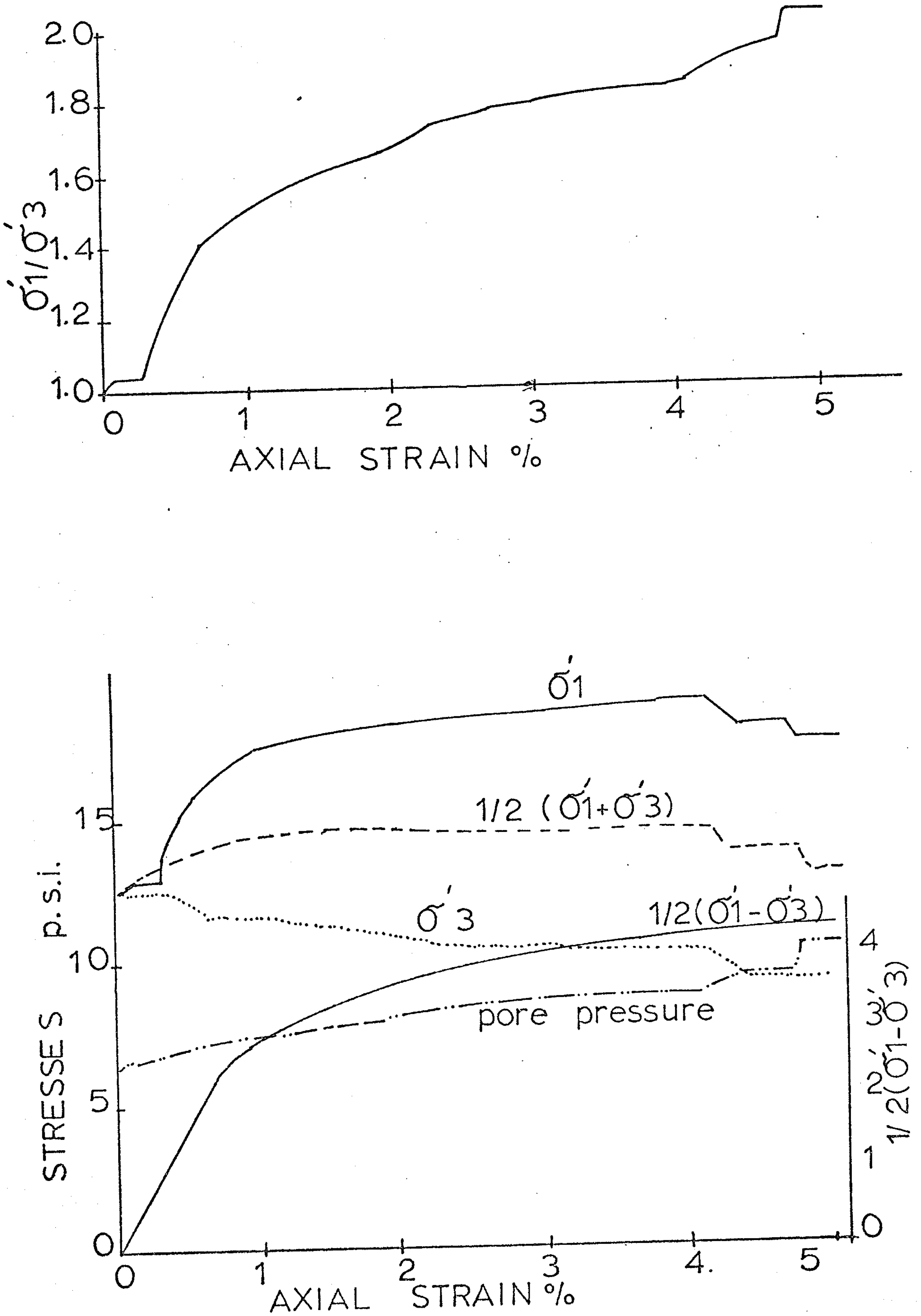

FIGURE A-30 RESULTS - TEST 2042

$w_f = 57.3\%$ $e_f = 1.68$ $\sigma'_c = 31.2$ psi.

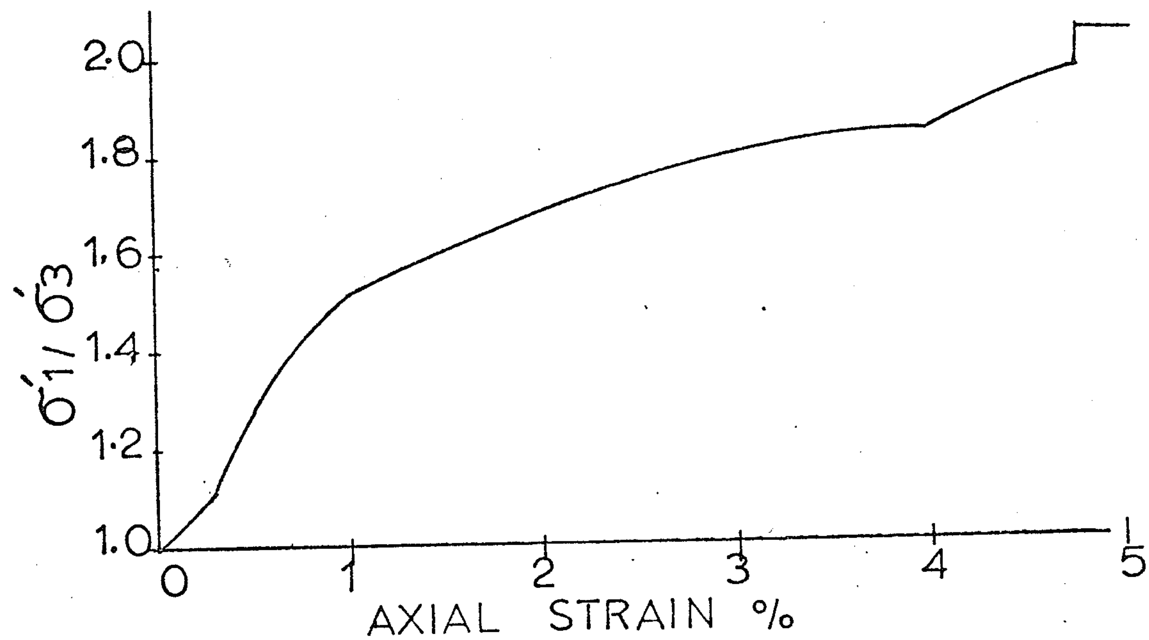

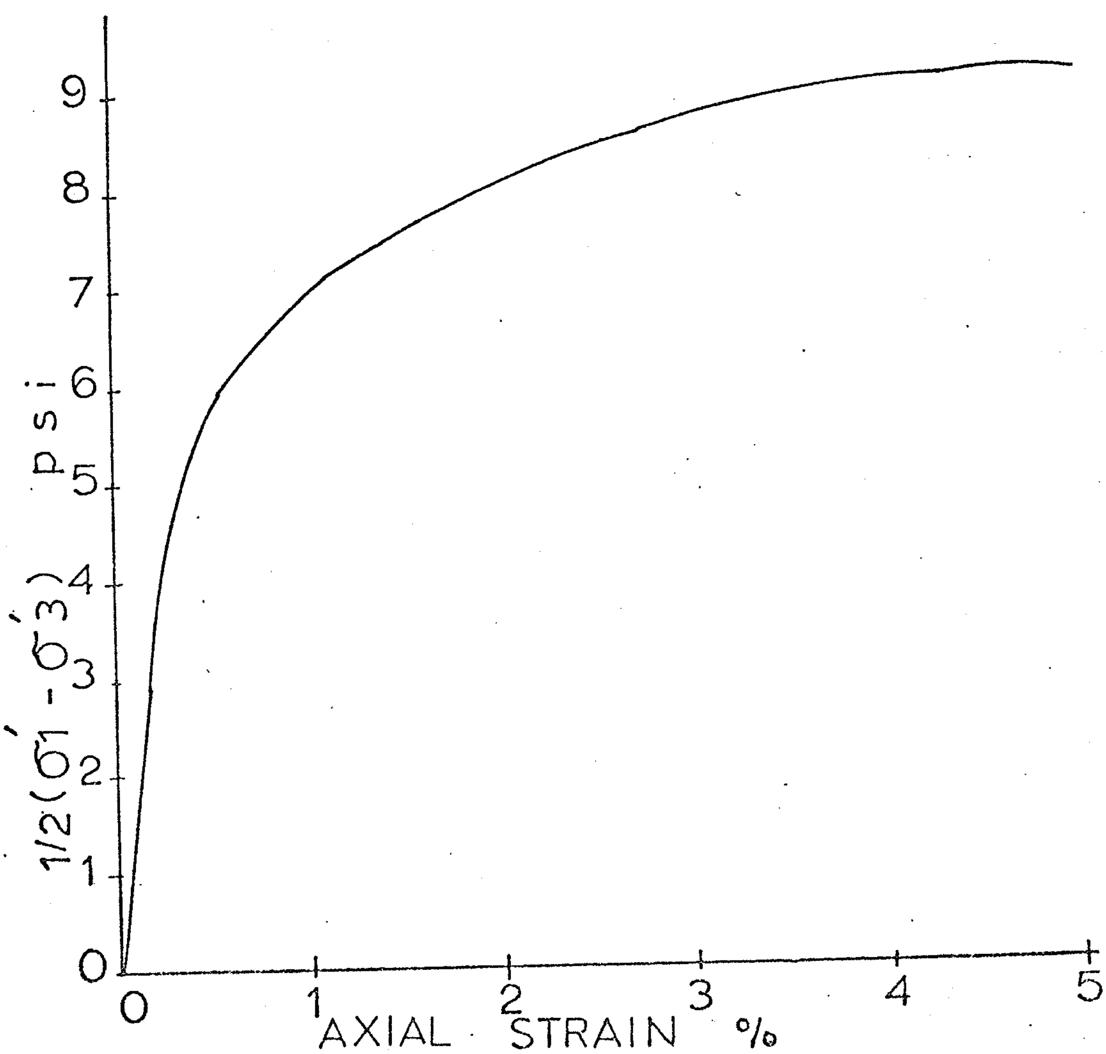

FIGURE A-31 RESULTS-TEST 204.2

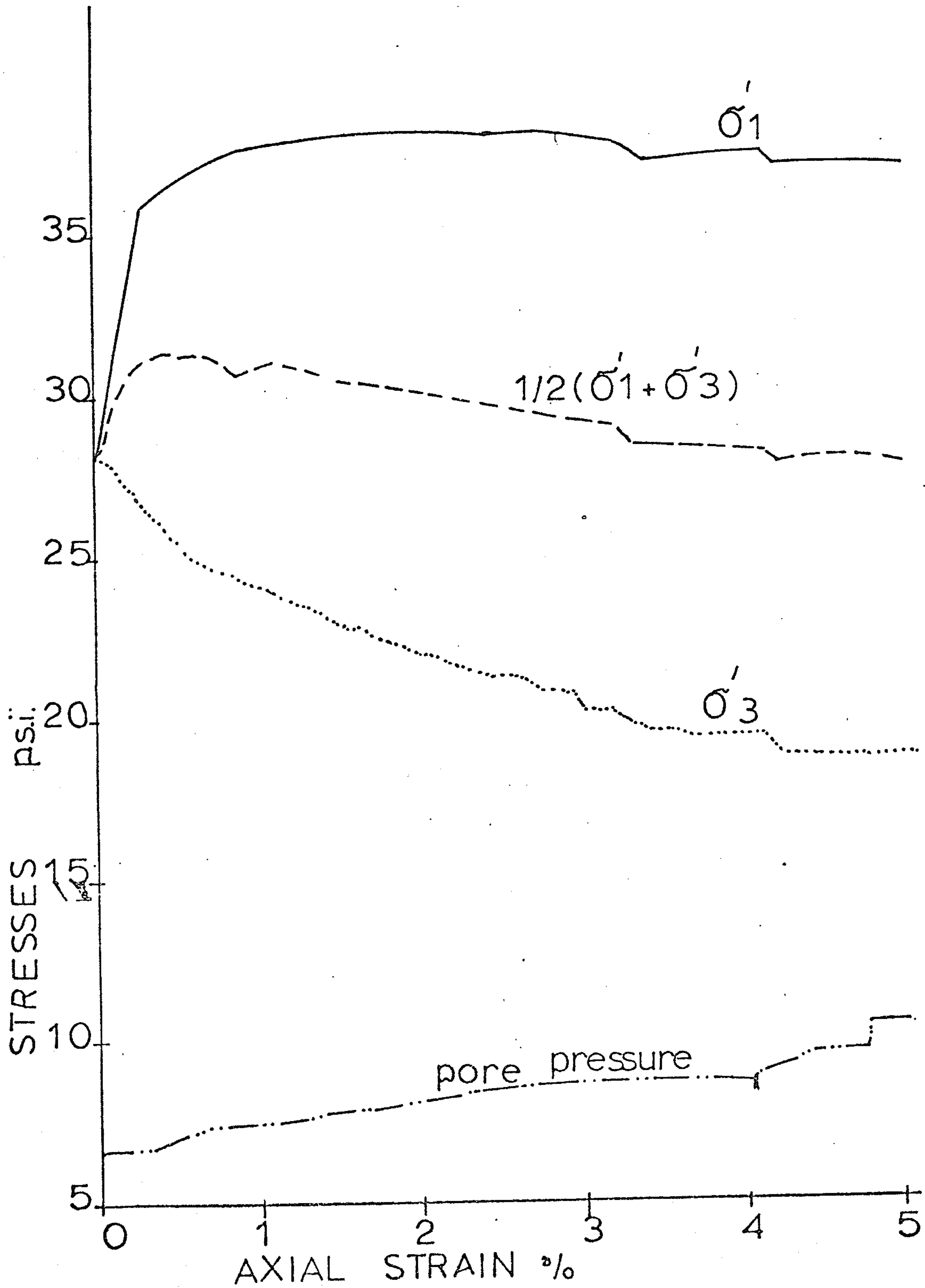

FIGURE A-32 RESULTS - TEST 301.1

IDS TEST

$w_i = 64.88\%$
$w_f = 68.50\%$
$\sigma'_c = 12.2$ psi

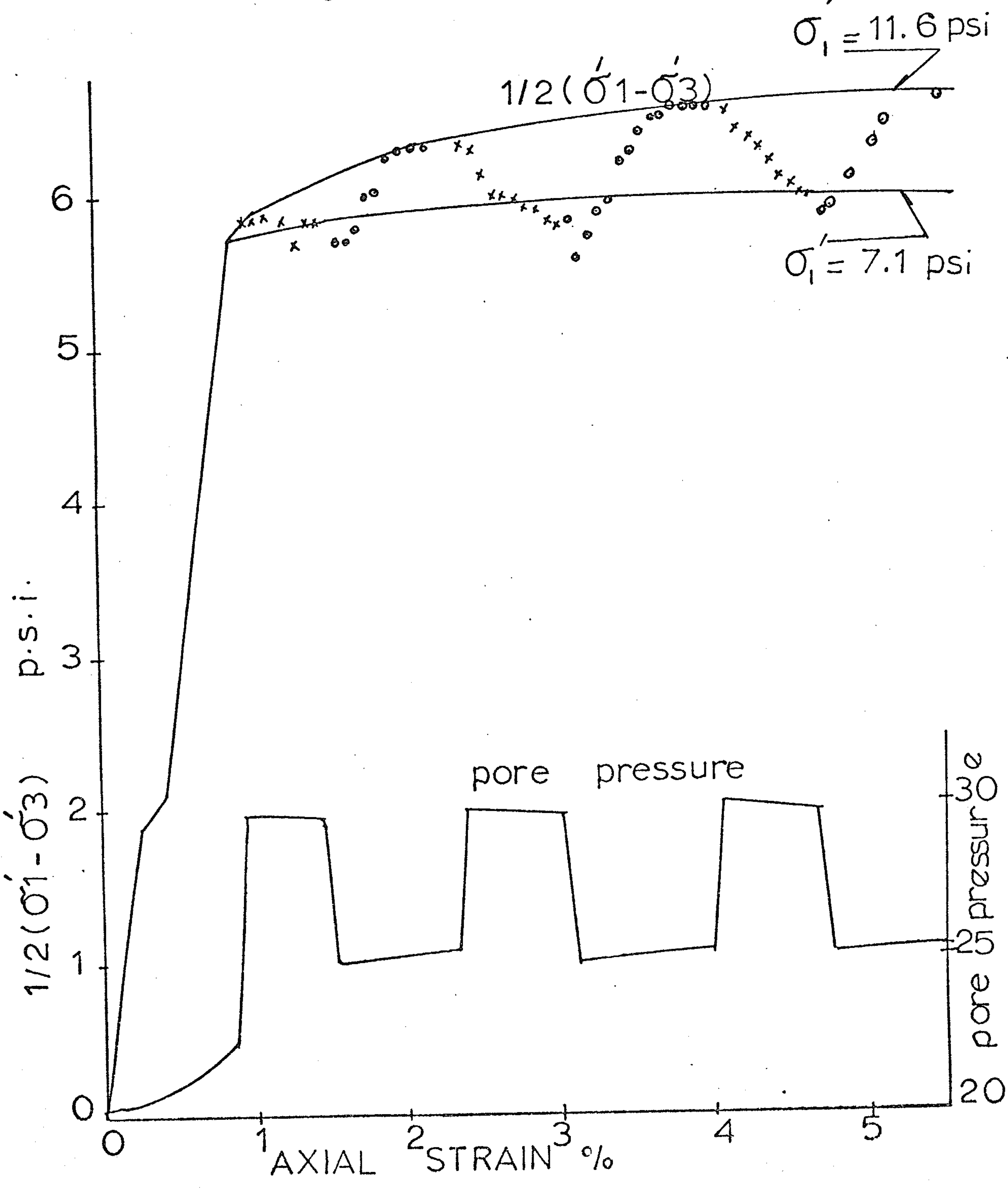

FIGURE A-33 RESULTS - TEST 301.2

IDS TEST

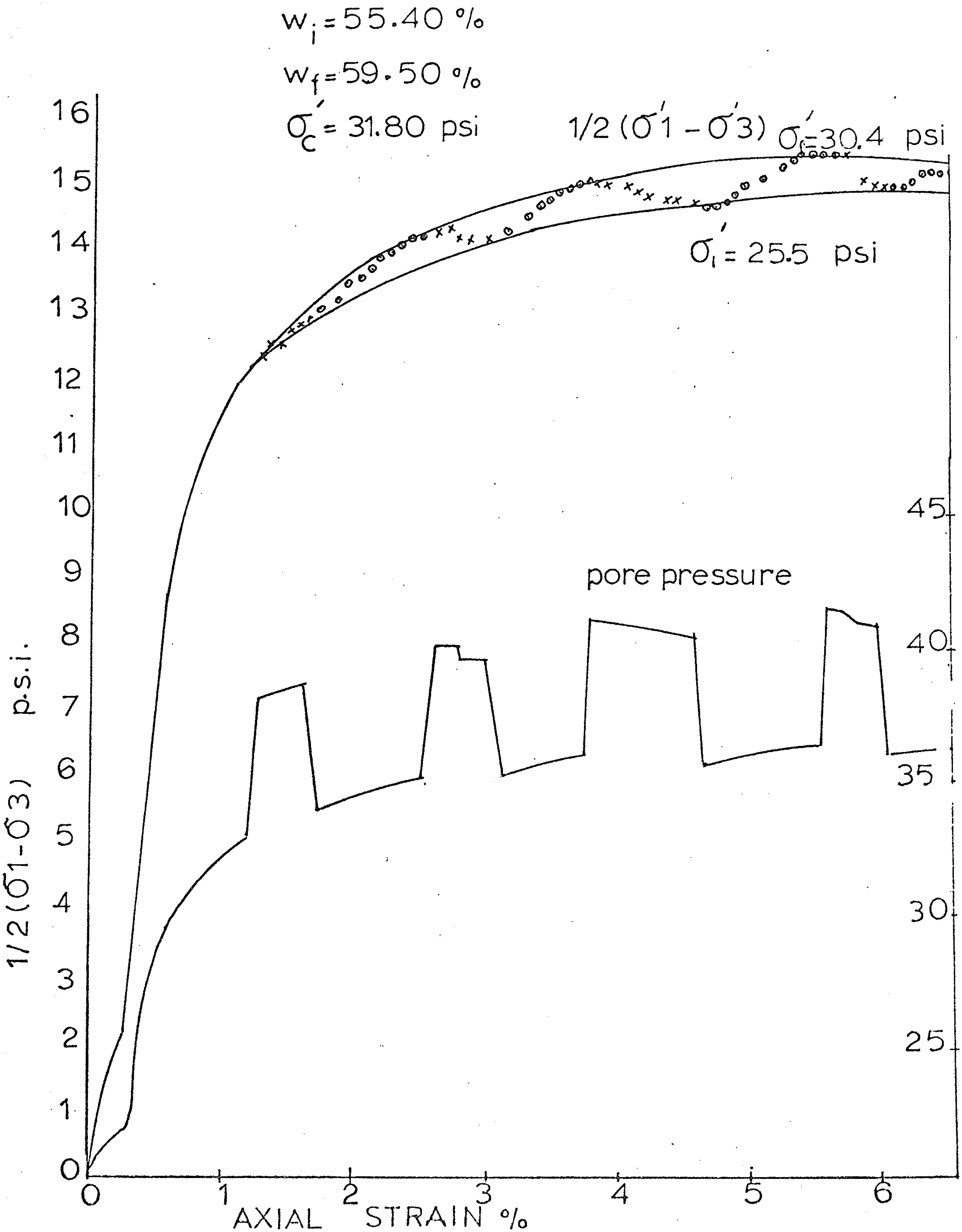

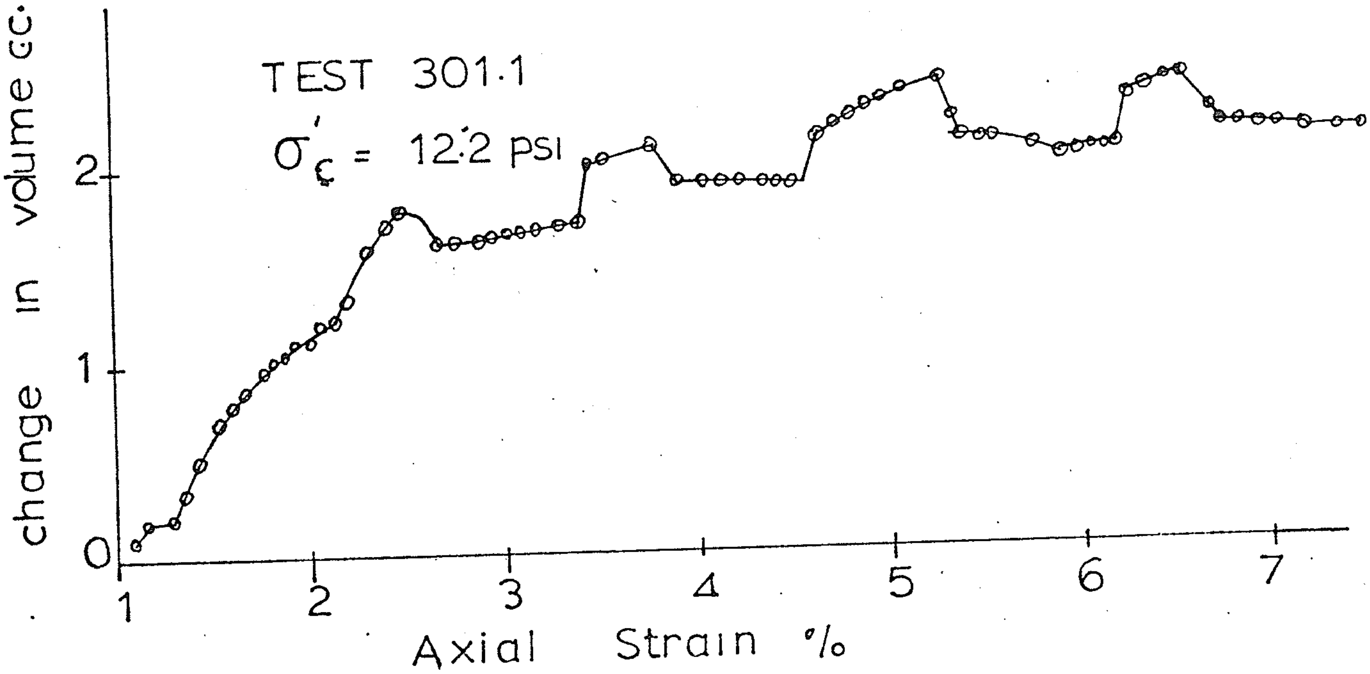

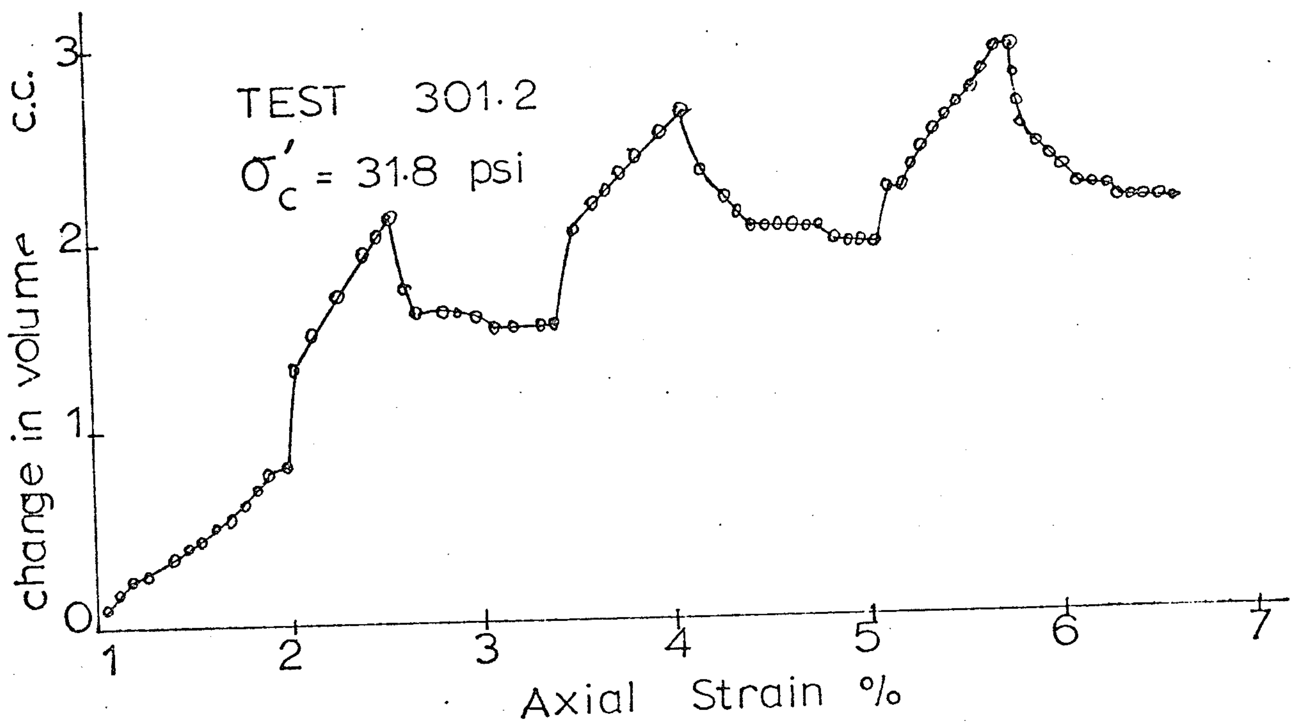

FIGURE A-34 Volume Change versus Strain Method (3)

Appendix B

Axial strain rate during tests

Appendix B

Table B-1 Axial strain rate in % strain /hour during tests

	Test number	101	102	103	104	201	202	203	204	IDS
Stage 1	Linear	0.935	0.632	0.810		0.675	0.660	0.667		0.638
	Non linear	0.873	0.916	0.890		0.984	0.975	0.955		1.020
	Average	0.886	0.826	0.864	1.050	0.935	0.925	0.905	0.850	0.916
Stage 2	Linear	0.675	0.650	0.715	0.730	1.120	0.624	1.200	1.020	0.700
	Non linear	0.867	0.939	0.967	0.897	0.915	0.870	0.885	0.895	0.970
	Average	0.835	0.892	0.917	0.860	0.922	0.830	0.888	0.910	0.900
Stage 3	Linear	0.636		0.795	0.650	0.600	0.678	0.650		
	Non linear	0.883		0.872	0.850	0.870	0.850	0.934		
	Average	0.832		0.852	0.812	0.830	0.815	0.875		

Appendix C

Effective octahedral normal stress at failure vs. water content at failure.

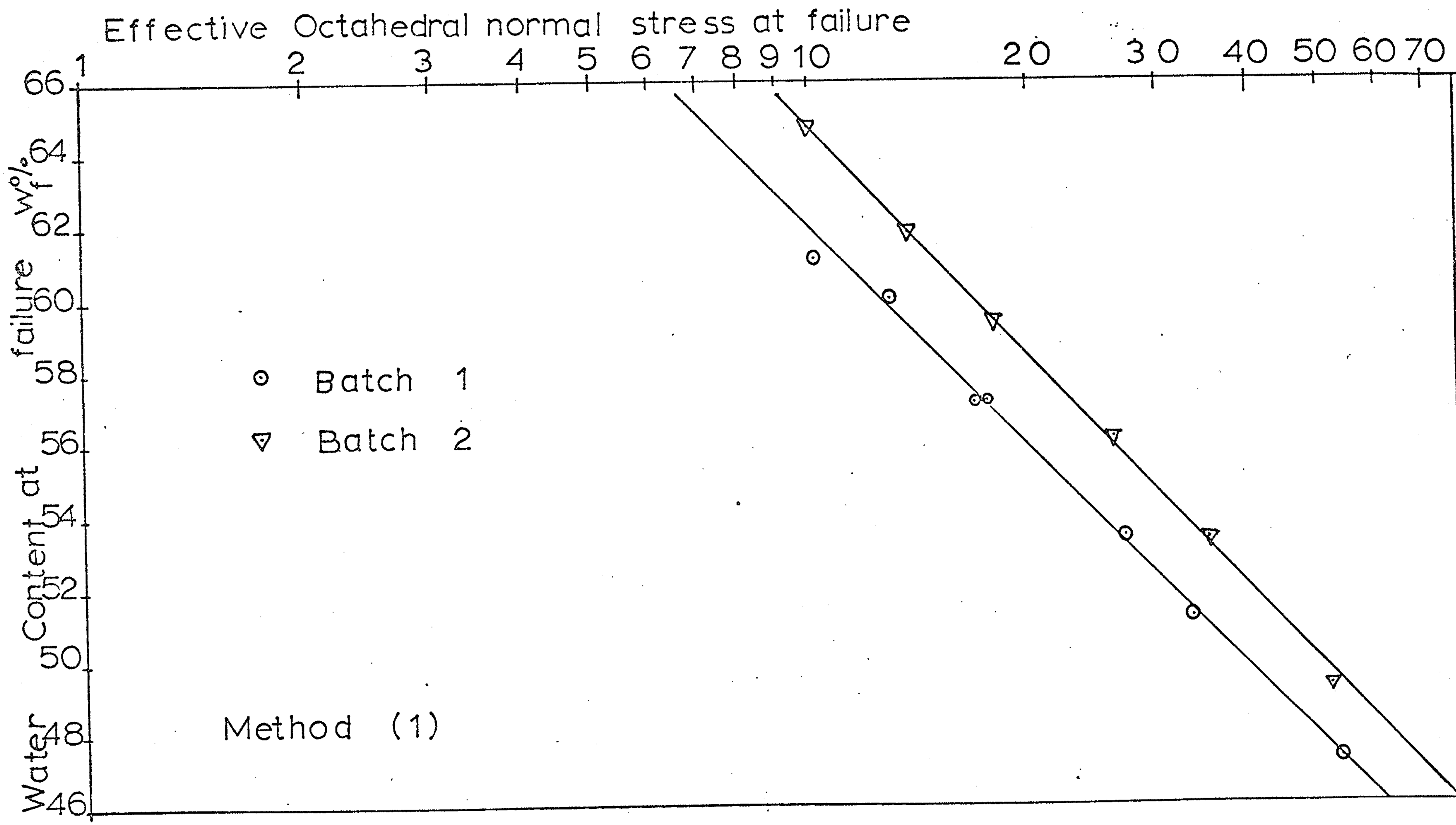

FIGURE C-1 Effective octahedral normal stress at failure vs water content at failure ; Method (1).

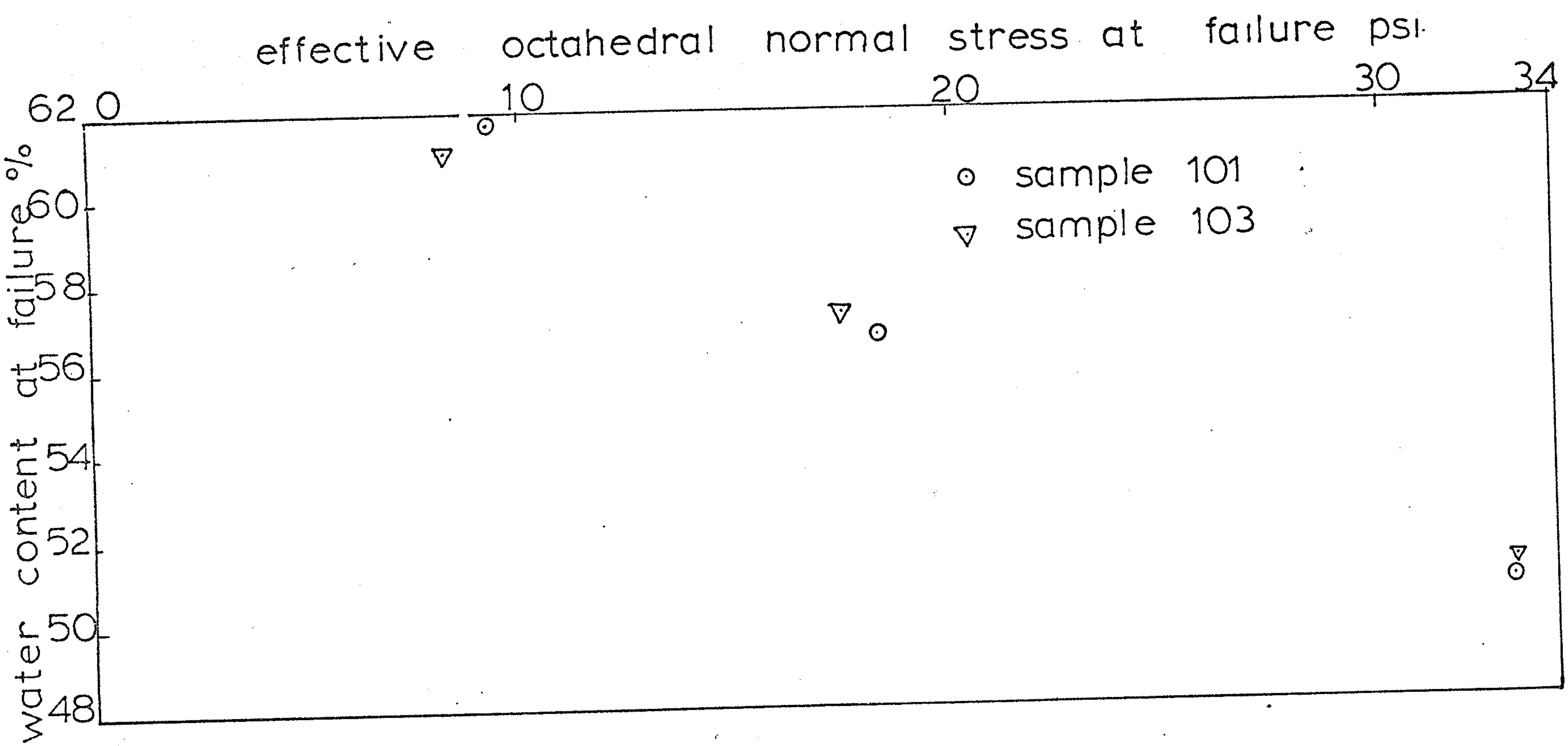

FIGURE C-2 Effective octahedral normal stress at failure vs. water content at failure ; Method (2).

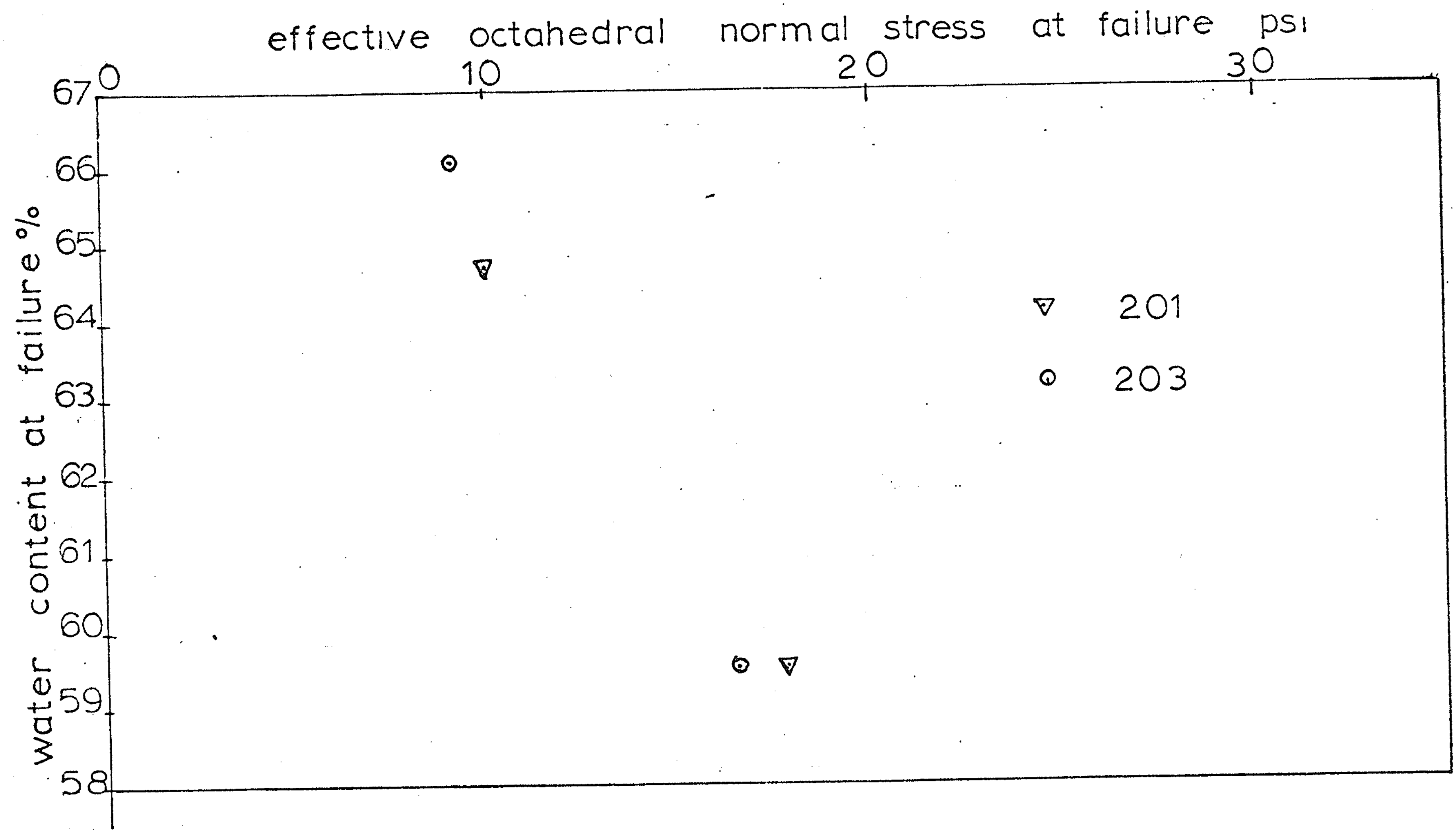

FIGURE C-3 Effective octahedral normal stress at failure vs. water content at failure; samples 201 - 203; Method (2)

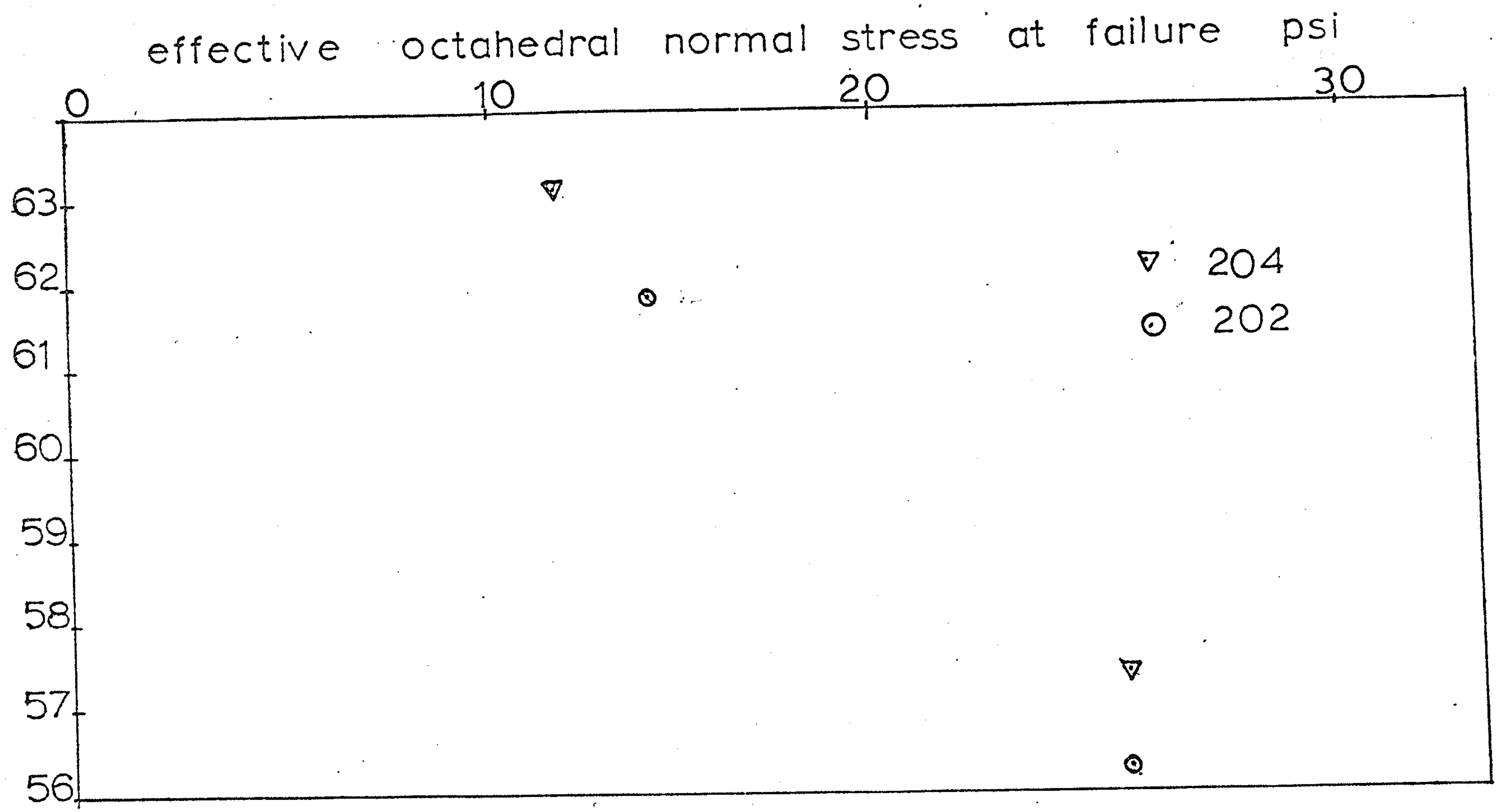

FIGURE C-4 . Effective octahedral normal stress at failure vs. water content at failure ; Method (2) ; samples 202-204.

Appendix D

Pore pressure and effective consolidation pressure vs. elapsed time.

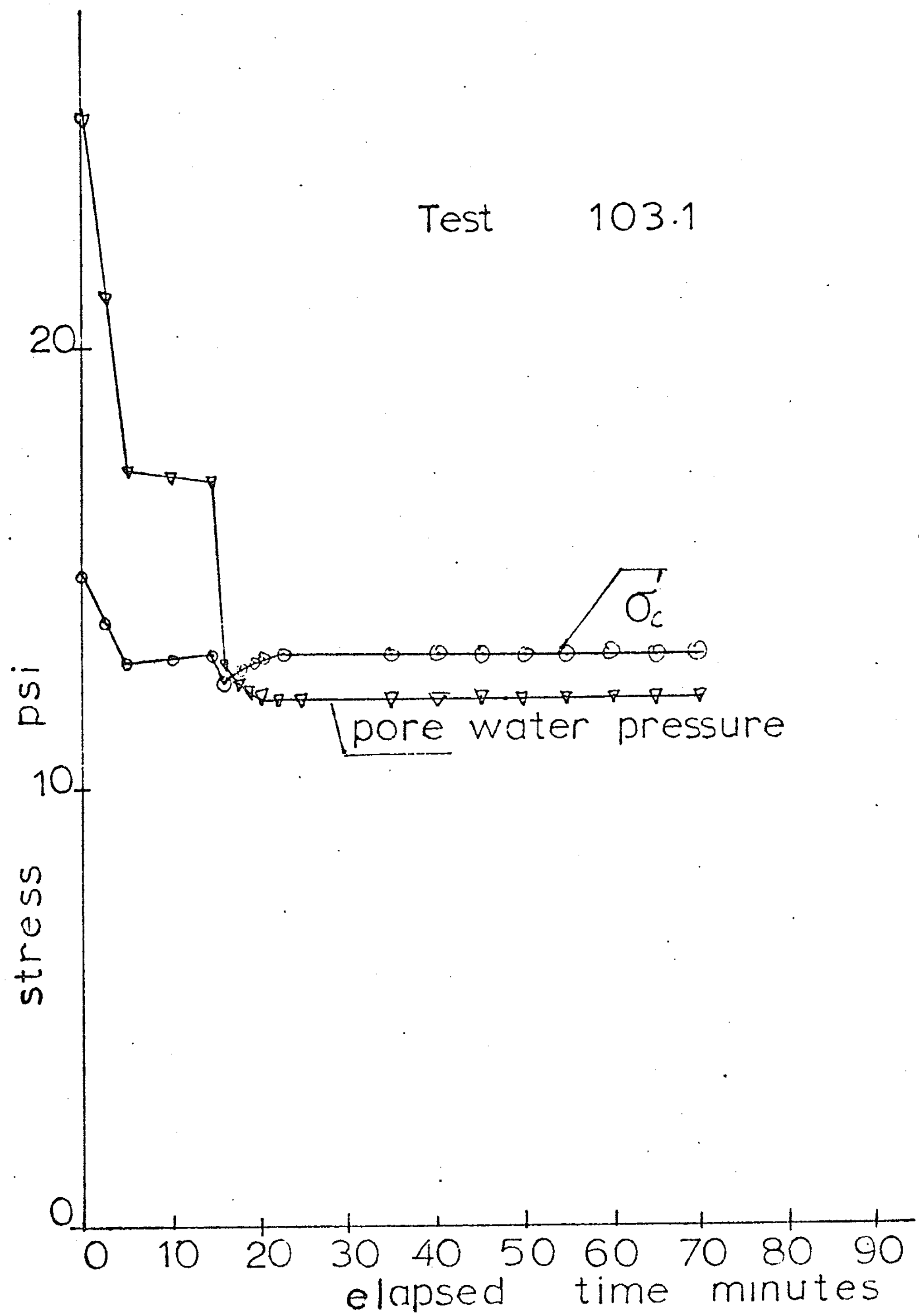

FIGURE D-1 Pore pressure & σ_c' vs. elapsed time ; Method (2)

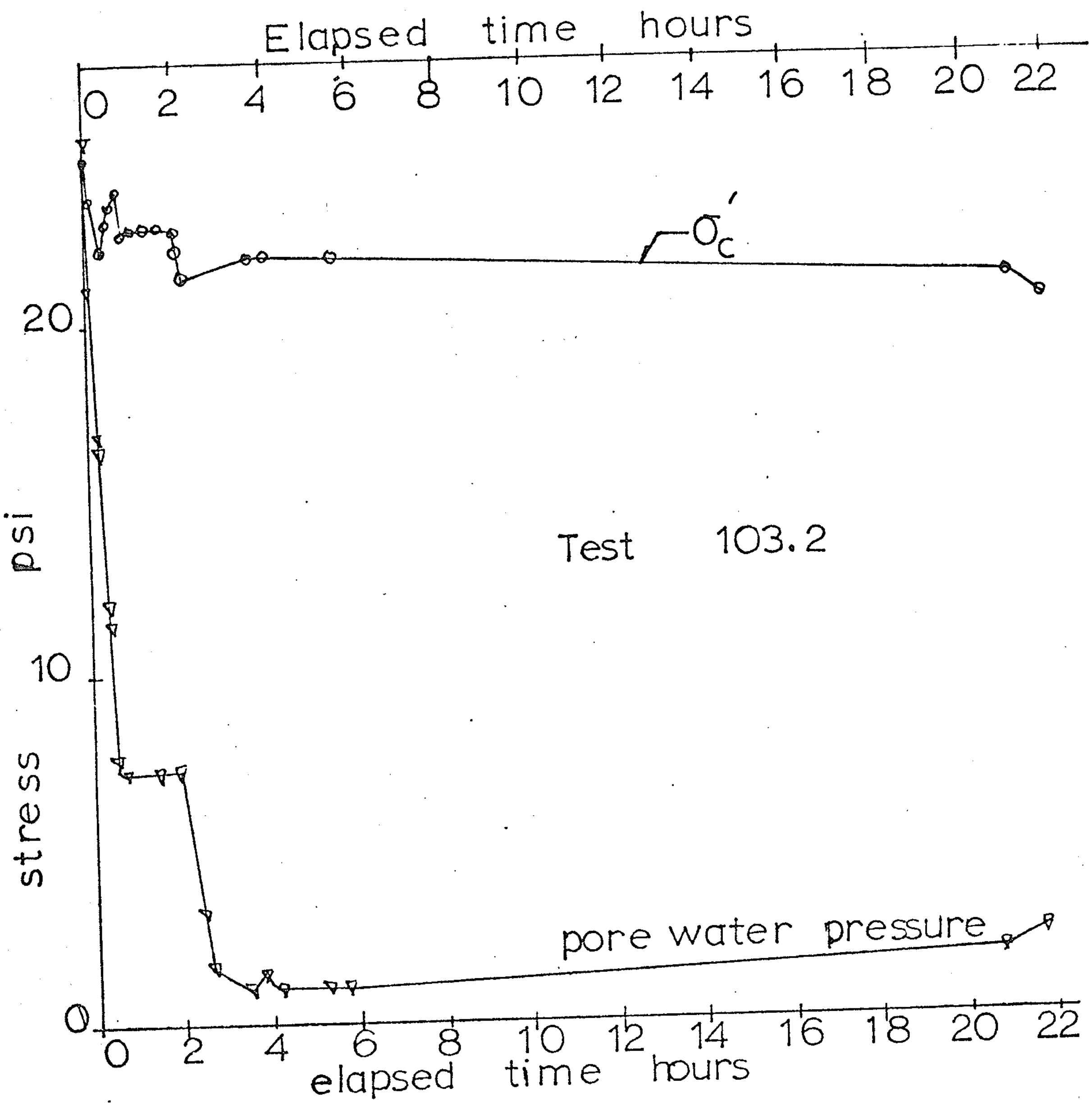

FIGURE D-2 Pore pressure & σ_c' vs. elapsed time ; Method (2)

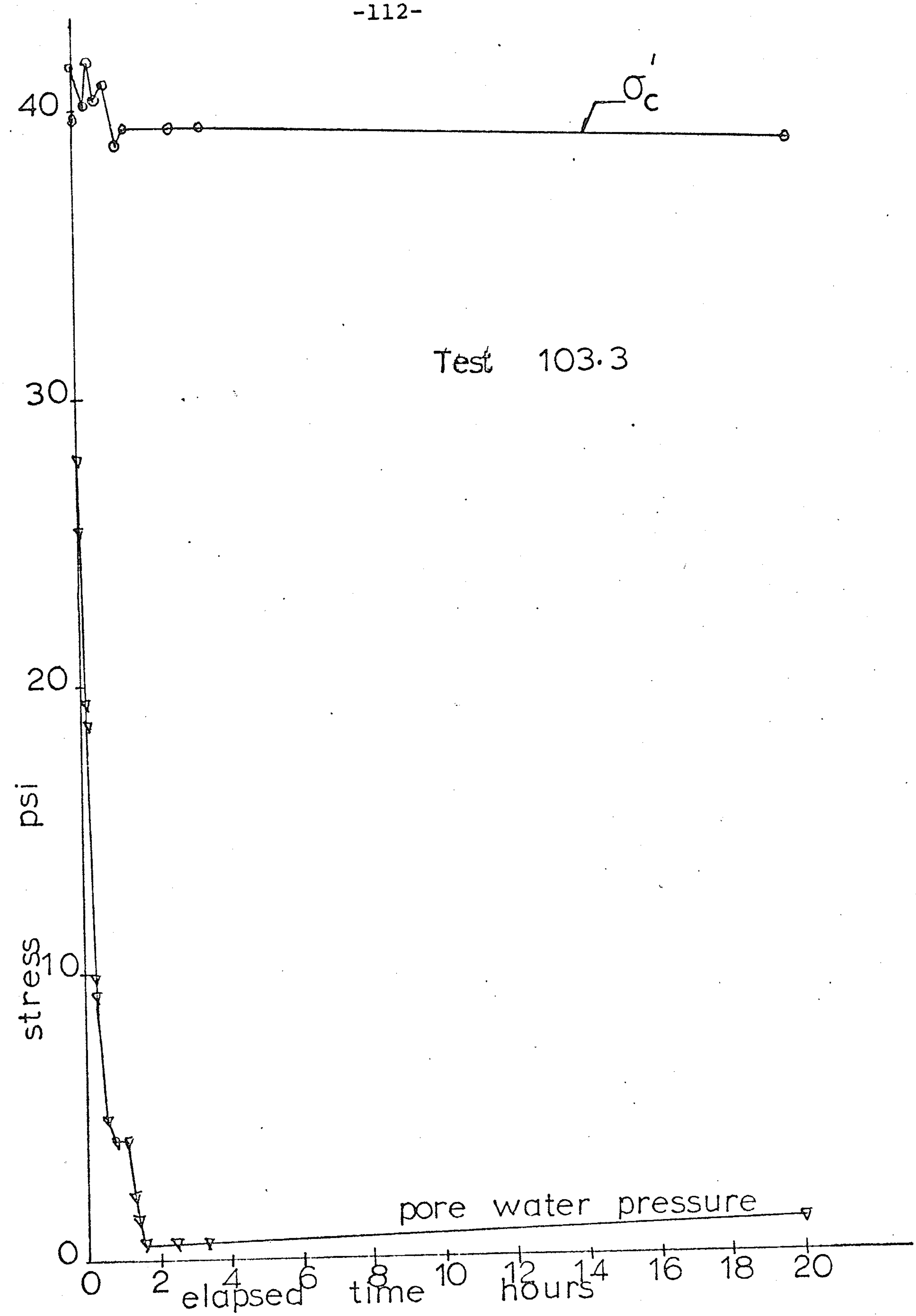

FIGURE D-3 Pore pressure & σ_c' vs elapsed time - , Method (2)

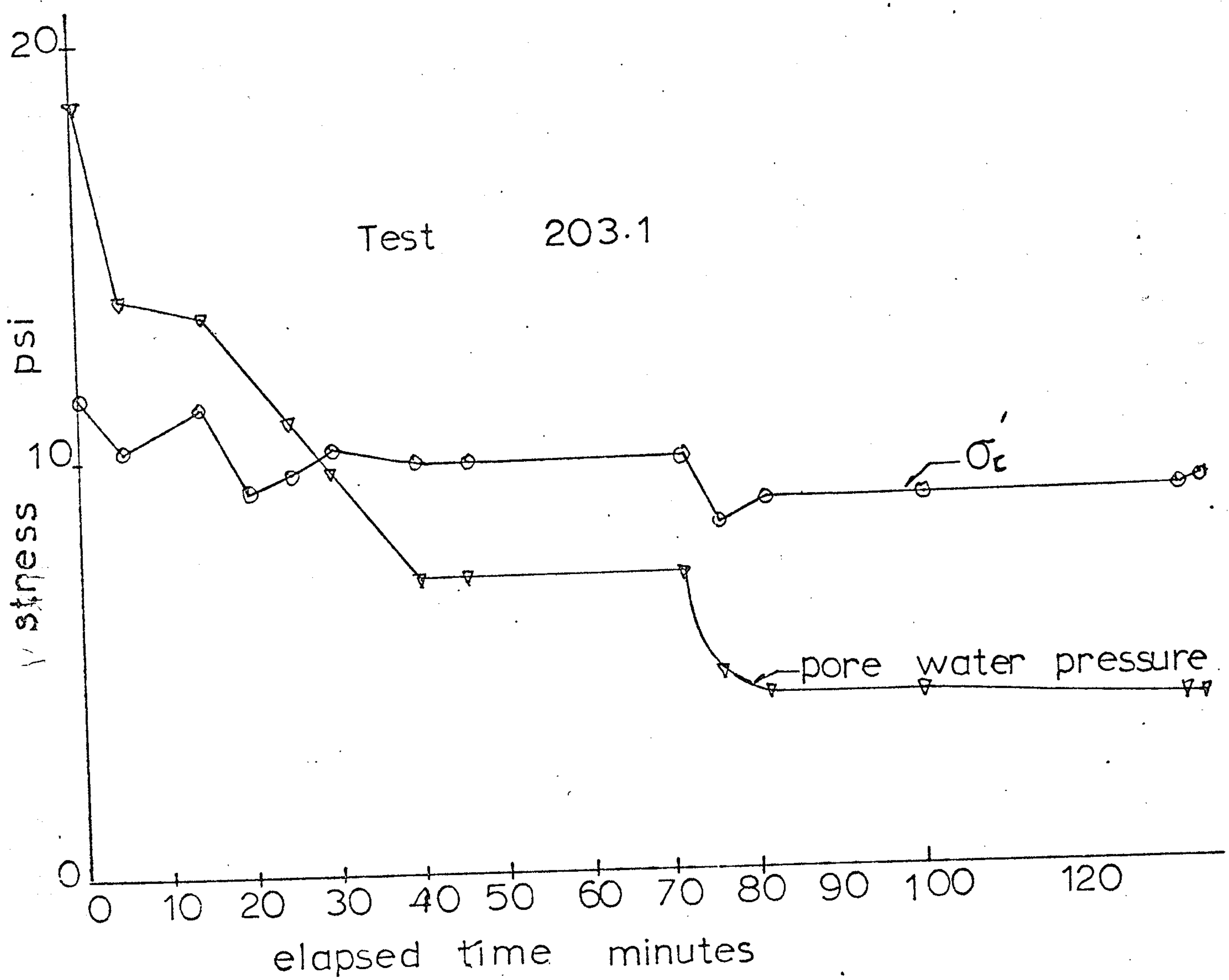

FIGURE D-4 Pore pressure & σ_c' vs. elapsed time ; Method (2)

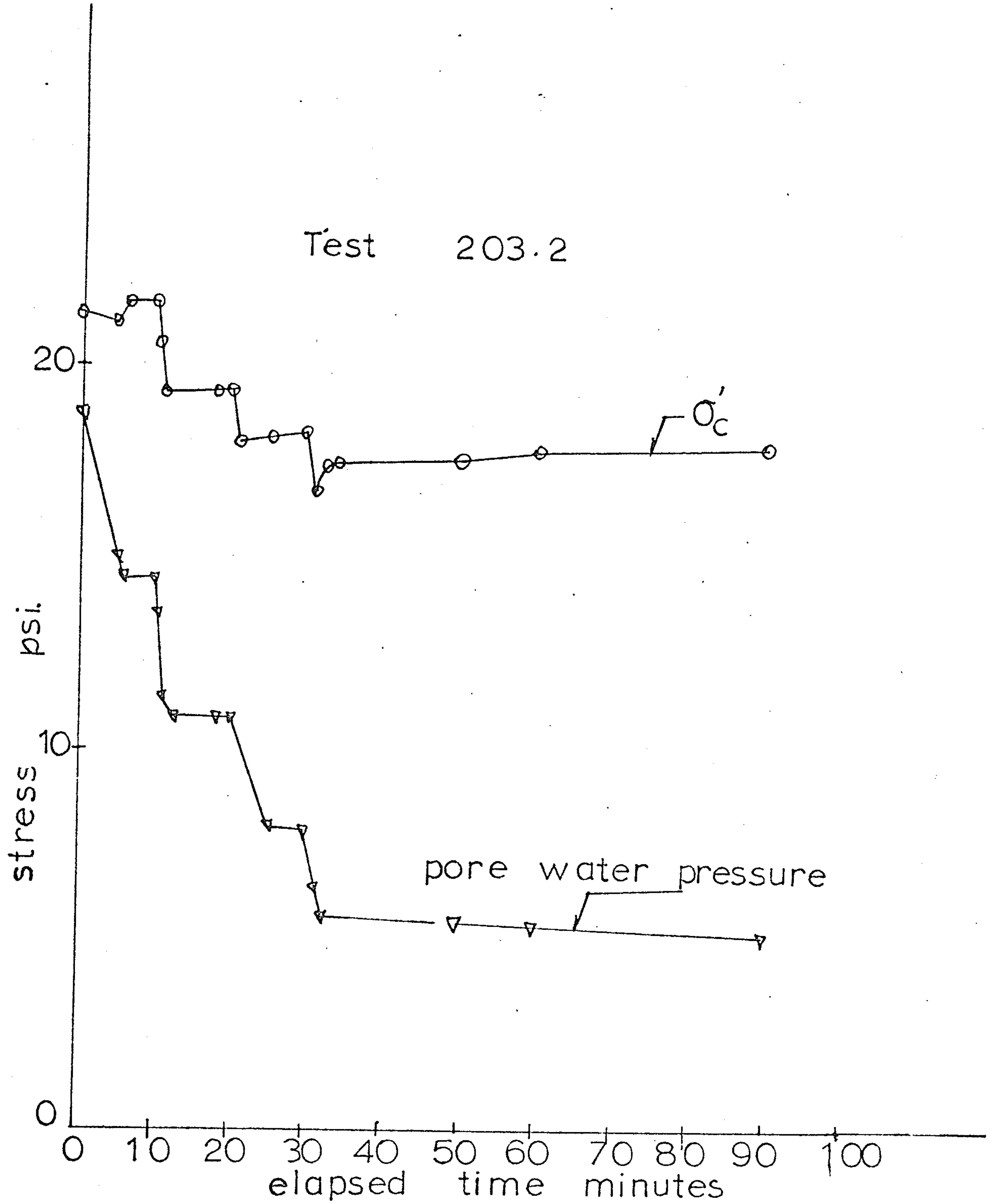

FIGURE D-5 Pore water pressure & σ_c' vs elapse time ; Method (2)

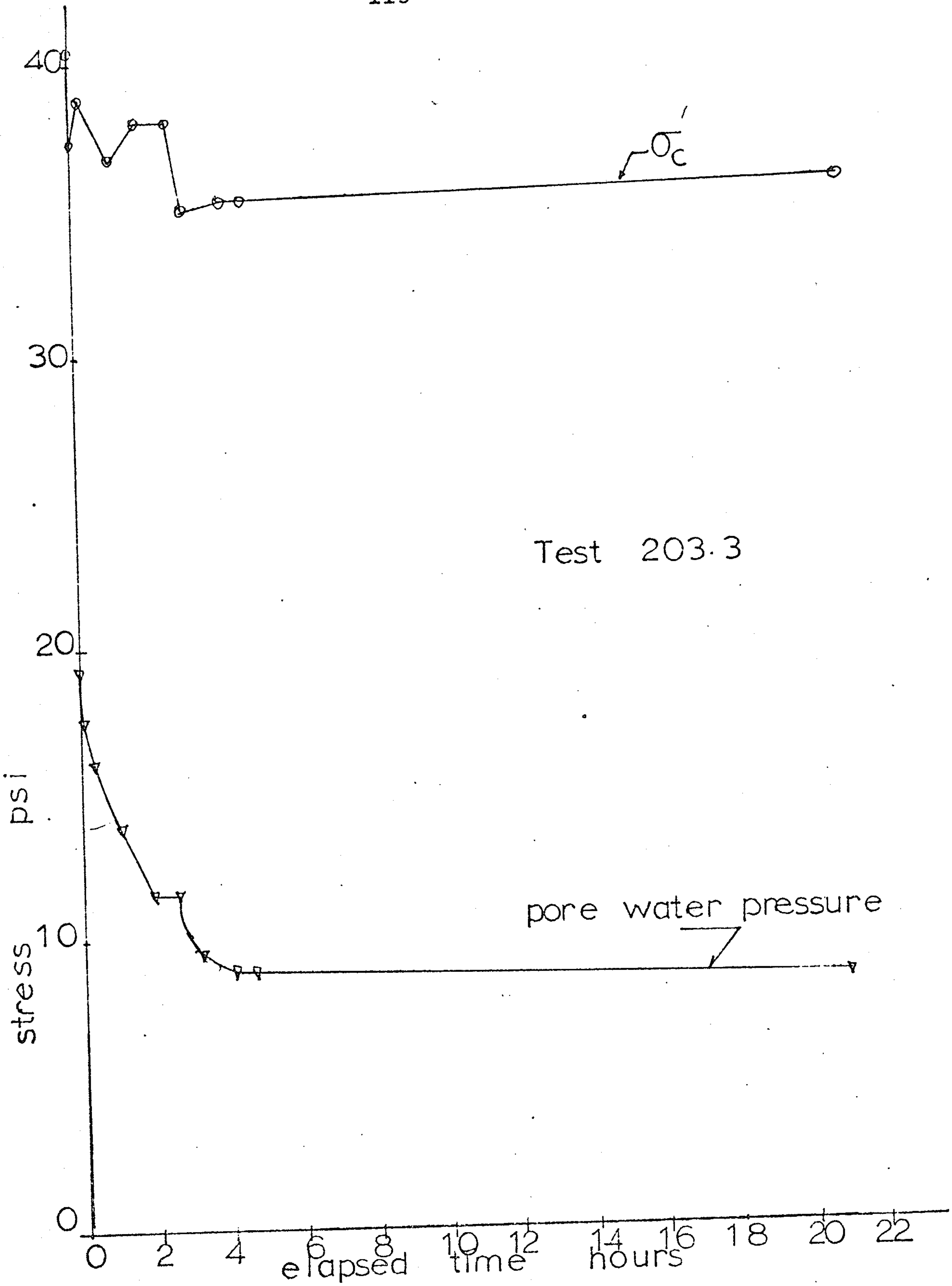

FIGURE D-6 Pore pressure & σ_c' vs elapsed time; Method (2)

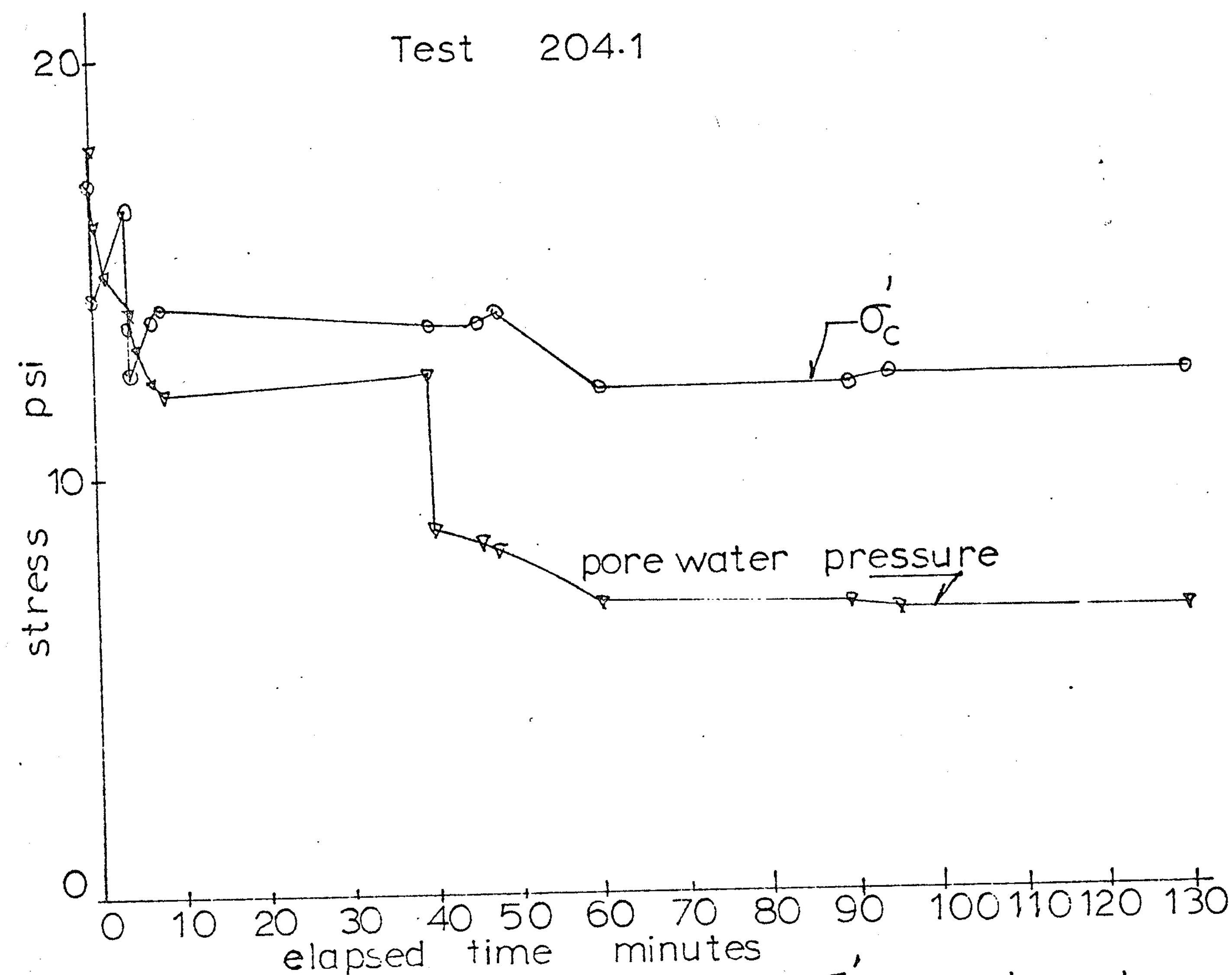

FIGURE D-7 Pore pressure & σ_c' vs elapsed time ; Method (2)

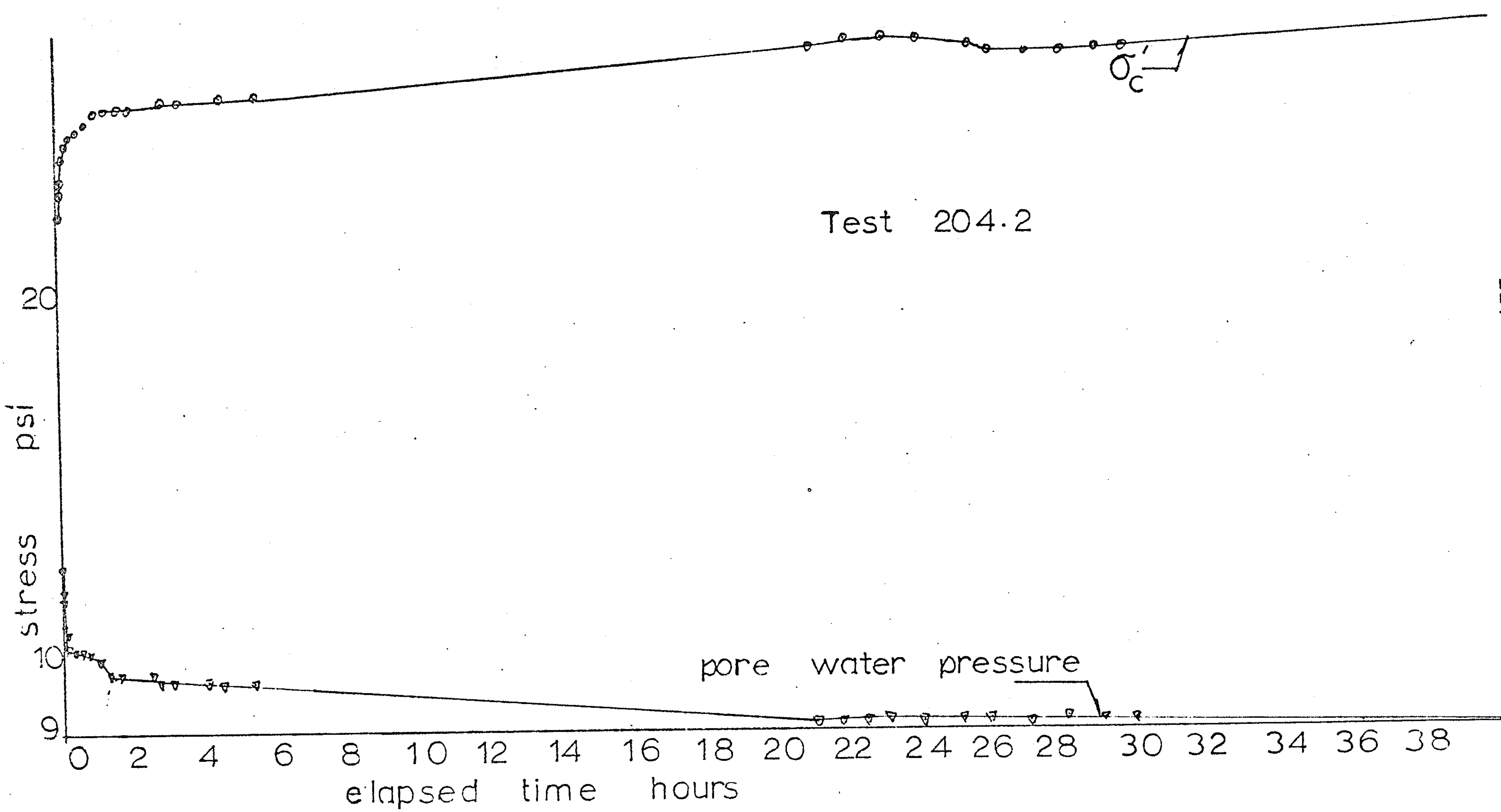

FIGURE D-8 Pore pressure & σ_c' vs elapsed time ; Method (2)

Appendix E

Independent-dependent-strain,IDS,technique.

Independent-dependent-strain,IDS,test.

Schmertmann and Osterberg (1960),and Schmertmann (1962),developed a new testing technique.The objective of this test is to separate the independent and dependent effective components of strength at any strain, hence the abreviation IDS test.

One sample of soil is required.The sample is consolidated and a back pressure is applied.The sample is then axially tested.The major principal stress,σ_1',is kept constant by increasing the pore pressure at the base of the sample.The changes in volumes and heights of the sample are recorded throughout the test.

Two effective stress conditions of the soil with identical structure at any strain are needed,to obtain the dependent and independent strength components.Schmertmann and Osterberg (1960) developed the hopping technique shown in Figure E-1.Two values of σ_1' are chosen;σ_1' (high) and σ_1' (low).The major principal stress,σ_1',range of about 75 to 100 % of the equivalent consolidation pressure,σ_e' ,produces strength changes that could be interpreted with sufficient accuracy and yet involves only a small void ratio change.As the sample is axially loaded σ_1' (high) is kept constant and points on σ_1' (high) deviator curve are obtained.The pore pressure is increased by an amount equal to the difference between σ_1' (high) and σ_1' (low). After some time, the deviator stress level off and points on σ_1' (low) deviator curve are obtained. Successive increase and decrease in the pore pressure leads to two deviator stress curves. At any strain two effective stresses are obtained and the strength components are readily calculated.

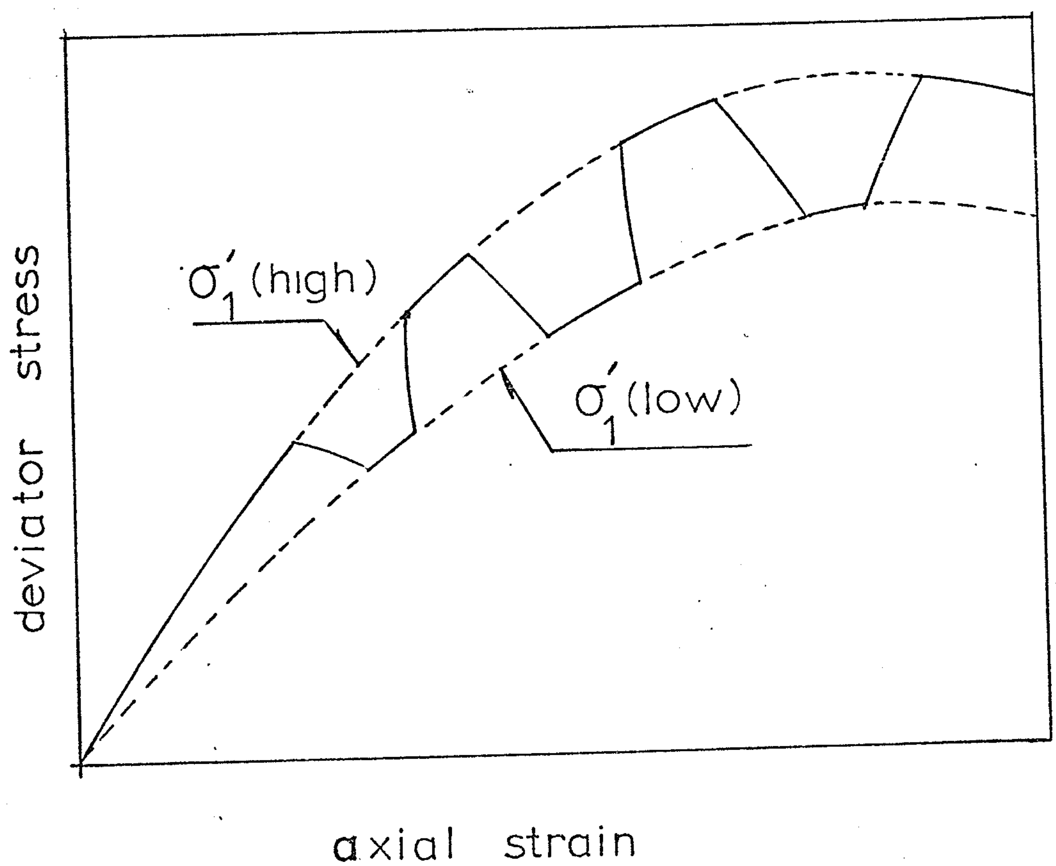

FIGURE E-1 Independent-dependent-strain, IDS, test.